RSC Advances

REVIEW

View Article Online
View Journal | View Issue

Cite this: *RSC Adv.*, 2024, **14**, 33681

Advancements in tantalum based nanoparticles for integrated imaging and photothermal therapy in cancer management

Ikhazuagbe H. Ifijen, *[a] Awoyemi Taiwo Christopher,[b] Ogunnaike Korede Lekan,[c] Omowunmi Rebecca Aworinde,[d] Emmanuel Faderin,[e] Oluwafunke Obembe,[f] Tawakalitu Folashade Abdulsalam_Akanji,[g] Juliet C. Igboanugo,[h] Uzochukwu Udogu,[i] Godwin Onogwu Ogidi,[j] Terungwa H. Iorkula[k] and Osasere Jude-Kelly Osayawe[k]

Tantalum-based nanoparticles (TaNPs) have emerged as promising tools in cancer management, owing to their unique properties that facilitate innovative imaging and photothermal therapy applications. This review provides a comprehensive overview of recent advancements in TaNPs, emphasizing their potential in oncology. Key features include excellent biocompatibility, efficient photothermal conversion, and the ability to integrate multifunctional capabilities, such as targeted drug delivery and enhanced imaging. Despite these advantages, challenges remain in establishing long-term biocompatibility, optimizing therapeutic efficacy through surface modifications, and advancing imaging techniques for real-time monitoring. Strategic approaches to address these challenges include surface modifications like PEGylation to improve biocompatibility, precise control over size and shape for effective photothermal therapy, and the development of biodegradable TaNPs for safe elimination from the body. Furthermore, integrating advanced imaging modalities—such as photoacoustic imaging, magnetic resonance imaging (MRI), and computed tomography (CT)—enable real-time tracking of TaNPs *in vivo*, which is crucial for clinical applications. Personalized medicine strategies that leverage biomarkers and genetic profiling also hold promise for tailoring TaNP-based therapies to individual patient profiles, thereby enhancing treatment efficacy and minimizing side effects. In conclusion, TaNPs represent a significant advancement in nanomedicine, poised to transform cancer treatment paradigms while expanding into various biomedical applications.

Received 7th August 2024
Accepted 6th October 2024

DOI: 10.1039/d4ra05732e

rsc.li/rsc-advances

1 Introduction

Cancer remains one of the most formidable challenges facing modern medicine, with its complex nature demanding innovative approaches for diagnosis and treatment.[1] In recent years, nanotechnology has emerged as a promising frontier in the fight against cancer, offering unprecedented opportunities to revolutionize both imaging and therapeutic modalities.[2–4] Among the myriad nanoparticles explored for their potential in cancer management, tantalum-based nanoparticles have garnered significant attention for their unique physicochemical properties and multifaceted applications in enhanced imaging and photothermal therapy. Nanoparticles exhibit distinct properties compared to their bulk counterparts due to their high surface area-to-volume ratio and quantum effects at the nanoscale,[5–7] making them promising candidates for various biomedical applications, including drug delivery, imaging, and theranostics.[8–10] In cancer therapy, nanoparticles offer targeted delivery of therapeutic agents to tumor sites, minimizing off-target effects and enhancing treatment efficacy. Their ability to accumulate preferentially in tumors through passive

[a]*Department of Research Outreach, Rubber Research Institute of Nigeria, Iyanomo, Benin City, Nigeria. E-mail: larylans4u@yahoo.com*
[b]*Laboratory Department, Covenant University Medical Centre, Canaan land, KM 10, Idiroko Road, Ota, Ogun State, Nigeria*
[c]*Department of Chemistry, Wichita State University, 1845 Fairmount, Box 150, Wichita, KS 67260-0150, USA*
[d]*Department of Chemistry, Michigan Technological University, 1400 Townsend Dr, Houghton, MI 49931, USA*
[e]*Department of Pharmaceutical Sciences, Southern Illinois University, Edwardsville, 1 Hairpin Drive, Edwardsville, IL 62026-001, USA*
[f]*Universite Paris-Cite, 4 Avenue de l'observatoire, 75006 Paris, France*
[g]*Department of Clinical Research and Vetenary, Vetplace Animal Hospital Lagos, Nigeria*
[h]*Department of Health, Human Performance, and Recreation, 155 Stadium Drive, Arkansas 72701, USA*
[i]*Department of Chemistry, Federal University of Technology Owerri, Nigeria*
[j]*Pharmacist at Saint Louis Catholic Hospital Owo Ondo State, Nigeria*
[k]*Department of Chemistry and Biochemistry, Brigham Young University Provo, Utah, USA*

targeting (enhanced permeability and retention effect) or active targeting strategies further enhances their utility in oncology.[11,12] Moreover, nanoparticles can be functionalized with targeting ligands, antibodies, or peptides to achieve specific interactions with cancer cells, enabling personalized medicine approaches.[13]

The development and application of tantalum-based nanoparticles represent a paradigm shift in the landscape of cancer diagnosis and treatment.[14–17] These nanoparticles, characterized by their high atomic number and biocompatibility, exhibit exceptional properties that makes them well-suited for various biomedical applications. In particular, their ability to serve as multimodal contrast agents for enhanced imaging and as agents for targeted photothermal therapy holds immense promise for improving cancer patient outcomes.[17–19] Tantalum-based nanomaterials, with their high photothermal conversion efficiency and compatibility with imaging modalities such as computed tomography (CT) and photoacoustic imaging (PAI), have shown great potential in targeted tumor ablation and real-time tracking of therapeutic progress, offering a dual-function strategy that significantly enhances therapeutic precision.

The quest to develop effective contrast agents for imaging modalities has been a longstanding endeavour in oncology. Traditional imaging techniques such as X-ray computed tomography (CT) and magnetic resonance imaging (MRI) rely on the use of exogenous contrast agents to enhance tissue contrast and delineate pathological lesions.[20,21] However, conventional contrast agents often suffer from limitations such as poor specificity, short circulation times, and potential toxicity. In this context, tantalum-based nanoparticles offer a compelling solution, leveraging their high X-ray attenuation coefficient and tunable surface properties to provide superior imaging contrast and resolution.[22,23] Furthermore, their compatibility with emerging imaging modalities such as photoacoustic imaging (PAI) holds promise for non-invasive, high-resolution imaging of deep-seated tumors.[24,25]

Beyond their role as contrast agents, tantalum-based nanoparticles exhibit remarkable potential in photothermal therapy (PTT), a minimally invasive approach for cancer treatment. PTT relies on the selective conversion of optical energy into heat by nanoparticles upon exposure to near-infrared (NIR) light, leading to localized hyperthermia and subsequent tumor ablation.[26,27] The unique optical properties of tantalum-based nanoparticles, coupled with their ability to accumulate preferentially within tumor tissues, make them ideal candidates for targeted PTT. By precisely controlling the distribution and intensity of NIR light, clinicians can achieve selective destruction of cancerous cells while minimizing damage to surrounding healthy tissue, thereby offering a promising alternative or adjunct to conventional cancer therapies.[28]

As tantalum-based nanoparticles continues to undergo rigorous preclinical and clinical evaluation, it is imperative to assess their safety, efficacy, and translational potential in cancer management. Moreover, ongoing research efforts are focused on refining nanoparticle synthesis techniques, optimizing surface functionalization strategies, and exploring novel therapeutic combinations to further enhance their performance in imaging and therapy.[16,17] By addressing these challenges and capitalizing on the unique properties of tantalum-based nanoparticles, researchers aim to realize their full potential as versatile tools in the personalized and precision-oriented approach to cancer treatment.

In light of these developments, this review aims to provide a comprehensive overview of the development and application of tantalum-based nanoparticles for enhanced imaging and photothermal therapy in cancer treatment. By synthesizing and critically evaluating existing literature, this review seeks to elucidate the current state-of-the-art, identify key challenges and opportunities, and delineate future directions for advancing tantalum-based nanoparticles towards clinical translation. Through this collective effort, tantalum-based nanoparticles stand poised to make significant contributions to the field of oncology, offering new hope and possibilities in the relentless pursuit of conquering cancer.

2 Synthesis methods of tantalum-based nanoparticles

Tantalum-based nanoparticles have emerged as promising candidates for various biomedical applications, including cancer imaging and therapy.[13,23] The synthesis of these nanoparticles encompasses a range of methods, each offering unique advantages and limitations. This section provides an overview of the synthesis methods for tantalum-based nanoparticles, including chemical precipitation, the sol–gel method, and other notable approaches. The advantages, limitations, and considerations associated with each method are discussed, along with recent advancements in synthesis methodologies and their implications for nanoparticle properties.

2.1 Sol–gel method

The sol–gel method is a versatile and widely utilized technique for the synthesis of tantalum-based nanoparticles, offering precise control over nanoparticle properties through a series of controlled chemical reactions.[14,29] In this method, tantalum alkoxide precursors, typically tantalum ethoxide or tantalum isopropoxide, undergo hydrolysis and condensation reactions to form a sol, which is then subjected to subsequent steps of drying and calcination to yield tantalum-based nanoparticles.[30,31]

One of the primary advantages of the sol–gel method lies in its ability to finely tune nanoparticle properties. Through careful control of precursor concentration, solvent composition, and processing conditions, researchers can adjust various parameters to achieve desired nanoparticle characteristics.[32,33] This fine-tuning capability enables precise control over particle size, morphology, and surface characteristics, allowing for the tailoring of nanoparticles to meet specific application requirements.[34,35]

The sol–gel method offers the potential for precise control over particle size, morphology, and surface characteristics. By modulating parameters such as precursor concentration, reaction temperature, and reaction time, researchers can influence

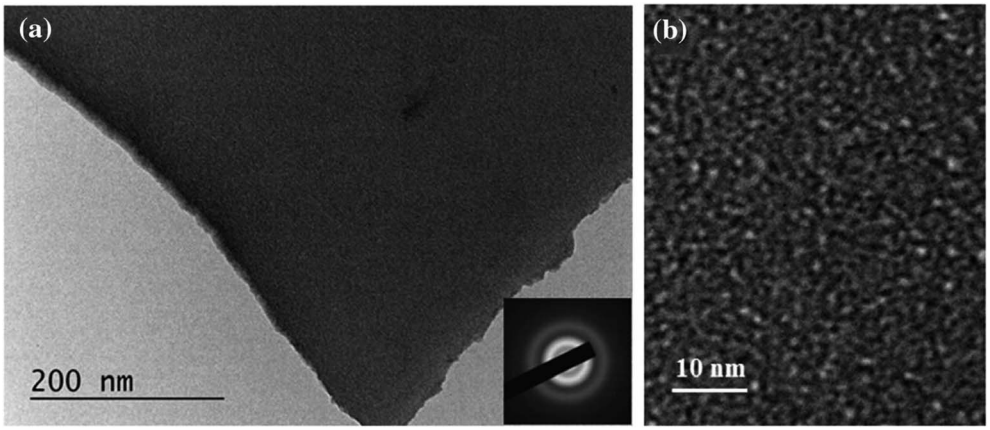

Fig. 1 TEM images and SAED pattern (inset) of dense Ta_2O_5 films at different magnifications (a) 40 000× and (b) 150 000× (Reproduced from ref. 43 with permission from Springer Nature copyright [2024]).

the nucleation and growth of nanoparticles, leading to the formation of uniform and well-defined structures.[36,37] This level of control is particularly valuable in biomedical applications, where the properties of nanoparticles play a crucial role in determining their performance in diagnostics and therapy.

The sol–gel method offers numerous advantages, yet it also has certain limitations. One major challenge is the multi-step process and the intricate chemistry involved, which require careful optimization to consistently obtain desired nanoparticle characteristics.[38] Each stage—hydrolysis, condensation, drying, and calcination—demands precise control over reaction parameters to prevent issues such as particle aggregation or phase impurities. Furthermore, the synthesis process may necessitate specialized equipment and expertise, increasing both complexity and cost.[39,40] When utilizing the sol–gel method for nanoparticle synthesis, several considerations must be taken into account. It is crucial to optimize reaction parameters to achieve reproducible results, which involves meticulous attention to factors such as temperature, pH, and reaction time. The choice of solvents, catalysts, and stabilizing agents can also significantly affect nanoparticle properties, highlighting the necessity for careful planning and systematic optimization throughout the synthesis process.[41,42]

In a nutshell, the sol–gel method represents a powerful approach for the synthesis of tantalum-based nanoparticles with tailored properties for various applications. While it offers advantages such as precise control over nanoparticle characteristics, researchers must navigate challenges such as complex chemistry and specialized equipment requirements. By carefully considering and optimizing reaction parameters, solvents, and catalysts, researchers can harness the full potential of the sol–gel method to develop tantalum-based nanoparticles with enhanced performance and efficacy in cancer treatment and other biomedical applications.

For example, the synthesis of tantalum-based nanoparticles using the sol–gel approach has been explored in recent research efforts, aiming to harness the unique properties of these nanoparticles for various biomedical applications, including cancer imaging and therapy.

In the study conducted by Georgiev *et al.* (2020), the synthesis of tantalum oxide (Ta_2O_5) nanoparticles using the sol–gel technique is detailed, with a focus on tailoring the refractive index for potential applications in optical detection of volatile organic compounds (VOCs).[43] The researchers aimed to introduce mesoporosity into the thin films to modulate their refractive index, employing a soft templating approach utilizing various co-polymers, specifically Pluronics, as structure-directing agents.

The tantalum sol was synthesized from $TaCl_5$ as a precursor and ethanol as a solvent, followed by spin-coating deposition to fabricate the thin films. Subsequent annealing at 320 °C facilitated the formation of the tantalum oxide lattice while decomposing the organic templates, thus introducing the desired mesoporosity. Transmission electron microscopy (TEM) was utilized to investigate the morphology of the films. Dense films exhibited a smooth surface with nanoscale pores, while porous films displayed a more irregular surface with mesoscale pores ranging from 5 to 8 nm (see Fig. 1). The concentration of the organic templates significantly influenced the porosity, with higher concentrations yielding more prominent and uniform pores. Selected area electron diffraction (SAED) confirmed the amorphous status of both dense and porous films, consistent with previous findings in the literature regarding Ta_2O_5 samples. Energy dispersive X-ray spectroscopy (EDX) analysis revealed uniform distribution of tantalum and oxygen across the films, indicating close-to-stoichiometric composition.

Overall, this study demonstrated the successful synthesis of tantalum oxide nanoparticles with tunable refractive index using the sol–gel technique, offering insights into the influence of organic templates on film morphology and porosity (see Fig. 2). These tailored structures hold promise for applications requiring precise optical properties, particularly in VOCs detection, thereby showcasing the versatility and potential of sol–gel synthesized tantalum-based materials.

In a Previous study by Ohishi *et al.* (1992), the growing interest in the sol–gel method for producing dielectric thin films with high dielectric constants has been highlighted.[44] Tantalum oxide (Ta_2O_5) films have emerged as promising

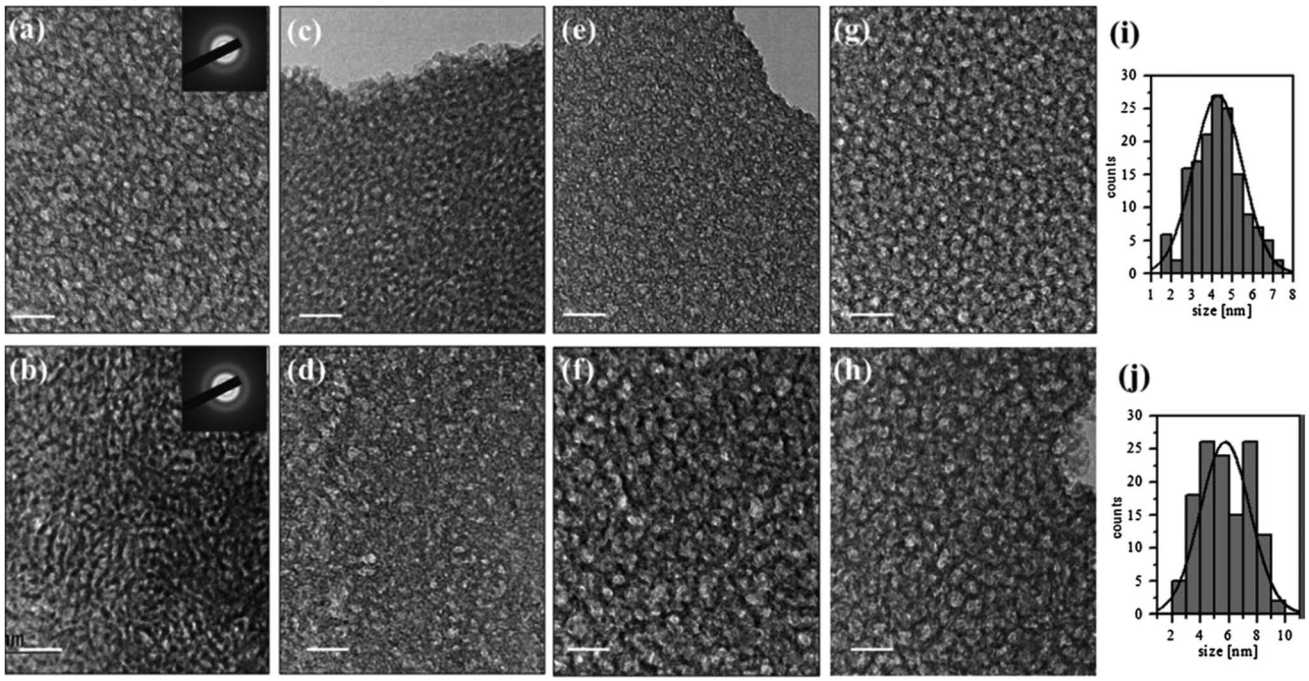

Fig. 2 TEM images of porous Ta_2O_5 films prepared with addition of 5% organic template of copolymers PE6200 (a), PE6400 (c), PE6800 (e) and PE9400 (g) and 20% of PE6200 (b), PE6400 (d), PE6800 (f) and 15% of PE9400 (h); size distribution of the pores of Ta_2O_5 templated with 5% PE9400 (i) and 15% PE9400 (j). (Inset): typical SAED (selected area electron diffraction) pattern. The bar is 20 nm (ref. 43) (Reproduced from ref. 43 with permission from Springer Nature copyright [2024]).

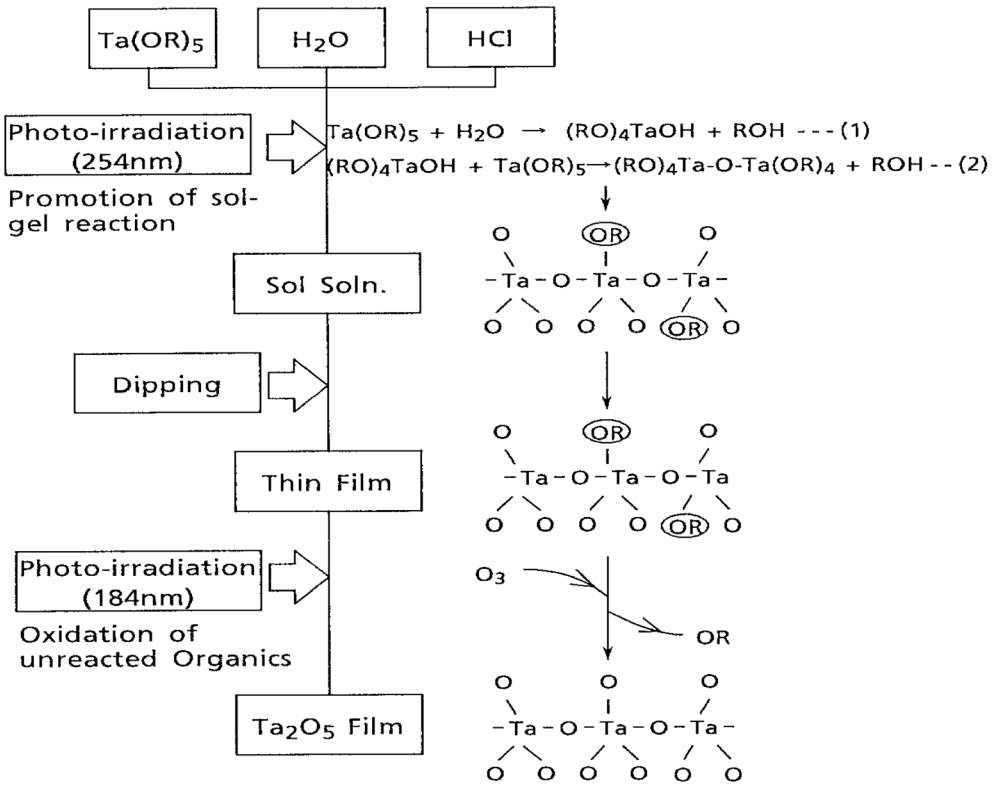

Fig. 3 Synthetic procedure of Ta_2O_5 films prepared by the sol–gel method using photo-irradiation (Reproduced from ref. 44 with permission from Elsevier copyright [2024]).

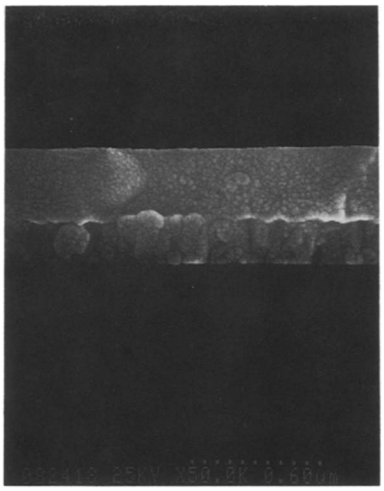

Fig. 4 Cross-section of Ta_2O_5 thin film prepared by the sol–gel method using photo-irradiation (Reproduced from ref. 44 with permission from Elsevier copyright [2024]).

candidates for insulators in various electronic devices such as LSI devices, electroluminescent devices, and film capacitors due to their large dielectric constant.

The paper reported a novel process for fabricating Ta_2O_5 films using a combination of the sol–gel process and photo-irradiation. This method enabled the deposition of thin films on substrate surfaces at low temperatures, expanding the range of feasible fabrication conditions. Remarkably, the electric characteristics of these Ta_2O_5 films closely matched those of films prepared using conventional techniques such as sputtering and chemical vapor deposition.

Fig. 3 illustrated the thin film deposition process on the substrate surfaces, demonstrating the feasibility and practicality of the proposed method. Moreover, Fig. 4 presents a scanning electron microscope (SEM) photograph revealing the cross-section of a Ta_2O_5 film prepared using this innovative process. Notably, the film exhibits a fine structure with uniform thickness, and the presence of minute Au–Pd particles forming a metallic coating for conductivity enhancement is evident. One notable observation is the absence of columnar structures typically found in Ta_2O_5 films prepared by sputtering methods, indicating a distinct advantage of the proposed sol–gel-based approach in achieving more uniform and controlled film morphologies.

Overall, this study highlighted the efficacy of the sol–gel method combined with photo-irradiation for fabricating Ta_2O_5 films with desirable electrical properties and structural characteristics, offering potential advancements in the development of electronic devices requiring high-quality dielectric thin films.

Gül *et al.* (2020) conducted a study focusing on the synthesis and characterization of tantalum oxide (Ta_2O_5) powders *via* the sol–gel method (see Fig. 5) and the investigation of Ta_2O_5 coating ability onto AZ91 Mg alloy surfaces.[45] The research aimed to explore the potential of Ta_2O_5 as a coating material for biomedical applications, considering its excellent corrosion and wear resistance, as well as biocompatibility.

The study involved the preparation of Ta_2O_5 solutions using the sol–gel method, which were subsequently utilized for both powder production and coating processes. AZ91 Mg alloy was chosen as the substrate due to its low density and mechanical properties similar to bone. However, surface treatments were necessary to ensure the alloy's mechanical integrity in biological environments over extended periods. The morphologies of the samples were examined using scanning electron microscopy with energy-dispersive spectroscopy (SEM-EDS) and X-ray diffraction (XRD). Additionally, the study showcased the microstructure of the Ta_2O_5 coatings, highlighting the presence of cracked regions and changes in coating morphology over multiple cycles of coating application (see Fig. 6).

Interestingly, each coating cycle formed coating islands of varying sizes, with larger islands observed in subsequent cycles. This phenomenon was associated with changes in the coating solution content throughout each cycle. Furthermore, the addition of acetic acid to the solution was found to significantly reduce cracks in the coating structure, suggesting its suitability for optimizing the coating morphology. The dried Ta_2O_5 powders were analyzed using combined thermogravimetry-differential thermal analysis (TG-DTA) to characterize their thermal properties. The coating ability of the tantalum oxide layer on the AZ91 Mg alloy surface was thoroughly discussed, emphasizing the importance of adding an optimum amount of deflocculating chemicals to optimize surface morphology.

Overall, the study contributes valuable insights into the sol–gel synthesis of Ta_2O_5 nanoparticles and their potential

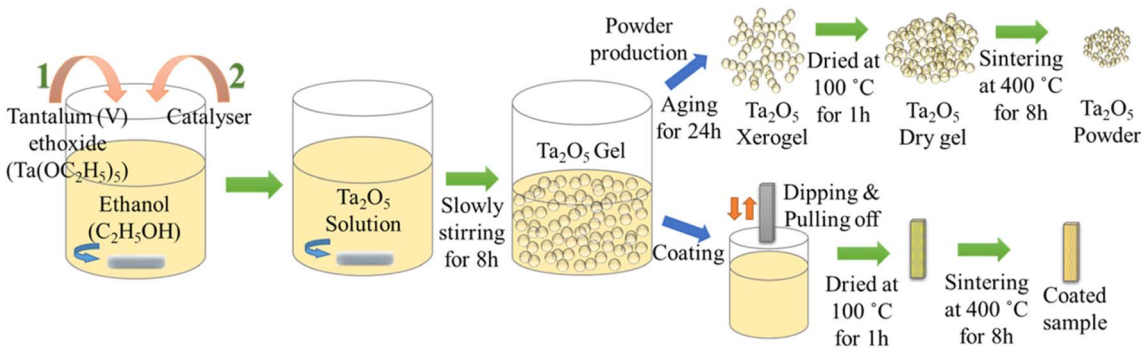

Fig. 5 Preparation of sol–gel solution and the steps for powder producing and coating processes (Reproduced from ref. 45 with permission from Springer Nature copyright [2024]).

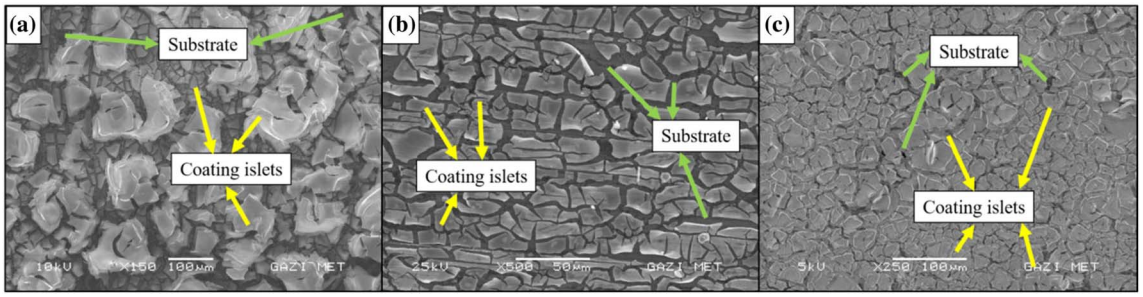

Fig. 6 SEM images of Ta_2O_5-coated AZ91 Mg alloy (a) C_1, (b) C_2, and (c) C_3 (Reproduced from ref. 45 with permission from Springer Nature copyright [2024]).

application as coatings for AZ91 Mg alloy surfaces. The research sheds light on the challenges and considerations associated with optimizing the coating process and highlighted avenues for further refinement in biomedical applications. Further investigation into the optimization of coating parameters and their impact on coating integrity and performance could pave the way for enhanced biomedical applications of Ta_2O_5 coatings.

In addition to the synthesis of tantalum oxide nanoparticles, researchers have explored various tantalum-based nanostructures, including hybrids, doped materials, composites, and coatings on other metals. Examples of these advancements encompass nickel tantalum oxide nanoparticles, tantalum-based photocurable hybrids, tantalum-doped ZnO nanoparticles, tantalum-incorporating silica hybrids, nanocrystalline potassium tantalum oxide, nanocrystalline mixed tantalum–zirconium carbide, tantalum sulfides, among others. These innovative approaches, achieved through the sol–gel technique, have yielded materials with significantly enhanced properties. Such advancements hold promise for a wide range of applications, from electronics to catalysis, owing to their tailored structures and improved performance characteristics. For example, in a study conducted by Liu *et al.* (2018), tantalum carbide (TaC) nanopowders were synthesized *via* a novel method combining the sol–gel and spark plasma sintering (SPS) processes.[46] Tantalum pentachloride ($TaCl_5$) and phenolic resin served as the sources of tantalum (Ta) and carbon (C), respectively, resulting in gels of Ta-containing chelate with good uniformity and high stability.

The synthesis process involved the preparation of gels followed by pyrolysis at 800 °C to obtain carbon-coated tantalum pentoxide (Ta_2O_5) structures. Subsequent heat treatment *via* SPS facilitated the rapid formation of TaC nanoparticles at relatively low temperatures. The study investigated the effects of the C/Ta molar ratio in the raw materials and the heat treatment temperature on the properties of the synthesized powders.

The results revealed that increasing the C/Ta molar ratio from 3.75 to 4.25 led to a decrease in the synthesis temperature, oxygen content, and average crystallite size of the TaC powders. Additionally, varying the heat treatment temperature from 1400 °C to 1600 °C resulted in a reduction of oxygen content, albeit accompanied by an increase in the mean crystallite size from 30 to 100 nm. The SEM images presented in Fig. 7 depicts

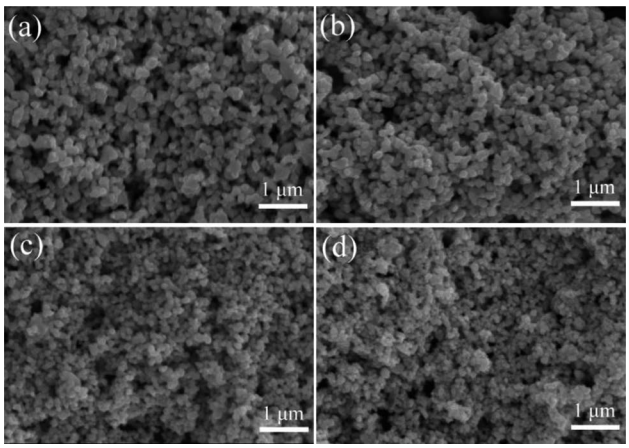

Fig. 7 SEM images of the powders prepared at different C/Ta molar ratios by SPS at 1500 °C for 5 min: (a) C/Ta = 3.75, (b) C/Ta = 4.00, (c) C/Ta = 4.25, (d) C/Ta = 4.50 (Reproduced from ref. 46 with permission from Elsevier copyright [2024]).

the particle size distributions of the powders prepared at different C/Ta molar ratios, showcasing relatively homogeneous distributions with pronounced reductions in particle size as the C/Ta molar ratio increased. This phenomenon may be attributed to the presence of free carbon among crystalline grains, acting as a diffusion barrier to prevent particle growth.

Fig. 8, on the other hand, illustrates FESEM images of powders synthesized at a C/Ta molar ratio of 4.25 at different temperatures. The increase in temperature from 1400 °C to 1600 °C resulted in a visible increase in particle size from 30 to 100 nm, indicating particle growth at elevated temperatures. Notably, TaC powders synthesized at a low C/Ta molar ratio of 4.25 at 1500 °C exhibited an average particle size of approximately 50 nm and a low oxygen content of about 0.43 wt%.

Overall, the sol–gel approach combined with SPS presents a promising method for synthesizing tantalum-based nanoparticles with tailored properties. By systematically exploring the effects of precursor composition and heat treatment conditions, researchers aim to optimize nanoparticle characteristics for enhanced performance in various biomedical applications, including cancer imaging and therapy.

Phani & Santucci (2001) reported the successful synthesis of crack-free, dense, and transparent tetragonal $NiTa_2O_6$ thin films

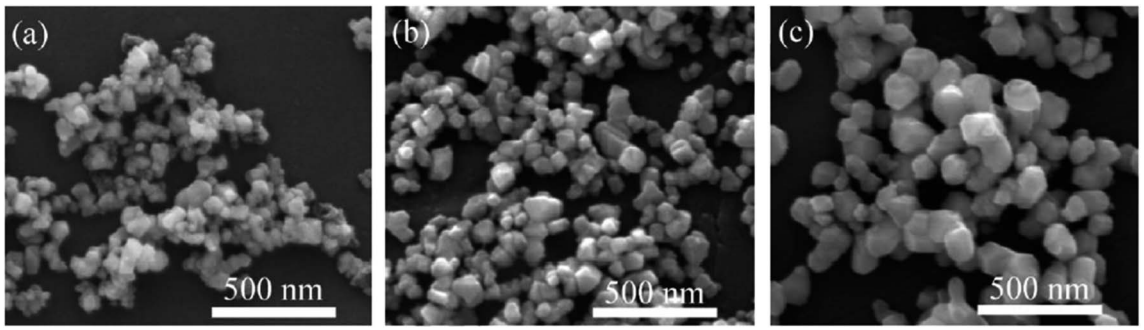

Fig. 8 FESEM images of powders synthesized at the C/Ta molar ratio of 4.25 at different temperatures: (a) 1400 °C, (b) 1500 °C, (c) 1600 °C (Reproduced from ref. 46 with permission from Elsevier copyright [2024]).

using a sol–gel approach.[47] Their study highlighted the formation process of $NiTa_2O_6$ phase, revealing its complete tetragonal structure on silicon substrates at specific annealing temperatures. Structural and morphological evolution of the thin films were thoroughly characterized using grazing incidence X-ray diffraction (GIXRD), tapping mode atomic force microscopy (TMAFM), and X-ray photoelectron spectroscopy (XPS), elucidating the growth mechanism and phase stability. In a similar vein, Phani & Santucci (2007) extended the sol–gel synthesis to produce dense tetragonal $Fe_2Ta_2O_8$ thin films. Their investigation delved into the structural evolution of $Fe_2Ta_2O_8$ phases under varying annealing conditions, shedding light on the formation mechanisms and phase transitions. By employing advanced characterization techniques such as GIXRD and tapping mode atomic force microscopy, they provided valuable insights into the morphological properties and structural stability of the thin films.

Oubaha *et al.* (2011) introduced a novel hybrid organic–inorganic sol–gel material based on tantalum ethoxide and 3-trimethoxysilylpropylmethacrylate, aimed at fabricating optical waveguides and three-dimensional structures.[48] Their study showcased the versatility of sol–gel techniques in photonics applications, demonstrating the successful fabrication of single-mode waveguides and stable three-dimensional woodpile structures. By correlating material composition with optical performance, they highlighted the importance of precise control over material formulation for achieving desired device functionalities. Richard *et al.* (2018) investigated the effects of Ta doping on the crystallinity and electrical properties of ZnO nanoparticles synthesized *via* sol–gel methods.[49] Their study revealed enhanced crystallinity and reduced resistivity in Ta-doped ZnO nanoparticles, indicative of improved electrical conductivity. By combining experimental measurements with first principles calculations, they provided comprehensive insights into the structural and electronic properties induced by Ta doping, offering valuable guidance for optimizing doping strategies in semiconductor materials. In a complementary study, Koshevaya *et al.* (2023) explored the doping of tantalum oxide (Ta_2O_5) nanoparticles with rare earth elements (REEs) to fine-tune their structural, optical, and electrochemical properties.[50] By employing sol–gel and solvothermal synthesis approaches, they obtained tantalum oxide powders with different textures and systematically studied their luminescent properties. Their findings revealed the potential of Ta_2O_5 nanoparticles as wide-spectrum luminescent materials, with tailored luminescence properties achieved through REE doping.

Each study contributes valuable insights into the synthesis, characterization, and potential applications of tantalum-based materials synthesized *via* sol–gel techniques. Phani & Santucci (2007) showcased the synthesis of different tantalum-based oxides, emphasizing phase control and film quality.[47] Oubaha *et al.* (2011) demonstrated the versatility of sol–gel synthesis in photonic applications,[48] while Richard *et al.* (2018) highlighted the doping effects on semiconductor properties.[49] Koshevaya *et al.* (2023) extended the exploration to luminescent properties, offering promising avenues for optoelectronic applications.[50]

In summary, these studies collectively underscored the versatility and significance of sol–gel synthesis in tailoring tantalum-based nanoparticles for various applications, ranging from thin film coatings to photonic devices and luminescent materials. Advanced characterization techniques and theoretical simulations have complemented experimental efforts, providing valuable insights into the structural, morphological, and optical properties of these nanoparticles. Continued research in this field holds promise for further optimizing synthesis parameters and unlocking novel material functionalities for diverse technological applications.

Furthermore, other studies have also synthesized tantalum-based nanoparticles using the sol–gel approach:

Blanc *et al.* (2006) introduced a novel acrylate-modified silica incorporating tantalum synthesized *via* a sol–gel route.[51] By depositing thin films and subsequently photo-polymerizing them through UV irradiation, they demonstrated the fabrication of micron-thick coatings with tunable refractive indices by varying tantalum concentration. These coatings exhibited good transparency in the blue range of the optical spectrum, making them suitable for integrated optics applications. Simonenko *et al.* (2015) explored the synthesis conditions of refractory tantalum-zirconium carbide using a sol–gel method.[52] By controlling synthesis parameters such as temperature and exposure time, they were able to manipulate the phase composition and oxidation resistance of the resulting carbide materials, which is crucial for their performance in high-temperature applications. Zhou *et al.* (2014) investigated non-

hydrolytic sol–gel synthesis for the preparation of tantalum sulfide (TaS_2) materials.[53] By reacting tantalum halides with thio-ethers, they demonstrated the direct synthesis of crystalline TaS_2 at low temperatures, offering a promising alternative to traditional high-temperature methods. This approach allowed for the tuning of crystallite sizes and the selective preparation of different TaS_2 modifications, expanding the range of tantalum sulfide materials accessible *via* sol–gel synthesis.

Çelikbıçak *et al.* (2013) developed a tantalum-based sol–gel material for the selective enrichment of phosphopeptides from complex biological samples.[54] By incorporating polyethylene glycol (PEG) into the sol–gel structure, they improved the material's chemical and physical properties, enhancing its performance in phosphopeptide enrichment compared to conventional tantalum oxide materials. This study demonstrated the potential of sol–gel-derived materials for bioanalytical applications, highlighting their versatility beyond traditional material synthesis. Rechberger *et al.* (2017) demonstrated the synthesis of amorphous indium tantalate nanoparticles *via* a non-aqueous sol–gel method, followed by annealing to produce crystalline nanoparticles and assembly into aerogel monoliths.[55] These nanoparticle-based aerogels exhibited high surface areas and mechanical stability, making them promising candidates for photocatalytic applications. However, the degradation of methylene blue showed limited success, indicating the need for further optimization of their photocatalytic properties.

Overall, these studies illustrate the versatility and potential of sol–gel synthesis for the preparation of tantalum-based materials with tailored properties for various applications, ranging from optics to catalysis and biotechnology. Further research in this field holds promise for the development of advanced materials with enhanced performance and functionality.

2.2 Hydrothermal/solvothermal synthesis

The synthesis of tantalum-based nanoparticles through hydrothermal or solvothermal methods stands at the forefront of nanomaterial research, offering unparalleled control over the fabrication process and resulting properties.[56,57] In hydrothermal synthesis, aqueous solutions serve as the reaction medium, allowing for the precise manipulation of reaction conditions such as temperature, pressure, and pH. Conversely, solvothermal methods utilize organic solvents, offering flexibility in tuning reaction parameters to achieve desired nanoparticle characteristics.[58]

These synthesis routes enable the creation of tantalum-based nanoparticles with tailored sizes, shapes, and compositions, which are crucial for optimizing their performance in diverse applications. For instance, in catalysis, the morphology and surface structure of nanoparticles play a pivotal role in catalytic activity and selectivity.[56] Similarly, in energy storage systems such as batteries and supercapacitors, nanoparticle size and morphology significantly impact charge storage capacity and cycling stability. Moreover, tantalum-based nanoparticles synthesized *via* hydrothermal or solvothermal routes exhibit promising potential in biomedical applications, including drug delivery, bioimaging, and tissue engineering.[57] The ability to finely tune nanoparticle properties ensures compatibility with biological systems while maximizing therapeutic efficacy.[58]

By further exploring and refining hydrothermal and solvothermal synthesis techniques, researchers can unlock new opportunities for advancing tantalum-based nanomaterials. Continued efforts in this area hold the potential to revolutionize various industries, addressing critical challenges and driving innovation in fields ranging from catalysis to biomedicine.

For example, Kominami *et al.* (2001) explored the synthesis of tantalum(v) oxide (Ta_2O_5) powders through solvothermal reactions and subsequent evaluation of their photocatalytic properties.[59] The authors synthesized Ta powders *via* a solvothermal reaction of tantalum pentabutoxide (TPB) in toluene at varying temperatures (473–573 K) in the presence of water.

At lower temperatures (473 and 523 K), they obtained Ta powder with a large surface area, characterized by X-ray diffraction (XRD) patterns showing no clear peaks of crystallites, indicative of amorphous structure. However, at 573 K, crystalline b-phase Ta was obtained. Moreover, post-calcination of the amorphous Ta at 973 K induced crystallization into the b-phase, suggesting a structural transformation under high temperature.

The authors then investigated the photocatalytic production of hydrogen from 2-propanol in aqueous solution using these Ta particles. Interestingly, they found that the as-synthesized amorphous and crystalline b-phase samples exhibited negligible rates of hydrogen evolution, while crystalline b-phase samples formed by post-calcination showed higher activity. This observation underscores the influence of crystallinity on the photocatalytic activity of Ta_2O_5. Furthermore, the authors explored the photocatalytic decomposition of organic compounds by mineralization of acetic acid under aerated conditions. They observed that solvothermal Ta exhibited a higher rate of formation compared to other Ta samples, indicating the importance of synthesis method in dictating photocatalytic performance.

In addition, the study delves into the role of water in the crystallization process, highlighting its significance in the formation of crystalline b-phase Ta. The authors found that the presence of water, fed into the autoclave and dissolved in toluene during the process, played a crucial role in the crystallization of amorphous Ta into the desired phase. Moreover, the authors examined the crystal growth behaviour, observing predominant growth along the (001) crystal plane in the solvothermal process, which was further enhanced with prolonged reaction time. Fig. 9a and b presented TEM photographs of Ta-1 and Ta-4, respectively, depicting agglomerates of very small particles. These images provide visual insight into the morphology of the synthesized Ta particles, underscoring the effectiveness of the solvothermal method in producing fine particles.

Generally, Kominami *et al.* (2001) presented a comprehensive investigation into the synthesis and photocatalytic activity

of Ta_2O_5 powders, shedding light on the influence of synthesis parameters and crystallinity on their performance.[59] Their findings contribute to the understanding of photocatalytic materials and may have implications in various environmental and energy-related applications.

Gömpel *et al.* (2014) study investigated the synthesis of alkali metal tantalates using hydrothermal methods, revealing the pH-dependent changes in nanoparticle morphology.[60] The authors demonstrated the synthesis of nanosized Ta_2O_5 rods and $MTaO_3$ cubes (M = Na, K, Rb) under varying pH conditions, revealing distinct morphological transformations (see Fig. 10). Notably, acidic conditions (pH 3 and 4) led to the formation of Ta_2O_5 nanoparticles, characterized by a mixture of small needles and agglomerates. Conversely, near-neutral pH values (7 and 8) yielded rod-shaped nanoparticles with improved dispersity and minimal agglomeration. At higher pH values (12 and 13), cube-shaped nanoparticles were synthesized, highlighting the pH-dependent morphological evolution facilitated by hydrothermal synthesis.

The TEM images provided visual evidence of the synthesized nanoparticles' morphologies, with distinct shapes observed under different pH conditions. Nanorods, cubes, and parallelepipeds were obtained depending on the pH of the reaction medium, underscoring the versatility of hydrothermal synthesis in tailoring nanoparticle morphology (see Fig. 11). Additionally, the influence of base cations (Na, K, Rb) on nanoparticle shape and size distribution was elucidated, with potassium and rubidium hydroxides yielding cubic nanoparticles with slightly broader size distributions compared to sodium hydroxide.

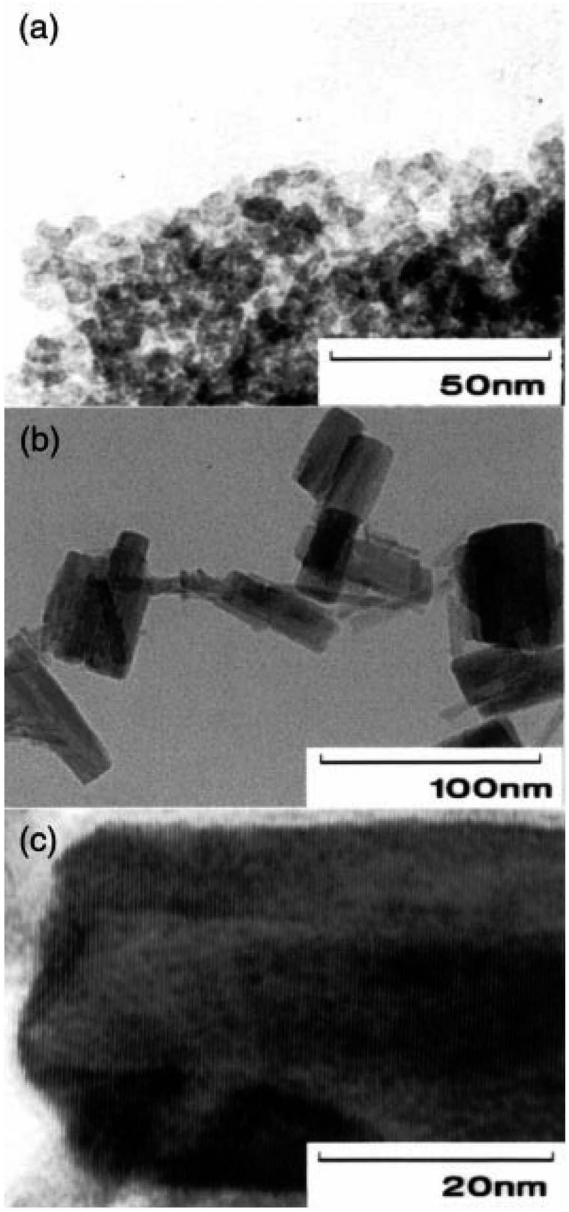

Fig. 9 TEM photographs of Ta-1 (a) and Ta-4 (b and c) (Reproduced from ref. 59 with permission from Royal Society of Chemistry copyright [2024]).

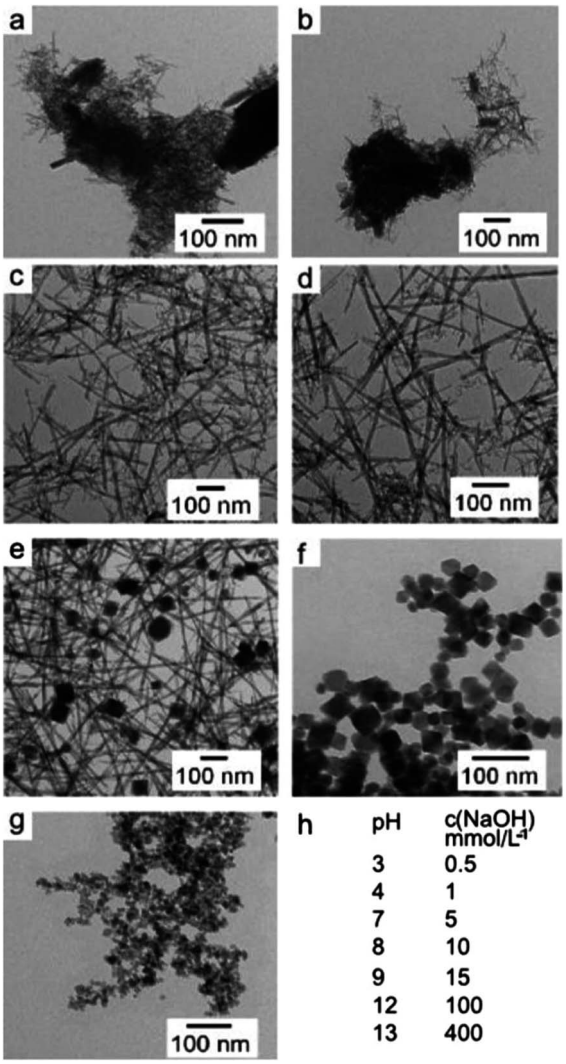

Fig. 10 Displays transmission electron microscopy (TEM) images (a–g) depicting tantalum oxide nanoparticles at various pH levels: (a) pH 3, (b) pH 4, (c) pH 7, (d) pH 8, (e) pH 9, (f) pH 12, and (g) pH 13. Additionally, (h) presents the pH values of the reaction mixtures prior to hydrothermal treatment, as determined by NaOH concentration (Reproduced from ref. 60 with permission from Royal Society of Chemistry copyright [2024]).

Furthermore, X-ray diffraction analysis revealed the crystalline phases present in the synthesized nanoparticles, confirming the formation of Ta_2O_5 at acidic pH values and defect-pyrochlore-type tantalic acid ($HTaO_3$) at higher pH values. The crystallinity and composition of the synthesized nanoparticles were found to be pH-dependent, with variations observed in crystallite size and phase composition. Despite challenges in resolving the exact crystal structure and composition of the synthesized nanoparticles, the study provided valuable insights into the role of pH in controlling nanoparticle morphology and composition.

In a nutshell, Gömpel *et al.* (2014) investigation highlighted the utility of hydrothermal synthesis in synthesizing alkali metal tantalates with tunable morphologies, offering opportunities for tailored applications in photocatalysis and materials science.[60] The pH-dependent synthesis approach provides a versatile platform for engineering tantalum oxide and tantalate nanoparticles with desired properties, paving the way for further exploration in diverse fields requiring nanomaterials with controlled morphology and composition.

In the study by Das & Ganguli (2013), tantalum-based oxide nanoparticles were synthesized using a template-free hydrothermal method under optimal alkaline conditions and suitable temperature.[61] The synthesized nanocubes of cadmium tantalate and cadmium niobate showed significantly higher photocatalytic activity compared to the same oxides obtained by the solid-state method. The hydrothermal synthesis was carried out at a much lower temperature (600 °C) than the solid-state method (1000 °C), resulting in the evolution of nanocubes with an edge size of approximately 15 nm. The X-ray diffraction (XRD) patterns of the synthesized nanoparticles indicated the formation of pure phases of $Cd_2Ta_2O_7$ and $Cd_2Nb_2O_7$, and the average crystallite size was found to be 20 nm and 25 nm, respectively. The pure phases of $Cd_2Ta_2O_7$ and $Cd_2Nb_2O_7$ were stabilized in the cubic phase at high alkali content. The role of alkali concentration, reaction time, and temperature in the synthesis process was thoroughly investigated to optimize the formation of monophasic cadmium tantalate and cadmium niobate phases.

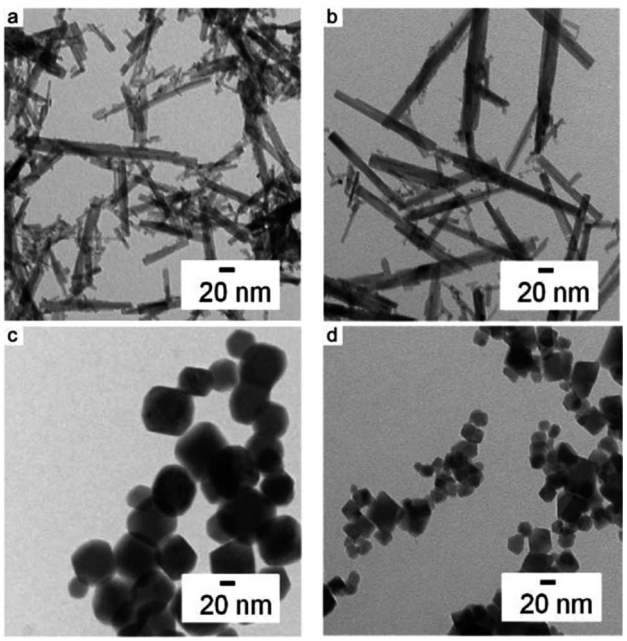

Fig. 11 TEM images of the nanoparticles yielded with different bases at different pH values. (a) pH 7 with KOH, (b) pH 7 with RbOH as the precursor base and (c) KOH and (d) RbOH as precursor bases both at pH 12 (Reproduced from ref. 60 with permission from Royal Society of Chemistry copyright [2024]).

The study also included the refinement of the crystallographic parameters of the synthesized nanoparticles using the Rietveld method, indicating a good quality fit. It was observed that the presence of alkaline hydroxylated Ta–Cl ionic groups under strongly alkaline conditions played a key role in stabilizing the phases of $Cd_2Ta_2O_7$ and $Cd_2Nb_2O_7$. The hydrothermal method conducted at 180 °C for 48 hours, followed by calcination at 600 °C for 8 hours, yielded nanocubes of $Cd_2Ta_2O_7$ and $Cd_2Nb_2O_7$ with sizes ranging from 15 to 30 nm. This method resulted in a larger specific surface area compared to solid-state synthesis, which is crucial for enhancing the photocatalytic efficiency of the nanoparticles. Furthermore, the optical properties and specific surface area of the synthesized nanocubes were investigated, demonstrating their potential for improved photocatalytic activity. In summary, the study successfully optimized the reaction parameters, leading to the formation of smaller-sized nanoparticles with increased specific surface area and improved photocatalytic performance.

The synthesis of tantalum pentoxide (Ta_2O_5) nanorods was carried out by Li *et al.* (2015) using hydrothermal methods with polyethylene glycol (PEG) as a guiding agent.[62] The resulting nanorods were extensively characterized using various techniques, including X-ray diffraction (XRD), scanning electron microscopy (SEM), transmission electron microscopy (TEM), as well as diffuse reflectance ultraviolet-visible (UV-vis) and photoluminescence spectroscopies. The study also investigated the effects of crystallization duration and the $Ta_2O_5/Sr(OH)_2$ ratio on the morphology of the synthesized nanoparticles and proposed a growth mechanism.

The presence of PEG and $Sr(OH)_2$ during the hydrothermal synthesis significantly affected the morphology of the resulting $Sr(OH)_2$ nanostructures. In the absence of PEG, irregular nanoparticles of varying sizes were formed, indicating the further growth of Ta_2O_5 during the hydrothermal treatment in the $Sr(OH)_2$ solution. Conversely, when both $Sr(OH)_2$ and PEG were present, homogeneous nanorods with controlled morphology were obtained. The X-ray diffraction patterns of the products revealed that phase-pure Ta_2O_5 was obtained under specific hydrothermal conditions, and the presence of $Sr(OH)_2$ also influenced the crystal phase of the product. Additionally, the UV-vis diffuse reflectance spectra showed that all samples exhibited similar UV absorption edges with negligible shifts, indicating that the Ta_2O_5 products were n-type semiconductors and potentially photocatalytically active under UV irradiation. The study also explored the effects of crystallization duration and the $Ta_2O_5/Sr(OH)_2$ ratio on product morphology, finding that the crystallization duration significantly influenced the morphology, resulting in Ta_2O_5 nanoparticles with different

length-to-diameter ratios. The $Ta_2O_5/Sr(OH)_2$ ratio also affected the morphology and crystal phase of the product, with nanoparticles of mixed phases obtained at certain ratios.

The growth mechanism of Ta_2O_5 nanorods was proposed based on the findings, indicating that polyethylene glycol (PEG) played a crucial role in controlling the nucleation and growth of the nanorods. The proposed mechanism involved the dissolution and hydroxylation of Ta_2O_5 in the presence of $Sr(OH)_2$ under hydrothermal conditions, with PEG adsorbing onto the resulting intermediates and favoring the formation of elongated nuclei, thus leading to the formation of one-dimensional (1D) nanorods. Overall, the study provided valuable insights into the hydrothermal synthesis of Ta_2O_5 nanorods and the factors influencing their morphology, crystal phase, and growth mechanism.

Hsieh *et al.* (2014) conducted an extensive study on the hydrothermal synthesis of tantalum-based pyrochlore nanoparticles combined with indium hydroxide, resulting in nanocomposites with remarkable photocatalytic properties under UV light.[63] The synthesis involved reacting tantalum sources with indium salts under high-temperature aqueous conditions, producing well-defined nanoparticles with distinct morphological and compositional characteristics. Scanning electron microscopy (SEM) analysis revealed that the samples primarily consisted of 30–40 nm octahedral-shaped nanoparticles, alongside a few larger particles (400–700 nm) identified as indium hydroxide ($In(OH)_3$). Transmission electron microscopy (TEM) further confirmed the single-crystalline nature of these nanoparticles, displaying clear lattice fringes corresponding to the (111) planes of pyrochlore. Additionally, dispersed clusters of $In(OH)_3$ were observed on the nanoparticles.

Inductively coupled plasma mass spectrometry (ICP-MS) indicated that the nanoparticles underwent extensive potassium/proton exchange during acid treatment, resulting in different K/In/Ta ratios before and after treatment. The structural analysis revealed that the nanoparticles possessed a defect pyrochlore structure ($A_2B_2O_6$) rather than an ideal pyrochlore structure ($A_2B_2O_7$), with TEM images showing non-uniform contrast indicative of extensive defects. Thermal gravimetric analysis (TGA) and proton nuclear magnetic resonance (^1H NMR) confirmed the presence of crystallization water and exchanged protons, respectively. The compositional analysis suggested that higher hydrothermal temperatures resulted in materials with more indium and fewer potassium, highlighting the influence of temperature on defect concentration and stoichiometry.

The synthesized nanocomposites displayed exceptional photocatalytic properties, absorbing UV light with main absorption edges around 270 nm, corresponding to band gaps of 4.6–4.8 eV. Among the samples, the acid-treated TIM-190-A exhibited the highest hydrogen (H_2) evolution rate of 5.82 mmol g^{-1} h^{-1} from a 10 vol% methanol aqueous solution, significantly outperforming the benchmark sodium tantalate ($NaTaO_3$). In terms of overall water splitting, TIM-190-A achieved a remarkable H_2 evolution rate of 357.7 mmol g^{-1} h^{-1}, more than twenty times higher than $NaTaO_3$. These results underscored the superior photocatalytic efficiency of the tantalum-based pyrochlore nanoparticles.

When compared to other photocatalysts like Degussa P25 TiO_2, Ta_2O_5, and NiO-loaded $SrTiO_3$, TIM-190-A demonstrated exceptional performance, with the H_2 evolution rates of these benchmarks being significantly lower. Moreover, the catalysts maintained their activity and structural integrity throughout prolonged photocatalytic reactions, consistently producing stoichiometric amounts of H_2 (or CO) and O_2, which highlighted their stability. This study by Hsieh *et al.* (2014) showcases the potential of tantalum-based pyrochlore nanoparticles for sustainable energy applications, emphasizing the effectiveness of defect engineering and precise compositional control in enhancing photocatalytic performance.[63]

In another study, Rafique *et al.* (2019) developed hydrophilic $NaYF_4$: Yb^{3+}/Er^{3+} nanoparticles (NPs) through a straightforward hydrothermal method, yielding lanthanide-doped upconversion (UC) materials with varied morphologies and crystal phases.[64] The synthesis parameters, including reactant concentrations, NaF concentrations, and reaction times, were meticulously optimized to influence the size, shape, and crystalline phase of the UCNPs. Scanning electron microscopy (SEM) revealed that adjusting the NaF concentration had a notable effect on the nanoparticle morphology. For instance, spherical nanoparticles were produced at a 1.0 M NaF concentration, with sizes ranging from 69.83 to 76.70 nm as the NaF volume increased from 7.5 to 9.0 mL. Conversely, decreasing NaF concentration to 0.5 M resulted in aggregated, irregular shapes, while increasing NaF volume to 9.0 mL led to more regular spheres of 67.93 nm size. These findings indicate that NaF concentration is critical in determining nanoparticle shape and size.

Further experiments at higher reactant concentrations (0.2 M) demonstrated that smaller, uniformly shaped nanoparticles (52.77 nm) could be synthesized with 1.0 M NaF and 7.5 mL volume. Increasing NaF volume to 9.0 mL, however, produced larger, less homogeneous nanoparticles (87.97 nm). The formation of fine, bitter gourd-shaped nanoparticles was observed at 0.25 M NaF and 7.5 mL volume, with significant variations in length and width when the NaF volume was increased. X-ray diffraction (XRD) analysis showed that the NaF content significantly influenced the crystalline phase of the nanoparticles, with different NaF concentrations resulting in various phases, such as α-$NaYF_4$, β-$NaYF_4$, and YF_3. This phase variation correlated with changes in nanoparticle shape and suggested that phase transitions contribute to structural defects.

Further experiments explored the impact of hydrothermal reaction time and dopant ion concentrations on nanoparticle size, homogeneity, and crystalline phase. SEM images and XRD patterns indicated that reaction times and increased Er^{3+} concentrations significantly influenced particle size and phase transitions from cubic to hexagonal phases, with longer reaction times yielding larger particles with enhanced hexagonal phase intensity.

In summary, the study by Rafique *et al.* (2019) demonstrated that careful optimization of synthesis parameters, such as

reactant and NaF concentrations and reaction time, can effectively control the morphology and crystalline phase of $NaYF_4$: Yb^{3+}/Er^{3+} upconversion nanoparticles. The ability to tailor these properties makes these UCNPs promising candidates for various applications requiring precise control over nanoparticle characteristics.

2.3 Synthesis of tantalum-based nanoparticles *via* magnetron sputtering approach

The synthesis of tantalum-based nanoparticles *via* the magnetron sputtering approach presents a sophisticated and scalable method to produce high-quality nanoparticles with controlled size, composition, and morphology.[65,66] Magnetron sputtering is a type of physical vapor deposition technique that relies on the ejection of atoms from a target material, in this case, tantalum, due to the impact of energetic ions generated from an argon plasma.[67] This method is favoured for its ability to produce uniform and pure nanoparticles, which are essential for a range of advanced applications.[68]

In magnetron sputtering, a high-purity tantalum target is utilized. The process can be carried out using either direct current (DC) or radio frequency (RF) magnetron sputtering, with RF sputtering being particularly advantageous for insulating targets or when precise control over the deposition process is required.[69,70] The choice of sputtering gas, typically argon, is critical due to its inert nature and appropriate atomic mass, which ensures effective momentum transfer during the collision process.[71,72] The pressure of the sputtering gas, generally maintained between 1 to 10 mTorr, significantly influences the mean free path of the sputtered atoms and the overall deposition rate.[73]

The power applied to the magnetron is another crucial parameter that affects the ion energy and sputtering rate. Higher power levels can enhance the deposition rate but may also lead to increased substrate heating, which needs to be carefully controlled.[74,75] Substrate temperature plays a vital role in determining the nucleation and growth kinetics of the nanoparticles. By adjusting the substrate temperature, researchers can tailor the physical properties of the nanoparticles to meet specific requirements.[76]

The synthesis process begins with the preparation of the tantalum target, ensuring it is free from surface contaminants. The sputtering chamber is evacuated to a base pressure of around 10^{-7} torr to minimize impurities.[77,78] Once the chamber is sufficiently evacuated, argon gas is introduced, and a plasma is ignited by applying a voltage to the magnetron. The unique magnetic field configuration of the magnetron traps electrons near the target surface, maintaining a high-density plasma that efficiently sputters tantalum atoms from the target.[79] These atoms travel through the chamber and condense into nanoparticles. The size and distribution of the resulting nanoparticles can be finely controlled by adjusting the sputtering parameters, such as gas pressure, power, and substrate conditions.[78] The nanoparticles can be deposited directly onto a substrate or collected in a liquid medium, depending on the intended application. Future research aims to optimize the synthesis parameters to tailor the properties of tantalum-based nanoparticles for specific applications, explore the potential of hybrid nanostructures, and scale up the production process for industrial use.[78] The magnetron sputtering approach thus offers a promising pathway for the synthesis of high-performance tantalum-based nanoparticles with diverse and impactful applications.[76]

For example, the synthesis of tantalum oxynitride (TaO_xN_y) thin films is crucial for various applications due to their unique optical and electronic properties. In a study by Lertvanithphol *et al.* (2019), the films were synthesized using a magnetron sputtering system with two different techniques: conventional reactive sputtering and reactive gas-timing (RGT).[68] The conventional reactive sputtering technique involves the simultaneous introduction of reactive gases, oxygen and nitrogen, during the sputtering process of a tantalum target. This steady method results in the formation of TaO_xN_y films with properties closely resembling those of tantalum oxide (TaO), primarily due to the consistent incorporation of oxygen and nitrogen.

On the other hand, the reactive gas-timing (RGT) technique alternates the introduction of oxygen and nitrogen gases during sputtering. This alternation enhances nitrogen incorporation by closing the oxygen supply and immediately switching to nitrogen. The RGT method allows the sputtered atoms to maintain relatively high particle energies, reducing collisions and enabling a higher nitrogen concentration. Consequently, this leads to variations in the optical properties of the films, as the nitrogen concentration can be effectively controlled by adjusting the timing of gas introduction.

Spectroscopic ellipsometry (SE) was employed to measure the optical properties of the films over the range of 0.75–5.0 eV at a 70° incident angle. The optical model based on the Tauc–Lorentz function was constructed to extract the properties of the films, revealing homogeneous growth with distinct optical characteristics depending on the deposition technique. Field-emission scanning electron microscopy (FE-SEM) confirmed the homogeneous growth and structural consistency of the films with the proposed model (Fig. 12). Furthermore, glazing-incident X-ray diffraction (GI-XRD) analysis showed that all the films were completely amorphous, consistent with the high binding energy of tantalum atoms, which prevents crystallization without substrate heating or bias.

X-ray photoelectron spectroscopy (XPS) was used to analyze the elemental composition and chemical states within the films. The results indicated a higher nitrogen content in the films synthesized using the RGT method, as evidenced by a significant N 1s peak at 396 eV, which was absent in the films produced by conventional sputtering. This confirmed that the RGT technique successfully incorporated nitrogen into the oxynitride films. The N K-edge X-ray absorption spectroscopy (XAS) measured in total fluorescence yield (TFY) mode further elucidated the nitrogen chemical states, showing a single peak at 400.6–400.9 eV in RGT films, which suggested effective nitrogen incorporation and hybridization with tantalum and oxygen.

The optical properties of the films, including the refractive index and extinction coefficient, were significantly influenced

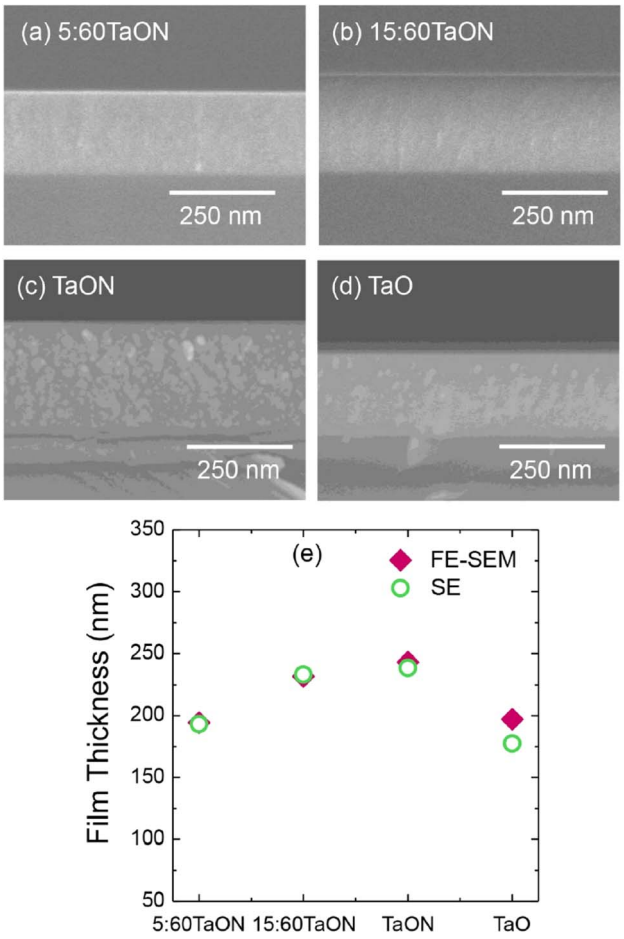

Fig. 12 (a–d). FE-SEM in cross-sectional view film morphologies of the prepared samples. (e) The film thicknesses obtained from both techniques (Reproduced from ref. 68 with permission from Elsevier copyright [2024]).

by the deposition technique. Films produced by the RGT method exhibited higher refractive indices and extinction coefficients compared to those made by conventional sputtering, indicating enhanced optical density and absorption. The optical band gap (E_g) of the films was determined using Tauc plots, revealing that RGT films had lower band gaps (2.17 eV for 5 : 60 timing, 2.88 eV for 15 : 60 timing) compared to the conventional films (4.21 eV). This tunability of the band gap through oxygen timing highlighted the versatility of the RGT method in modifying film properties.

The study demonstrated the superior ability of the RGT method to control nitrogen incorporation, resulting in films with higher refractive indices and lower band gaps, which are beneficial for various optoelectronic applications. The findings align with previous research showing that nitrogen content significantly affects the optical properties of TaO_xN_y films. However, the RGT technique offers a more efficient approach to nitrogen incorporation compared to other advanced sputtering methods, such as high-power impulse magnetron sputtering (HiPIMS).

The study by Lertvanithphol *et al.* (2019) effectively illustrated the synthesis of tantalum oxynitride thin films using magnetron sputtering, comparing conventional reactive sputtering and the innovative reactive gas-timing technique.[68] The results emphasize RGT's superior ability to tune optical properties by controlling nitrogen incorporation, providing valuable insights for designing advanced materials for optoelectronic applications. Future research could further optimize gas timing parameters and explore the use of other reactive gases to enhance the material's potential applications.

Baker *et al.* (2022) successfully synthesized tantalum suboxide nanoparticles using reactive direct-current (DC) magnetron sputtering.[80] The composition of the films was controlled kinetically by varying chamber pressure and deposition rate, maintaining a constant Ar-5%O_2 gas mixture. The resulting films had oxygen contents from 46% to 71%, achieving stoichiometric Ta_2O_5 at higher oxygen levels.

The synthesized films were X-ray amorphous, indicating a lack of crystallinity, and SEM analysis confirmed smooth, uniform surfaces. Electrical resistivity varied over seven orders of magnitude, with a sharp transition at 55% oxygen content: lower oxygen films exhibited metallic conduction, while higher oxygen films showed semiconducting behaviour due to activated tunnelling. The mass density of the films decreased with increasing oxygen content, attributed to the lower density of tantalum oxide and the presence of porosity in higher oxygen content films.

Temperature-dependent measurements and Hall effect data revealed a significant drop in carrier density with increasing oxygen content, especially at low temperatures, indicating a transition from metallic to insulating behaviour. Overall, the study demonstrated precise control over the synthesis and properties of tantalum suboxide nanoparticles, making them suitable for advanced applications like hohlraums in magnetized inertial confinement fusion.

Cristea *et al.* (2021) explored the synthesis of tantalum-titanium oxynitride (TaTiON) thin films through DC reactive magnetron co-sputtering.[81] The synthesis was carefully controlled by varying the Ti and Ta target currents, which ranged between 0.00 and 1.00 A, while maintaining a constant sum of 1.00 A for the two currents. The deposition was performed under a −50 V bias voltage at a substrate temperature of 100 °C, with a reactive gas flow consisting of nitrogen and oxygen in a constant N_2/O_2 ratio of 85%/15%.

The structure and properties of the resulting films were found to depend significantly on the elemental composition. Single metal oxynitrides (TaON and TiON) exhibited a low degree of crystallinity, while the co-sputtered films were predominantly amorphous. The TaON film demonstrated the highest hardness (14.8 GPa), whereas the TiON film had a significantly lower hardness (8.8 GPa). Co-sputtered films showed intermediate hardness values. The oxygen content in the films increased notably when the Ti concentration exceeded that of Ta, influencing both the optical and electrical properties. The sheet resistivity of the co-sputtered films was strongly dependent on the O/(Ta + Ti) atomic ratio.

Further structural analysis using grazing incidence XRD revealed that the single-metal oxynitrides (TaON and TiON) had certain degrees of crystallinity, whereas co-sputtered films were

amorphous. The presence of characteristic diffraction peaks suggested that the TaON film was polycrystalline, forming face-centered cubic (fcc) TaN, likely doped with some oxygen. Conversely, the TiON film displayed peaks corresponding to the rutile phase of TiO2_22, indicating a predominance of oxide formation over nitride, due to the higher O/Ti ratio compared to N/Ti.

Mechanical property analysis showed a variation in indentation hardness and elastic modulus depending on the applied target currents. Hardness values ranged from ~7 GPa to ~15 GPa, and the indentation elastic modulus ranged from ~70 GPa to ~220 GPa. These properties were linked to the oxygen content promoted by higher Ti target currents. Additionally, coatings with high hardness and low elastic modulus exhibited improved fracture toughness, as indicated by higher H/E and H3/E2 ratios.

Adhesion and wear behaviour were evaluated through scratch and tribometer tests. Films with higher Ta content, particularly the TaON film, demonstrated better adhesion and higher critical loads for delamination. Interestingly, the TiON film, despite its lower thickness, showed adequate wear resistance, attributed to its ductility and amorphous nature. The study highlighted the potential of tailoring the composition and structure of TaTiON films to achieve desired mechanical and electrical properties for various applications.

Furthermore, Singh *et al.* (2014),[66] Beline *et al.* (2019),[82] Baker *et al.* (2022),[80] and Rudolph *et al.* (2017)[83] have conducted comprehensive studies on the synthesis of tantalum-based nanoparticles (TaNPs) using a magnetron sputtering approach, each contributing unique insights to the field.

Singh *et al.* (2014) meticulously explored a gas-aggregated magnetron sputtering system, beginning with the sputtering of tantalum atoms from a target that aggregate into nanoparticles within the gas phase.[66] These size-selected, amorphous nanoparticles are then deposited onto a substrate, initially forming a monolayer. As deposition continues, multi-layered structures form through nanoparticle coalescence. Upon exposure to ambient air, the tantalum-based nanoparticles oxidize, resulting in a core–shell structure with a metallic tantalum core and a tantalum oxide shell. The metallic core is approximately 3 nm in diameter, surrounded by a 2 nm thick oxide shell. High-angle annular dark-field scanning transmission electron microscopy (HAADF-STEM) and grazing incidence X-ray diffraction (GIXRD) confirm the amorphous nature of the films. Additionally, atomic force microscopy (AFM) and scanning electron microscopy (SEM) reveal a highly porous structure, with surface roughness increasing upon oxidation. X-ray photoelectron spectroscopy (XPS) analysis demonstrates a graded oxidation profile from tantalum pentoxide (Ta_2O_5) at the surface to metallic tantalum deeper within, providing a gradation in oxidation states advantageous for specific applications.

Building on these findings, Beline *et al.* (2019) refined the deposition parameters of magnetron sputtering to synthesize tantalum oxide (Ta_xO_y) films on commercially pure titanium (cpTi).[82] They systematically evaluated the structural and optical properties, morphology, roughness, elemental composition, and surface energy of these films. By varying the oxygen flow rates and other deposition parameters, they produced Ta_xO_y films with differing thicknesses and structures, ranging from amorphous to crystalline (specifically the β-Ta_2O_5 phase). Optical analysis revealed regular and large-amplitude interference oscillations, indicating that the films had high optical homogeneity.

The crystalline β-Ta_2O_5 coatings, in particular, exhibited increased roughness and surface energy, which positively influenced pre-osteoblastic cell spreading and morphology. These coatings demonstrated biocompatibility, making them suitable for biomedical applications. Importantly, compared to cpTi, the tantalum oxide films did not increase bacterial adhesion, further underscoring their potential utility in medical devices where both biocompatibility and resistance to bacterial colonization are crucial.

In a related study, Baker *et al.* (2022) synthesized tantalum suboxide films with varying oxygen content using reactive direct-current magnetron sputtering.[80] This method involved controlling the composition kinetically by adjusting the chamber pressure and deposition rate while keeping the working gas mix constant. The resultant films were X-ray amorphous, displaying significant variation in electrical resistivity across seven orders of magnitude. Notably, the dominant conduction mechanism shifted from metallic to activated tunnelling when the oxygen content exceeded approximately 55 at%, which was marked by a sharp increase in resistivity and a corresponding decrease in carrier density at low temperatures. This study highlighted the critical influence of oxygen content on the electrical properties of tantalum suboxide films and demonstrates the ability to tailor these properties through precise control of the sputtering parameters.

Further extending the application of magnetron sputtering, Rudolph *et al.* (2017) conducted an in-depth exploration into the synthesis of Ta_3N_5 using a magnetron sputtering technique, which was notably enhanced with an axial magnetic field.[80] This innovative approach aimed to guide ionic species more precisely onto the growing film, thereby optimizing the deposition process. The introduction of the axial magnetic field was crucial in achieving a high degree of crystallinity within the Ta_3N_5 films, a significant improvement over the amorphous content that typically characterizes conventionally sputtered films.

The enhanced ion-assisted growth not only improved the crystallinity but also contributed to the formation of a highly nanostructured surface. This surface was densely populated with grains, which are essential for increasing the active surface area. The dense grain population is beneficial for various applications, especially for solar water splitting, where the increased surface area can enhance light absorption and catalytic efficiency. By using this method, Rudolph *et al.* (2017) effectively demonstrated that modifying the conventional magnetron sputtering setup with an axial magnetic field can lead to superior structural and morphological properties in Ta_3N_5 films.[80] This advancement underscores the potential for fine-tuning sputtering parameters to achieve desired material characteristics, paving the way for improved performance in practical applications such as solar energy conversion and other photoactive technologies.

Overall, magnetron sputtering emerges as a versatile method for synthesizing tantalum-based nanoparticles and films, offering control over structural, morphological, and electrical properties. Each study highlights different aspects and potential applications, from biomedical coatings to advanced materials for fusion energy and solar water splitting. The ability of this synthesis method to produce both amorphous and crystalline structures, along with tailored porosity and oxidation profiles, underscores its potential in various technological domains.

In addition to well-established methods like the Sol–Gel Method, hydrothermal/solvothermal approaches, and magnetron sputtering, several other techniques have been instrumental in synthesizing tantalum-based nanoparticles.[81–83] Chemical vapor deposition (CVD) stands out for its ability to deposit thin films or nanoparticles by chemical reactions in the vapor phase, ensuring precise control over composition and film thickness.[84,85] This method is favoured in applications requiring uniform and conformal coatings of tantalum compounds, though careful parameter optimization is essential to avoid by-products and ensure substrate integrity[86–88] Electrodeposition offers another robust approach, leveraging electrochemical processes to deposit tantalum-based nanoparticles from solution onto conductive substrates. It excels in scalability and allows fine-tuning of nanoparticle size and morphology by adjusting deposition parameters such as voltage and solution composition. This makes electrodeposition ideal for producing dense, pure coatings suitable for electronics and catalysis.[89–91]

Laser ablation provides a non-contact method to produce tantalum-based nanoparticles by vaporizing a target material with a high-energy laser in controlled environments. It offers precise control over nanoparticle size, shape, and crystallinity without introducing contaminants from solvents or chemicals.[85] Gas-phase condensation, meanwhile, involves the condensation of vapor-phase precursors onto a substrate under controlled conditions, yielding nanoparticles with uniform size distributions and high purity.[86,87] Solvated metal atom dispersion (SMAD) is effective for producing colloidal nanoparticles by solvating tantalum atoms in a liquid matrix and subsequently reducing them to form well-defined nanoparticles.[88,89] Finally, ball milling mechanically grinds tantalum precursors with grinding balls, facilitating nanoparticle formation through mechanical alloying and reduction reactions.[90,91] These diverse synthesis methods underscore the versatility in tailoring tantalum-based nanoparticles for applications spanning biomedical devices to

Table 1 Advantages and disadvantages of various synthesis methods for tantalum-based nanoparticles

Synthesis method	Advantages	Disadvantages
Sol–gel method	Allows for control over composition and morphology. Suitable for producing nanocomposites. Low-temperature processing. Scalable. Versatile	Requires careful control of processing conditions to avoid phase separation or unwanted crystallization. Long processing times. Limited to certain compositions
Hydrothermal/solvothermal	High purity of synthesized nanoparticles. Scalable for industrial production. Able to control nanoparticle size and morphology. Environmentally friendly	High temperatures and pressures required. Slow reaction kinetics. Complex control over reaction conditions
Magnetron sputtering	Precise control over film thickness and composition. High deposition rates. Suitable for thin film coatings. Can produce uniform and conformal coatings	Equipment costs can be high. Limited to certain substrate sizes and shapes. Challenges in scaling up for large-area coatings
Chemical vapor deposition (CVD)	Precise control over film thickness, composition, and uniformity. High purity coatings. Suitable for complex shapes and large-scale production	Requires high temperatures and vacuum conditions. Hazardous precursor chemicals. Complex equipment and maintenance requirements
Electrodeposition	Scalable and cost-effective. Allows for precise control over nanoparticle size and morphology. High purity of coatings. Simple operation	Limited to conductive substrates. Deposition rate dependent on current density. Electrolyte chemistry must be carefully controlled
Laser ablation	Precise control over nanoparticle size and shape. High purity without chemical additives. Suitable for various materials and complex compositions	Expensive equipment. Limited to small batch production. Energy-intensive process. Potential for particle aggregation
Gas-phase condensation	Uniform nanoparticle size distribution. High purity of synthesized nanoparticles. Scalable for large-scale production. Minimal contamination	Requires precise control over vapor phase conditions. Limited to specific nanoparticle compositions. Complex handling of precursor gases
Solvated metal atom dispersion (SMAD)	Produces colloidal nanoparticles with controlled size and shape. Scalable. Low-cost precursor materials. Versatile for various metals	Requires careful control over reduction conditions. Limited to specific solvent systems. Potential for agglomeration of nanoparticles
Ball milling	Scalable. Simple and low-cost equipment. Allows for control over nanoparticle size and morphology. Suitable for a wide range of materials	Mechanical energy input may lead to contamination. Requires long milling times. Particle size distribution may not be uniform

advanced materials in electronics and energy technologies, each method offering distinct advantages in controlling nanoparticle properties critical for specific applications.[92,93] Table 1 shows the advantages and disadvantages of various synthesis methods for tantalum-based nanoparticles.[81–93]

3 Multimodal imaging applications

3.1 Utilization of tantalum-based nanoparticles as X-ray contrast agents in computed tomography (CT) and other imaging modalities

Tantalum-based nanoparticles (TaNPs) have emerged as promising contrast agents for various imaging modalities due to their unique physical and chemical properties. In computed tomography (CT), TaNPs are particularly valuable because of tantalum's high atomic number ($Z = 73$), which provides strong X-ray attenuation. This characteristic makes TaNPs excellent candidates for enhancing image contrast in CT scans, allowing for more precise visualization of anatomical structures and pathological conditions.[94]

The utilization of TaNPs in CT imaging involves synthesizing nanoparticles that are biocompatible and stable within the biological environment.[95] Surface modifications, such as coating with biocompatible polymers or functionalizing with targeting ligands, are often employed to improve the nanoparticles' stability and targeting capabilities.[96] These modifications help TaNPs to accumulate preferentially in the tissues of interest, such as tumors, thereby enhancing the contrast in the CT images.[95,96]

Beyond CT, TaNPs are being explored for use in other imaging modalities such as magnetic resonance imaging (MRI), optical imaging, and photoacoustic imaging. In MRI, although tantalum is not inherently magnetic, it can be combined with other magnetic materials to create composite nanoparticles that serve as dual-modal imaging agents.[97,98] For optical imaging, the strong light absorption properties of tantalum can be exploited to enhance image contrast. In photoacoustic imaging, TaNPs can convert absorbed light into sound waves, providing high-resolution images of tissues based on their optical properties.[99,100]

For example, in the study by Bonitatibus *et al.* (2010), the primary focus was on the imaging potential of water-soluble tantalum oxide nanoparticles (TaO_x NPs) with diameters $\leq$6 nm as X-ray contrast agents for computed tomography (CT) imaging and other modalities.[101] This research sought to overcome the limitations of traditional iodine-based contrast agents by leveraging tantalum's superior X-ray attenuation properties, particularly at higher diagnostic energies.

The nanoparticles demonstrated enhanced image contrast compared to iodine at equivalent molar concentrations across the diagnostic X-ray spectrum. This advantage was especially evident at higher X-ray energies, where tantalum's K-edge absorption provided a more consistent image contrast profile than iodine-based agents, which tend to show decreased attenuation with increasing X-ray energy. Such properties position tantalum oxide nanoparticles as highly effective candidates for improving CT imaging resolution and diagnostic accuracy.

In vivo validation involved administering the nanoparticles intravenously to rats, followed by imaging with a clinical 64-slice CT scanner. The imaging results highlighted excellent temporal resolution and a dynamic distribution of the contrast agent from the vena cava to the arterial system. Furthermore, the rapid clearance of tantalum oxide nanoparticles from the bloodstream indicates their suitability for real-time imaging applications, minimizing potential long-term retention issues within the body.

The study concluded by emphasizing the promising role of tantalum oxide nanoparticles as next-generation X-ray contrast agents, showcasing significant advantages over traditional iodine-based agents in terms of imaging performance and biocompatibility. Future research should focus on comprehensive safety evaluations and clinical trials to validate their efficacy and safety for routine medical use.

In a different study carried out by Oh *et al.* (2011), tantalum oxide nanoparticles (TaO_x NPs) were explored as cost-effective, bioinert nanoprobes for high-performance X-ray CT imaging.[102] The synthesis of uniformly sized TaO_x NPs was achieved using a microemulsion method, which allowed for precise control over particle size through variations in ethanol content. The surface modification of these nanoparticles was accomplished *via* a simple *in situ* sol–gel reaction using various silane derivatives. This modification facilitated the attachment of functional moieties such as polyethylene glycol (PEG) and fluorescent dyes, enhancing the biocompatibility and multifunctionality of the nanoparticles. The PEG coating provided antifouling properties, ensuring long circulation times *in vivo*, while the fluorescent dye enabled bimodal imaging capabilities, combining fluorescence with X-ray CT imaging.

The performance of TaO_x NPs in CT imaging was thoroughly evaluated. The nanoparticles exhibited a linear increase in Hounsfield units (HU) with concentration, demonstrating superior contrast enhancement compared to traditional iodine-based agents. *In vivo* studies highlighted the efficacy of TaO_x NPs in X-ray CT angiography, where they provided bright, well-resolved images of blood vessels, heart, liver, spleen, and kidneys with prolonged circulation times (Fig. 13). Additionally, the PEGylated nanoparticles showed no significant cytotoxicity, as confirmed by MTT assays, and minimal *in vivo* toxicity, as evidenced by histological analyses and serum liver function tests. Beyond CT, the bimodal imaging capability of TaO_x NPs was showcased in sentinel lymph node mapping, where the nanoparticles facilitated both fluorescence and X-ray imaging, aiding in precise tumor metastasis detection and image-guided surgery (Fig. 14). The study concluded that TaO_x nanoparticles hold significant potential for various medical applications, including angiography and metastasis detection in liver and lymph nodes, due to their excellent imaging performance, biocompatibility, and multifunctional capabilities.

Torres *et al.* (2012) investigated the potential of metal-containing nanoparticles, specifically core–shell tantalum oxide (TaO) nanoparticles, as X-ray contrast media for CT imaging.[103] Their study aimed to achieve reduced radiation

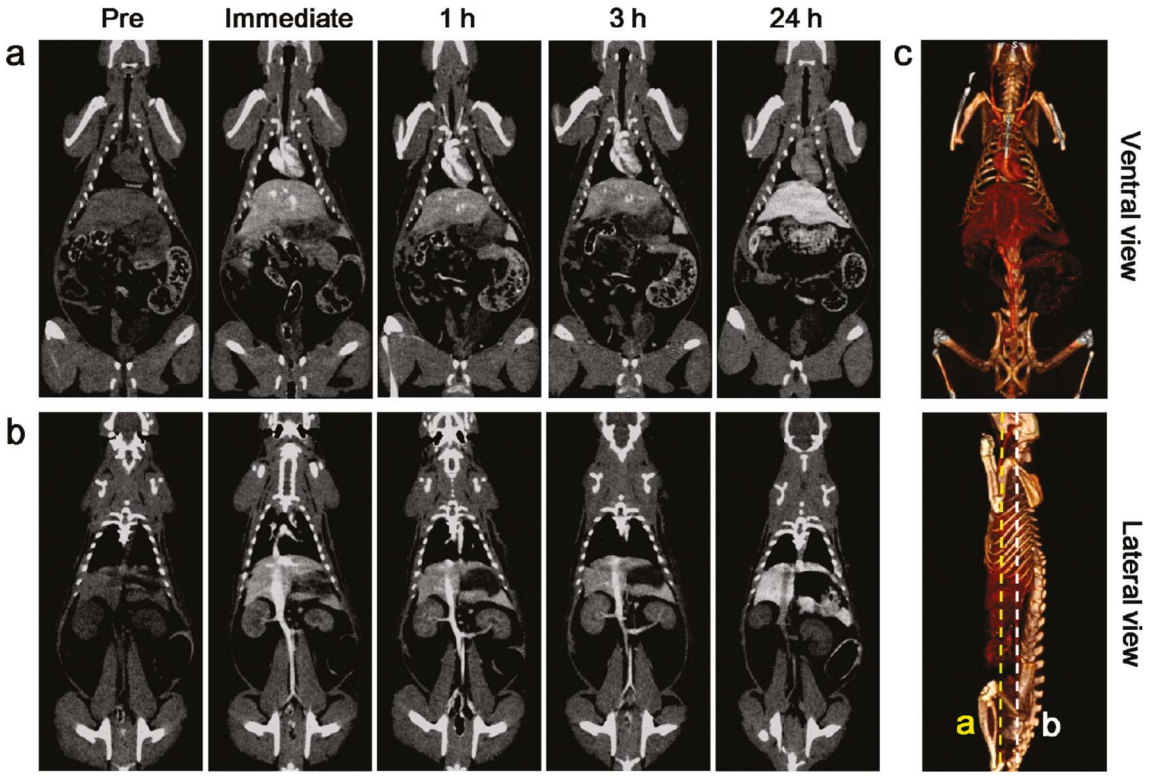

Fig. 13 *In vivo* X-ray CT imaging. (a and b) Serial CT coronal views of a rat following injection of 1 mL of PEG-RITC-TaO_x solution (840 mg kg^{-1}) into the tail vein. (a) Heart and liver (coronal view cut along the yellow dotted line in (c)). (b) Spleen, kidney, and inferior vena cava (coronal view cut along the white dotted line in (c)). (c) 3D-renderings of *in vivo* CT images reveal the ventral (top) and lateral (bottom) sides of the heart and great vessels. The images were obtained immediately after injection (Reproduced from ref. 102 with permission from American Chemical Society copyright [2024]).

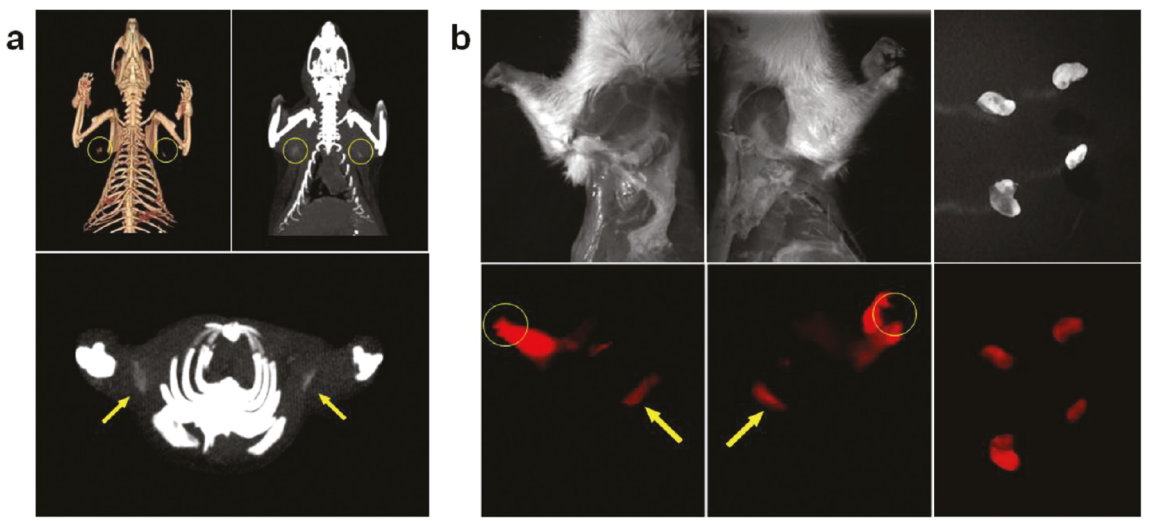

Fig. 14 Sentinel lymph node mapping and resection. (a) *In vivo* CT volume-rendered (upper left) and maximum intensity projections (MIP) images (upper right and lower panels) of the sentinel lymph node of the rat were obtained 2 h after intradermal injection of 100 μL of PEG-RITCTaO_x solution (210 mg mL^{-1}) in both paws. The yellow circles and arrows indicate the locations of the lymph nodes. (b) White light photographs (upper panels) and fluorescence images (lower panels) of the rat injected intradermally with 100 μL of PEG-RITC-TaO_x solution in both paws. Lateral views of the rat 2 h after injection show highly intense red emission from the lymph node and injected part (left and middle). Arrows and circles indicate the putative axillary sentinel lymph nodes and injection point, respectively. Sentinel lymph nodes of the two rats dissected by bimodalimage-guided surgery (right) (Reproduced from ref. 102 with permission from American Chemical Society copyright [2024]).

dose, increased contrast, and improved visualization of smaller anatomical features. The authors synthesized size-fractionated TaO nanoparticles and evaluated their biodistribution, blood half-life, organ retention, and histopathology in preclinical settings.

The fractionated TaO nanoparticles were injected at both the anticipated clinical dose and three times that dose to assess their biological performance. The results demonstrated that improved control over the size of 2-diethylphosphatoethylsilane-TaO nanoparticles significantly reduced the retention of injected tantalum. *In vivo* and *in vitro* CT imaging studies revealed differences in short-term biodistribution in the kidney when comparing the TaO nanoparticles to small-molecule iodinated contrast media. Furthermore, the study provided preliminary data on new imaging applications utilizing "Ta-only" imaging through multienergy CT image acquisition.

In a nutshell, Torres *et al.* (2012) highlighted that size-fractionated core–shell TaO nanoparticles, with a well-defined particle size distribution, possess several essential characteristics for clinically viable vascular imaging compounds.[103] These nanoparticles show promise in advancing multienergy CT imaging applications, potentially offering more detailed and accurate imaging with reduced radiation exposure.

Wang *et al.* (2013) explored the utilization of tantalum oxide (TaO_x) nanoparticles as X-ray contrast agents in CT imaging, demonstrating their superior performance compared to traditional iodine-based agents.[104] The TaO_x nanoparticles maintain consistent X-ray attenuation across clinically relevant energy levels (100–140 kVp), providing enhanced image clarity and diagnostic accuracy.

Integrating these nanoparticles into hydrogel microparticles allows for controlled size and shape, optimizing their use in medical imaging. The hydrogels offer biocompatibility and potential for targeted delivery, enhancing the effectiveness of the contrast agents. *In vivo* studies showed significant vascular contrast enhancement with PEGylated TaO_x nanoparticles, which is crucial for visualizing blood vessels and diagnosing vascular diseases.

TaO_x nanoparticles offer several advantages over iodine-based agents, such as maintaining consistent attenuation at higher energy levels and presenting a lower risk of adverse reactions like allergies and nephrotoxicity. This makes them safer for a broader range of patients. Furthermore, the potential for functional imaging with TaO_x nanoparticles, due to their stable attenuation properties, adds another layer of diagnostic capability.

The study also highlighted the potential application of TaO_x nanoparticles in other imaging modalities, such as dual-modality techniques combining CT with MRI or PET. These multimodal contrast agents can provide complementary information, enhancing diagnostic capabilities. For instance, functionalized TaO_x nanoparticles could offer simultaneous CT and MRI imaging or carry radiolabels for PET imaging, providing detailed insights into disease processes.

Wang *et al.* (2013) discussed future prospects, including scaling down the fabrication technique to produce hydrogel nanorods with controlled size and elasticity.[104] This could lead to more sophisticated contrast agents capable of precise targeting and controlled therapeutic release. Nanoscale hydrogel particles could navigate complex vascular structures, providing high-resolution images at the cellular level and enabling targeted theranostic applications.

In summary, Wang *et al.* (2013) presented tantalum-based nanoparticles as a promising alternative to iodine-based contrast agents in CT imaging, with superior attenuation properties, enhanced safety, and potential applications in multimodal imaging and theranostics.

In 2014, Freedman *et al.* conducted a compelling study exploring tantalum oxide (Ta_2O_5) nanoparticles as novel X-ray contrast agents for micro-computed tomography (μCT) imaging of articular cartilage.[105] These nanoparticles, ranging in size from 5 to 10 nm, feature distinct surface charges and were synthesized using different ligands with varied end functional groups. The study employed μCT to visualize articular cartilage, demonstrating effective detection of cartilage defects in a human cadaver joint. The synthesized nanoparticles exhibited preferential uptake around the defect sites, highlighting their potential utility for targeted imaging within cartilage structures. Furthermore, the study evaluated a non-toxic cationic nanoparticle contrast agent in an *in vivo* murine model, further emphasizing the importance of surface charge in optimizing nanoparticulate agents for targeting both the surface and interior zones of articular cartilage.

In another study by Jin *et al.* (2014), a nanotheranostic agent was developed for bimodal imaging-guided photothermal ablation of tumors. This involved encapsulating tantalum oxide (TaO_x) nanoparticles within polypyrrole (PPy) nanoparticles to enhance both X-ray CT and photoacoustic (PA) imaging capabilities *in vivo*.[106] The composite nanoparticles were designed to passively accumulate at tumor sites during circulation, enabling effective imaging and subsequent photothermal therapy upon near-infrared laser irradiation. This dual-modal approach underscores the potential of these nanoparticles as versatile contrast agents for enhancing diagnostic accuracy and therapeutic efficacy in tumor imaging and treatment.

Additionally, Jin *et al.* (2015) expanded on this work by developing multifunctional theranostic tantalum oxide nanoparticles (TaO_xNPs).[107] These nanoparticles were engineered for actively targeted delivery, pH-responsive drug release, and bimodal imaging employing fluorescence and CT imaging modalities. The study demonstrated the nanoparticles' biocompatibility, efficient drug release in acidic environments, prolonged circulation in the bloodstream, superior tumor-targeting capabilities, and enhanced therapeutic outcomes. The multifunctional nature of TaO_x@Cy7-DOX-PEG-HA NPs highlighted their potential as robust contrast agents for simultaneous fluorescence and X-ray CT imaging, alongside their promise in personalized cancer detection and treatment strategies.[107]

In 2016, Fitzgerald *et al.* aimed to develop and evaluate a proposed computed tomography (CT) contrast agent utilizing carboxybetaine zwitterionic (CZ) coated soluble tantalum oxide (TaO) nanoparticles (NPs).[108] Their investigation included

comparing the CT imaging performance of CZ-TaO NPs against conventional iodinated agents in live rats, alongside *in vitro* and *in vivo* assessments. The study demonstrated that CZ-TaO NPs provided significantly improved image contrast in CT scans compared to iodinated agents. Moreover, these nanoparticles exhibited no adverse effects upon injection in healthy rats and were efficiently cleared *via* urine, suggesting their potential suitability for widespread clinical CT imaging applications.[108]

Collectively, these studies underscore the diverse and promising applications of tantalum oxide nanoparticles in biomedical imaging. From enhancing the visualization of specific biological structures like articular cartilage to serving as efficient contrast agents for multiple imaging modalities, tantalum oxide nanoparticles continue to show significant potential in advancing diagnostic accuracy and therapeutic interventions in medicine.

In the study by Dai *et al.* (2017), tantalum-based nanoparticles, specifically tantalum carbide (Ta_4C_3) MXene-based composite nanosheets, have been effectively utilized as contrast agents for various imaging modalities, particularly X-ray computed tomography (CT).[109] The high atomic number of tantalum ($Z = 73$) and its significant X-ray attenuation coefficient make it an ideal candidate for CT imaging. When incorporated into the MnO_x/Ta_4C_3 composite nanosheets, tantalum provides excellent contrast-enhanced CT imaging capabilities. The study demonstrated that these composite nanosheets exhibited significantly improved brightness and enhanced Hounsfield units (HU) values in CT images, indicating a strong linear relationship between HU values and tantalum concentration (Fig. 15a and b). This enhancement was notably higher than that achieved with clinically used iodine-based contrast agents, underscoring the superior performance of the tantalum-based agents.

Further *in vivo* investigations involved injecting MnO_x/Ta_4C_3-SP composite nanosheets into mice bearing 4T1 tumors. The results showed significant contrast enhancement in the tumors, as evidenced by the increase in HU values post-injection. This suggests that the composite nanosheets are promising candidates for *in vivo* contrast-enhanced CT imaging, providing detailed anatomical and functional information with high spatial resolution and deep tissue penetration (Fig. 15c–e).

In addition to CT imaging, the study explored the use of these nanosheets in magnetic resonance imaging (MRI). The manganese oxide (MnO_x) component of the composite nanosheets responds to the tumor microenvironment, enabling T1-weighted MR imaging. Manganese, a biocompatible element, offers a safer alternative to gadolinium-based agents commonly used in clinical MRI. The MnO_x functionalization allows the nanosheets to exploit the mildly acidic and glutathione-rich conditions of the tumor microenvironment, leading to pH-responsive and GSH-sensitive MRI contrast enhancement. *In vitro* tests confirmed the increase in relaxivity (r1) and corresponding brightening effects of T1-weighted MR images under these conditions, which were further validated through *in vivo* imaging of tumor-bearing mice, showing significant signal enhancement post-injection.

The photothermal conversion capabilities of the MnO_x/Ta_4C_3 composite nanosheets also enabled their use in photoacoustic (PA) imaging. The study reported a linear relationship between PA signal intensity and tantalum concentration, demonstrating effective contrast enhancement for PA imaging. *In vivo* PA imaging further validated the performance of these nanosheets, showing clear acoustic emission signals and enhanced imaging of tumor tissues upon laser pulse illumination.

Overall, the Dai *et al.* (2017) study highlighted the multifunctional capabilities of tantalum carbide MXene-based composite nanosheets as versatile contrast agents.[109] These nanosheets not only enhance CT imaging due to the high X-ray attenuation properties of tantalum but also provide responsive MRI contrast and effective PA imaging capabilities, making them highly valuable for comprehensive cancer theranostics.

In a separate study, Liu *et al.* (2017) introduce tantalum sulfide (TaS_2) nanosheets (NSs) as a versatile nanoplatform designed not only for cancer therapy but also for enhancing computed tomography (CT) imaging capabilities.[110] Tantalum, known for its biocompatibility and high X-ray attenuation coefficient, forms the core of TaS_2 NSs, making them highly effective as CT contrast agents. The primary focus of the research revolves around TaS_2 NSs' ability to provide robust CT imaging contrast, a critical requirement in clinical diagnostics for visualizing anatomical structures and detecting pathological conditions with precision. The study demonstrates that TaS_2 NSs exhibit a linear increase in Hounsfield units (HU) with concentration across different X-ray spectra (100–140 kVp), indicating their capability to enhance image contrast effectively.

Moreover, *in vivo* experiments conducted in PC3 tumor-bearing mice highlight the prolonged circulation and enhanced CT signals observed in tumors following intravenous administration of TaS_2 NSs. This finding underscores the potential of TaS_2 NSs not only as imaging agents but also for imaging-guided therapeutic interventions. The ability to capitalize on the enhanced permeability and retention (EPR) effect in tumors further positions TaS_2 NSs as promising tools for personalized cancer treatment strategies. The study revealed the dual functionality of TaS_2 NSs, serving both as therapeutic agents for NIR-mediated hyperthermia and as diagnostic tools for CT imaging. This multifunctional approach not only enhances diagnostic accuracy but also opens avenues for combining imaging with targeted therapies, potentially improving patient outcomes.

Looking forward, further advancements in the synthesis and functionalization of TaS_2 NSs could optimize their imaging performance and therapeutic efficacy in clinical applications. Future research may focus on refining these nanosystems to achieve tailored diagnostic and therapeutic outcomes, paving the way for their integration into mainstream medical practice.

Freedman *et al.* (2014) conducted pioneering research into the synthesis and characterization of tantalum oxide (Ta_2O_5) nanoparticles as novel X-ray contrast agents specifically tailored for micro-computed tomography (μCT) imaging of articular cartilage.[105] The nanoparticles, sized approximately 5–10 nm, were engineered to possess distinct surface charges by

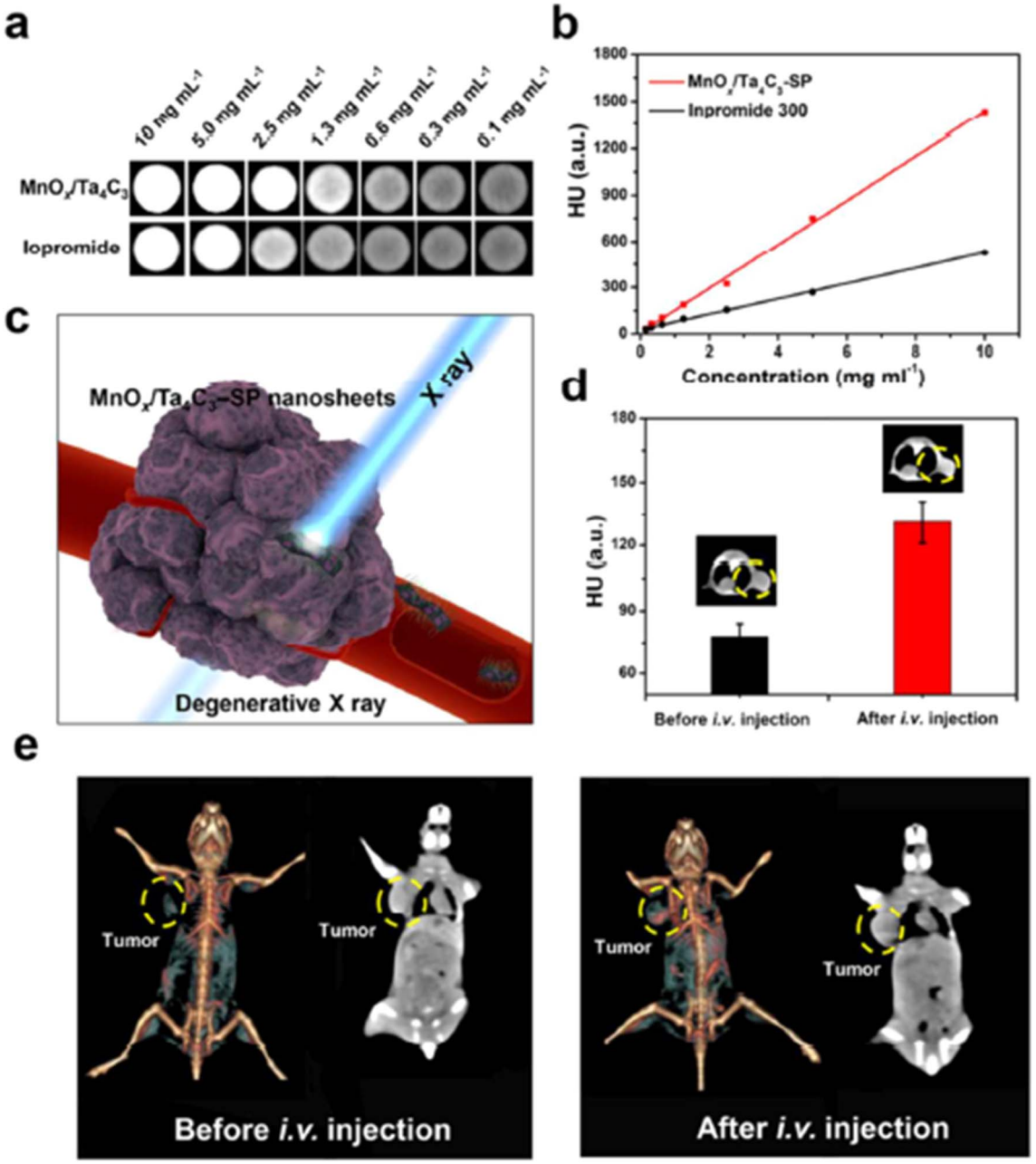

Fig. 15 (a) *In vitro* CT images and (b) CT contrasts of MnO_x/Ta_4C_3-SP composite nanosheet solutions and iopromide solutions at varied concentrations (0.1, 0.3, 0.6, 1.3, 2.5, 5.0, and 10 mg mL^{-1} with respect to Ta and I, respectively). (c) Schematic of *in vivo* CT imaging by using MnO_x/Ta_4C_3-SP composite nanosheets as the contrast agents. (d) *In vivo* CT contrasts of tumor tissue before and after i.v. administration of MnO_x/Ta_4C_3-SP composite nanosheets. (e) *In vivo* 3D reconstruction CT images (left) and contrast images (right) of mice before and after i.v. administration of MnO_x/Ta_4C_3-SP composite nanosheets (20 mg kg^{-1}, 100 μL) for 2 h (Reproduced from ref. 109 with permission from American Chemical Society copyright [2024]).

employing different ligands as end functional groups during synthesis. This strategic design was critical for enhancing the interaction of the nanoparticles with biological tissues, particularly the negatively charged components of articular cartilage.

The study leveraged the high spatial resolution of μCT to visualize cartilage structures in unprecedented detail. By integrating these nanoparticles, the researchers achieved superior visualization of cartilage defects in a human cadaver joint. Remarkably, the synthesized nanoparticles demonstrated preferential uptake in the regions surrounding cartilage defects, indicating their potential for targeted imaging applications. This preferential localization is attributed to the surface charge characteristics of the nanoparticles, which play a pivotal role in their interaction with the tissue matrix.

Additionally, the study extended its scope to *in vivo* applications, where an optimized, non-toxic cationic nanoparticle

contrast agent was evaluated using a murine model. This agent facilitated enhanced imaging of cartilage, underscoring the importance of nanoparticle surface charge in designing agents that can target both surface and interior zones of articular cartilage. These findings suggest that Ta_2O_5 nanoparticles represent a promising new class of contrast agents for articular cartilage imaging, providing critical insights into their potential clinical applications.

Jin *et al.* (2014) introduced an innovative nanotheranostic agent designed for bimodal imaging and photothermal ablation of tumors.[106] This study encapsulated tantalum oxide (TaO_x) nanoparticles within polypyrrole (PPy) nanoparticles to significantly enhance both X-ray CT and photoacoustic (PA) imaging capabilities *in vivo*. The dual functionality of the composite nanoparticles allowed them to serve as efficient contrast agents for both imaging modalities, providing comprehensive visualization of tumor sites.

The nanoparticles' ability to passively accumulate at tumor sites during blood circulation was a key finding of the study. This passive targeting was crucial for effective imaging, as it ensured that the nanoparticles were preferentially localized in the tumor tissue, thereby enhancing the contrast in both X-ray CT and PA imaging. Furthermore, under near-infrared laser irradiation, the nanoparticles exhibited photothermal cytotoxicity, effectively abating tumor cells. This dual modality not only improved imaging clarity but also provided a therapeutic avenue, showcasing the potential of these composite nanoparticles as a multifaceted tool for tumor imaging and treatment.

In a subsequent study, Jin *et al.* (2015) developed multifunctional theranostic tantalum oxide nanoparticles (TaO_xNPs) with capabilities for active targeting, pH-responsive drug release, and bimodal imaging.[107] These nanoparticles were meticulously designed to exhibit excellent biocompatibility, ensuring their safety for *in vivo* applications. The nanoparticles were engineered to have a high cumulative release rate in acidic microenvironments, typical of tumor sites, thereby enhancing their therapeutic efficacy.

The study highlighted the nanoparticles' prolonged circulation time in the bloodstream, which is essential for ensuring that the nanoparticles reach the target tumor tissue efficiently. Superior tumor-targeting ability was demonstrated, significantly enhancing the therapeutic outcomes. The theranostic nanoparticles were evaluated using fluorescence imaging and CT imaging, both of which showed substantial improvement in imaging quality. The multifunctional nature of TaO_x@Cy7-DOX-PEG-HA nanoparticles enabled their use in fluorescence/X-ray CT bimodal imaging and remote-controlled therapeutics for cancer treatment, paving the way for personalized cancer detection and treatment with high efficacy.

Fitzgerald *et al.* (2016) focused on developing and evaluating a computed tomography (CT) contrast agent based on carboxybetaine zwitterionic (CZ) coated soluble tantalum oxide (TaO) nanoparticles (NPs).[108] This study aimed to address the limitations of traditional iodinated contrast agents by providing a more effective and safer alternative. The CZ-TaO nanoparticles were meticulously synthesized and characterized for their CT imaging performance.

The study involved a comprehensive evaluation of the CZ-TaO NPs, comparing their performance with that of conventional iodinated agents in live rats, as well as through *in vitro* and *in vivo* examinations. The results demonstrated that CZ-TaO NPs provided substantially improved image contrast in CT scans, significantly enhancing visualization. Additionally, these nanoparticles exhibited rapid clearance in urine and showed no adverse effects post-injection in healthy rats, highlighting their potential as a viable option for clinical CT imaging.

Collectively, these studies illustrate the versatile applications of tantalum oxide nanoparticles in biomedical imaging. From enhancing the visualization of specific biological structures such as articular cartilage to serving as efficient contrast agents for various imaging modalities including μCT, X-ray CT, PA imaging, and fluorescence imaging, tantalum oxide nanoparticles have shown remarkable potential. Their unique properties, including biocompatibility, surface charge tunability, and multifunctionality, position them as promising candidates for advancing diagnostic and therapeutic practices in medicine. These advancements underscore the potential for tantalum oxide nanoparticles to revolutionize imaging techniques, offering new avenues for early diagnosis, targeted therapy, and personalized medicine.

In the study by Koshevaya *et al.* (2020), biocompatible Ta_2O_5 nanoparticles were synthesized *using a* solvothermal method, resulting in stable hydrosols suitable for medical imaging applications.[111] These nanoparticles were characterized by their small size (approximately 2 nm) and demonstrated colloidal stability in physiological conditions, crucial for their use *in vivo*.

Fig. 16 in the study depicted the *in vivo* application of Ta_2O_5 nanoparticles as a contrast agent in CT imaging of rat gastrointestinal tracts. The concentration of the nanoparticle hydrosol used (20 mg mL^{-1}) was chosen based on measurements of Hounsfield Units (HU) to achieve optimal contrast enhancement. Initially, native CT values of the rat stomachs were measured at 47.1 ± 5.7 HU. Following oral administration of the Ta_2O_5 nanoparticle dispersion, CT imaging revealed significant enhancement within 10 minutes, with a peak accumulation observed (426.1 ± 2.8 HU). Even after 4 h, the nanoparticles remained detectable within the stomach (414.1 ± 2.8 HU), indicating prolonged retention and circulation within the gastrointestinal tract under physiological conditions. This capability is crucial for improving diagnostic accuracy and early detection of gastrointestinal abnormalities. The nanoparticles' biocompatibility and prolonged circulation within the digestive system further underscore their potential for clinical applications, offering insights into their use in both diagnostic imaging and potentially in theranostic approaches such as drug delivery systems or combined imaging and therapy modalities.

In general, Ta_2O_5 nanoparticles represent a significant advancement in CT imaging technology, as demonstrated by their robust contrast enhancement capabilities illustrated in Fig. 16. Their stability, biocompatibility, and effective contrast properties make them promising candidates for future

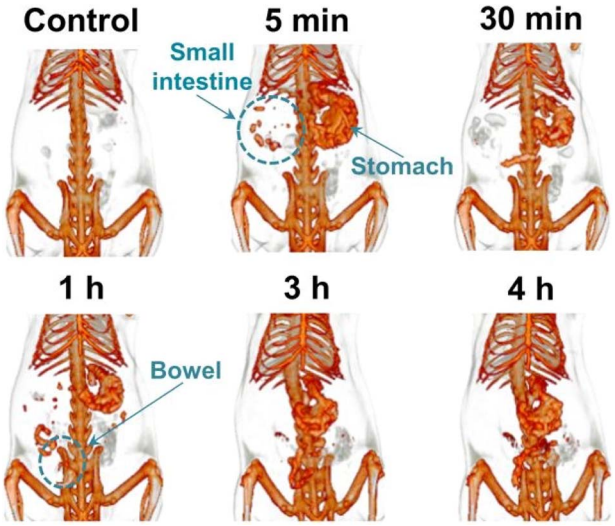

Fig. 16 CT coronal views of GI tract of the rat administered with Ta_2O_5 NPs (Reproduced from ref. 111 with permission from Royal Society of Chemistry copyright [2024]).

developments in medical imaging, aimed at enhancing patient care through improved diagnostic precision and therapeutic efficacy.

In a study carried out in 2020, Chakravarty *et al.* explored the synthesis, characterization, and application of tantalum oxide (TaO_x) nanoparticles (NPs) as advanced contrast agents for computed tomography (CT).[112] The research focused on developing five distinct versions of 9–12 nm diameter silane-coated TaO_x nanocrystals (NCs) using a sol–gel method. These NCs varied in hydrophilicity and fluorescence capabilities, achieving a high tantalum content of 78%, the highest reported to date.

Highly hydrophilic NCs, left uncoated, were evaluated *in vivo* in mice for micro-CT imaging of full-body vasculature. Upon intravenous injection, these NCs provided exceptional vascular contrast and circulated in the bloodstream for approximately 3 h hours before accumulating in reticuloendothelial system (RES) organs. Additionally, when injected locally into the mammary gland, these NCs enabled clear delineation of the full ductal tree structure, showcasing their utility in detailed imaging of complex biological structures.

The study also explored partially hydrophilic NCs encapsulated within mesoporous silica nanoparticles (TaO_x@MSNPs) and hydrophobic NCs encapsulated within poly(lactic-*co*-glycolic acid) (PLGA; TaO_x@PLGA) NPs. These encapsulated forms were designed as potential CT-imagable drug delivery vehicles. Bolus intramuscular injections of TaO_x@PLGA NPs and TaO_x@MSNPs, simulating tumor site accumulation, resulted in high signal enhancement in mice. *In vitro* studies revealed high cytocompatibility and low dissolution rates for both bare NCs and formulated NPs, underscoring their stability and biocompatibility.

This comprehensive work by Chakravarty *et al.* (2020) solidifies the versatility and efficacy of TaO_x-based NPs as CT contrast agents. Their ability to provide high contrast, target specific tissues, and potentially serve as drug delivery vehicles opens new avenues for diagnostic imaging and therapeutic applications.

Lawson *et al.* (2021) focused on enhancing the diagnostic capabilities of computed tomography (CT) through the use of tantalum oxide (Ta_2O_5) nanoparticles (NPs) for contrast-enhanced CT (CECT).[113] The primary objective was to develop nanoparticle-based contrast agents that could provide rapid, nondestructive, and quantitative imaging of human metacarpal phalangeal joint (MCPJ) articular cartilage. The study synthesized Ta_2O_5 NPs with diameters of 3–6 nm, coated with either non-ionic poly(ethylene) glycol (PEG) or cationic trimethylammonium ligands.

The choice of coatings was crucial for optimizing the diffusion of NPs into both healthy and osteoarthritic cartilage. The study demonstrated that these NPs could effectively enhance CT imaging by correlating CECT attenuation with the glycosaminoglycan (GAG) content and biomechanical integrity of the cartilage. Specifically, the cationic NPs showed a strong correlation ($R^2 = 0.8975$, $p < 0.05$) with GAG content and a significant correlation with the equilibrium modulus ($R^2 = 0.9312$, $p < 0.05$). Similarly, the neutral NPs also displayed a notable correlation ($R^2 = 0.7054$ and $R^2 = 0.8285$, respectively) with these parameters.

This study highlighted the importance of nanoparticle surface charge and size in designing effective contrast agents for targeting and imaging articular cartilage. The use of nanoparticle CECT allowed for the visualization of both soft tissue and underlying bone, a significant advantage over plain radiography, which is typically limited to imaging bone in musculoskeletal diseases. Additionally, the ability to provide real-time, quantitative assessments of both hard and soft tissues offered a comprehensive image of the disease stage, making nanoparticle CECT a valuable tool in diagnosing and monitoring musculoskeletal conditions.[114]

Both studies by Chakravarty *et al.* (2020)[112] and Lawson *et al.* (2021)[113] underscore the promising applications of tantalum oxide nanoparticles in the field of imaging. Chakravarty *et al.* (2020) demonstrated the versatility of TaO_x-based NPs in CT imaging of vascular structures and potential tumor sites, highlighting their high contrast and stability.[112] Lawson *et al.* (2021) focused on the quantitative assessment of articular cartilage using Ta_2O_5 NPs, emphasizing the importance of surface charge and size in designing effective contrast agents. Collectively, these studies illustrate the significant advancements in nanoparticle-based CT imaging, offering improved visualization, targeted imaging, and potential therapeutic applications, thereby paving the way for enhanced diagnostic and treatment strategies in various medical fields.

Narasimhan *et al.* (2021) explored the application of X-ray excited optical luminescence (XEOL) imaging using Europium-doped tantalum oxide nanoparticles (Eu NPs), emphasizing the critical role of tantalum oxide (TaO_x) in this advanced imaging technique.[115] XEOL offers a promising alternative to traditional *in vivo* optical imaging, enabling enhanced visualization of deep tissues. The choice of host material is crucial for generating highly luminescent XEOL probes, which are essential for acquiring detailed molecular information about diseases. Tantalum oxide was selected due to

its known biocompatibility and efficacy as a CT contrast agent, making it an ideal candidate for this application.

The researchers synthesized Europium-doped TaO_x nanoparticles using an oil-in-water micro-emulsion technique, with doping concentrations of 2%, 5%, 7%, and 10%. The optical properties of these nanoparticles were meticulously studied under varying X-ray voltages (50–200 keV). TaO_x NPs alone exhibited blue luminescence, while Eu NPs displayed a shift to reddish-orange luminescence, which intensified with increasing X-ray voltages. This shift and enhancement in luminescence are attributed to the effective energy transfer from the TaO_x host material to the Europium luminescent centers.

The impact of TaO_x nanoparticles on XEOL imaging is profound. The luminescence properties of the Eu NPs were highly responsive to changes in X-ray energy levels. At lower voltages, the emission from Europium was relatively mild. However, at higher voltages, specifically between 150 and 200 keV, there was a marked increase in luminescence intensity. This enhanced luminescence significantly improves the ability to visualize deep tissue structures with greater clarity and detail, which is essential for effective medical imaging.

The study demonstrates that the integration of TaO_x in the nanoparticle structure is pivotal for achieving the desired luminescent properties necessary for XEOL imaging. The high atomic number of tantalum contributes to its superior X-ray attenuation capability, which in turn enhances the efficiency of energy transfer to the Europium centers. This results in a brighter and more pronounced luminescence, facilitating detailed three-dimensional fluorescence-based tomography of tumors.

In practical terms, the enhanced luminescence provided by Europium-doped tantalum oxide nanoparticles under X-ray excitation means that these nanoparticles can be used to produce clearer, more detailed images of biological structures, even deep within tissues. This capability is particularly valuable for medical diagnostics, as it allows for more precise detection and characterization of tumors, potentially improving the accuracy of diagnosis and guiding more effective treatment strategies. In a nutshell, Narasimhan *et al.* (2021) underscore the significant impact of tantalum oxide nanoparticles in XEOL imaging applications. By serving as an effective host material that enhances luminescence through efficient energy transfer, TaO_x nanoparticles enable the detailed visualization of deep tissue structures. This advancement in imaging technology holds great promise for improving diagnostic accuracy and therapeutic outcomes in medical practice.

4 Synergies between various imaging modalities using tantalum-based nanoparticles as a contrast agent for comprehensive cancer diagnosis and monitoring

The advent of advanced imaging technologies has revolutionized cancer diagnosis and monitoring, allowing for early detection, precise treatment planning, and effective monitoring of therapeutic outcomes. Among the various imaging modalities, each has distinct advantages and limitations.[115,116] The development of multifunctional contrast agents, such as tantalum-based nanoparticles (TaO_x), presents a promising approach to leverage the strengths of multiple imaging techniques. This review explores the synergies between different imaging modalities facilitated by TaO_x nanoparticles for comprehensive cancer diagnosis and monitoring.[117]

Cancer remains a leading cause of morbidity and mortality worldwide, necessitating improved diagnostic and monitoring techniques. Imaging plays a crucial role in oncology, aiding in the visualization of tumors, assessment of treatment response, and detection of recurrence.[118,119] Traditional imaging modalities include computed tomography (CT), magnetic resonance imaging (MRI), positron emission tomography (PET), single-photon emission computed tomography (SPECT), and ultrasound (US). Each modality offers unique benefits, such as high spatial resolution, excellent soft tissue contrast, and functional imaging capabilities.[120] However, no single modality provides all the necessary information for comprehensive cancer care. Tantalum-based nanoparticles have emerged as a versatile contrast agent with the potential to enhance multiple imaging modalities.[16,121] Tantalum, a high atomic number element, provides excellent radiodensity for CT imaging and has favourable properties for functionalization, allowing for integration with other imaging techniques.[121]

MicroCT imaging is widely used for high-resolution anatomical imaging, particularly in preclinical studies. TaO_x nanoparticles have demonstrated superior performance as a contrast agent in microCT, offering high signal intensity and clear visualization of fine anatomical details.[122–124] Studies have shown that TaO_x nanoparticles provide nitid visualization of structures such as the ductal tree, with minimal outward diffusion and high homogeneity.[124] This capability is crucial for detailed anatomical studies and image-guided interventions, where precise localization and visualization are required (Fig. 17).[125]

Fluoroscopy provides real-time imaging, essential for guiding interventional procedures such as biopsies and catheter placements. The high radiodensity of TaO_x nanoparticles enhances contrast in fluoroscopic imaging, facilitating the accurate placement of instruments and monitoring of procedures.[126] The rapid visualization and high retention of TaO_x within the target area improve procedural accuracy and safety, making it an invaluable tool in interventional oncology. MRI is renowned for its excellent soft tissue contrast and is a cornerstone of cancer imaging.[127] While TaO_x nanoparticles are primarily designed for CT, their potential use in MRI is under investigation. Tantalum's paramagnetic properties could be harnessed to develop novel MRI contrast agents, enhancing contrast and improving delineation of soft tissues. Combining CT and MRI contrast capabilities in a single agent could provide comprehensive anatomical and functional imaging, improving diagnostic accuracy and treatment planning.[128,129]

Hybrid imaging techniques, such as PET/CT and SPECT/CT, combine the anatomical information of CT with the functional

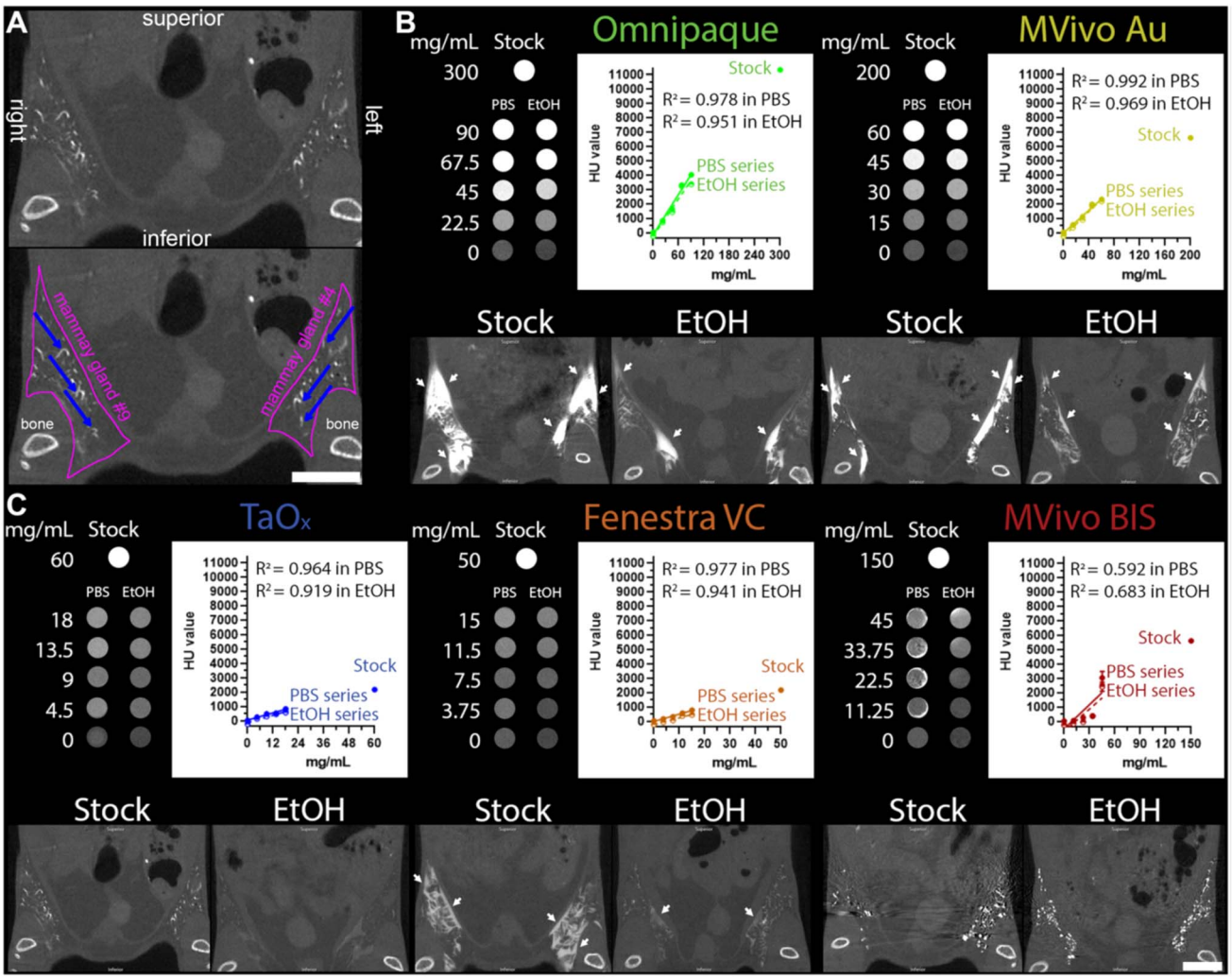

Fig. 17 Characteristics of contrast agents and their signal attenuation profiles in various solutions. (A) Annotated microCT images of TaO_x-infused mammary glands (36 mg Ta per ml stock, also shown at lower magnification in (C)); pink lines outline the abdominal mammary glands, and blue arrows indicate filled branches of the ductal tree. (B and C) Tissue phantoms and mice were scanned using the same microCT imaging parameters. Top panels (tissue phantoms): each contrast agent was diluted from stock reagent (maximal concentration) in PBS or 70% ethanol (EtOH) at the indicated concentrations (mg of metal per ml). Linear fitting of signal attenuation as a function of the metal concentration in each solution. Bottom panels: representative single-slice micro CT images of the lower body of animals captured immediately after the last ID injection of each indicated solution: Omnipaque (300 mg I per ml stock, 90 mg I per ml in EtOH), MVivo Au (200 mg Au per ml stock, 60 mg Au per ml in EtOH), TaO_x (36 mg Ta per ml stock, 10.8 mg Ta per ml in EtOH), Fenestra VC (50 mg I per ml stock, 15 mg I per ml in EtOH), MVivo BIS (150 mg Bis per ml stock, 45 mg Bis per ml in EtOH). Arrows indicate areas where leaked contrast agent accumulates on the fascia boundary. Scale bar is 10 mm in images at different magnifications (Reproduced from ref. 125 with permission from Springer Nature copyright [2024]).

data of PET or SPECT. TaO_x nanoparticles can be functionalized with radioisotopes or targeting ligands, enabling their use in hybrid imaging.[130–133] This approach allows for the simultaneous acquisition of anatomical and functional information, providing a more complete picture of tumor biology and metabolism. The integration of TaO_x nanoparticles in hybrid imaging could improve tumor localization, characterization, and monitoring of therapeutic response.[105,106] Longitudinal monitoring of cancer requires repeated imaging to assess treatment response and detect recurrence. The low toxicity and rapid systemic clearance of TaO_x nanoparticles make them suitable for repeated use. Their minimal long-term retention reduces the risk of cumulative side effects, enhancing patient safety.[107] The consistent and clear imaging provided by TaO_x nanoparticles over extended periods supports their use in serial imaging sessions, crucial for ongoing cancer monitoring.[107]

The use of tantalum-based nanoparticles as a multifunctional contrast agent presents a significant advancement in cancer imaging. By leveraging the strengths of various imaging modalities, TaO_x nanoparticles facilitate comprehensive cancer diagnosis and monitoring.[134] Their superior performance in microCT, potential applicability in MRI, and integration in hybrid imaging techniques provide a robust platform for precise and detailed imaging. The ability to use TaO_x nanoparticles in longitudinal studies further enhances their utility in clinical oncology.[110] As research advances, the development of TaO_x nanoparticles for multimodal imaging shows great promise for enhancing cancer care. These nanoparticles

facilitate early detection, precise treatment planning, and effective monitoring of therapeutic outcomes.[115] Tantalum-based nanoparticles have demonstrated remarkable potential in revolutionizing cancer imaging and diagnostics, particularly through their ability to enhance multiple imaging techniques.[134] For example, several studies have conducted extensive investigations into the use of tantalum-based nanomaterials as contrast agents for comprehensive and precise cancer diagnosis and monitoring. In the study by Lee *et al.* (2012), the researchers synthesized multifunctional Fe_3O_4/TaO_x core/shell nanoparticles (NPs) using a sol–gel reaction of tantalum(v) ethoxide in a microemulsion containing Fe_3O_4 nanoparticles.[95] The incorporation of tantalum in these NPs significantly contributed to their unique properties, making them highly suitable for simultaneous magnetic resonance imaging (MRI) and X-ray computed tomography (CT). The Fe_3O_4/TaO_x core/shell NPs exhibited excellent biocompatibility and prolonged circulation times, which are crucial for biomedical applications. When intravenously injected into rats with subcutaneously inoculated tumors, these NPs demonstrated distinct imaging capabilities that enhanced both MRI and CT modalities.

CT imaging with Fe_3O_4/TaO_x NPs enabled clear visualization of tumor-associated blood vessels, providing high-resolution 3D reconstructions of the vasculature. This capability is particularly advantageous for tumor therapy, as targeting tumor-associated vessels is critical for effective cancer treatment. The tantalum component of the NPs played a vital role in enhancing CT imaging due to its high atomic number, which provides strong X-ray attenuation and, consequently, high contrast in CT images. Simultaneously, MRI provided detailed insights into the tumor microenvironment by distinguishing between oxygenated and hypoxic regions within the tumor. Before the injection of the NPs, MRI images depicted the tumor as homogeneous and bright. Following the injection, MRI images revealed inhomogeneous signal attenuation within the tumor, with dark peripheral regions and a gray core, corresponding to oxygenated and hypoxic areas, respectively. The presence of Fe_3O_4 in the core of the NPs contributed to their effectiveness as T_2-weighted MRI contrast agents, enhancing the ability to capture detailed internal tumor structures.

The dual imaging capabilities of Fe_3O_4/TaO_x NPs stemmed from their unique properties. The tantalum component provided high-resolution imaging of blood vessels in CT without significant sensitivity to soft tissue contrast. Meanwhile, the Fe_3O_4 component enabled T_2-weighted MRI to capture the internal structure of the tumor with high sensitivity and excellent soft-tissue contrast, highlighting areas with reduced signal intensity due to the NPs. The study demonstrated that these multifunctional NPs could provide complementary information from both CT and MRI. CT was utilized to image the newly formed blood vessels associated with the tumor, which is crucial for targeting in cancer therapy. On the other hand, MRI was employed to evaluate the tumor microenvironment, including distinguishing between hypoxic and oxygenated regions. The integration of tantalum in these NPs was pivotal in enhancing CT imaging, while Fe_3O_4 improved MRI capabilities. This bimodal imaging approach, leveraging the unique electric, magnetic, and optical properties of the tantalum-based NPs, shows significant potential for accurate cancer diagnosis and monitoring, aiding in the visualization of tumor vessels, evaluation of tumor status, and planning of effective therapy strategies.

Jin *et al.* (2017) explored this potential by focusing on early detection and therapy of esophageal cancer, a critical factor in improving patient prognosis and survival rates.[135] They developed a theranostic agent combining multimodal imaging with cancer therapy by synthesizing hollow tantalum oxide (TaO_x) nanoparticles. These nanoparticles were engineered by encapsulating polypyrrole (PPy) and doxorubicin (DOX) in the core and conjugating them with a near-infrared fluorescence dye (NIRDye800) on the shell.

The core/shell nanoparticles exhibited multimodal imaging capabilities, including computed tomography (CT) for preliminary tumor location, photoacoustic (PA) imaging for anatomical localization, and fluorescence imaging for real-time monitoring of tumor margins. Additionally, these nanoparticles featured pH- and thermal-sensitive drug release, enhancing their utility in both imaging and therapeutic contexts. Using a subcutaneous thigh model to simulate early esophageal carcinoma, the nanoparticles demonstrated high imaging contrast between tumors and adjacent tissues, enabling controllable photothermal therapy (PTT) and chemotherapy.

CT imaging, known for its high resolution, depth penetration, and 3D reconstruction capabilities, is a widely used clinical modality. Tantalum's X-ray attenuation coefficient, comparable to gold and higher than iodine, makes these nanoparticles effective CT contrast agents. When tested in a CT phantom with varying nanoparticle concentrations, the CT signals were significantly enhanced. The CT values of PPy&DOX@TaO_x-NIRDye800-PEG nanoparticles increased linearly with concentration, nearly doubling the slope compared to omnipaque. *In vivo* CT imaging, performed by administering PPy&DOX@TaO_x-NIRDye800-PEG nanoparticles to KYSE30 tumor-bearing mice, showed a noticeable increase in CT signal at the tumor site 24 hours post-injection, indicating strong nanoparticle accumulation due to the enhanced permeability and retention effect typical of cancerous tumors.

PA imaging, valued for its deep imaging depth and high spatial resolution, was used to achieve precise anatomical localization of tumors. The PA signals from PPy&DOX@TaO_x-NIRDye800-PEG nanoparticles were dose-dependent. PA imaging of KYSE30 tumor-bearing mice, following intravenous injection of the nanoparticles, showed a progressive increase in PA signal intensity at the tumor site over time, confirming effective nanoparticle accumulation.

NIR-fluorescence imaging, known for its ultra-high sensitivity, was used to precisely identify tumor boundaries. The fluorescence intensity of PPy@DOX@TaO_x-NIRDye800-PEG solutions increased with concentration up to a point before decreasing due to self-quenching effects. *In vivo* fluorescence experiments showed a significant increase in tumor fluorescence intensity following nanoparticle injection, peaking at 24 hours and achieving a 5.7-fold signal enhancement over

surrounding tissues. This enhancement was consistent with the results from CT and PA imaging, demonstrating the nanoparticles' capability to differentiate effectively between tumor and normal tissues.

These findings indicate that the inherent physical properties of PPy&DOX@TaO_x-NIRDye800-PEG nanoparticles provide significant contrast enhancement across CT, PA, and fluorescence imaging modalities. By integrating these three imaging techniques, Jin *et al.* (2015) could precisely localize the tumor and delineate its boundaries, highlighting the substantial promise of tantalum-based nanoparticles in improving cancer diagnostics and treatment.

The exploration of tantalum-based nanomaterials for imaging purposes highlighted their potential to synergistically enhance multiple imaging modalities, providing comprehensive diagnostic and monitoring capabilities for cancer. The study by Dai *et al.* (2017) on MnO_x/Ta_4C_3 composite nanosheets exemplifies this integration, leveraging the unique properties of tantalum for CT, MRI, and PA imaging.[109]

CT imaging is widely utilized in clinical settings due to its high spatial resolution, deep tissue penetration, and ability to provide detailed anatomical and functional information. Tantalum, with its high atomic number ($Z = 73$) and significant X-ray attenuation coefficient, is particularly well-suited as a CT contrast agent. In the study by Dai *et al.* (2017) the MnO_x/Ta_4C_3 composite nanosheets demonstrated a substantial increase in brightness and Hounsfield units (HU) values in CT imaging as the concentration of tantalum increased.[109] This linear relationship between Ta concentration and HU values, along with significantly higher contrast than clinically used iodine-based agents, underscores the efficacy of MnO_x/Ta_4C_3 nanosheets as CT contrast agents.

MRI is another crucial imaging modality that provides high-resolution images of soft tissues without the use of ionizing radiation. The study by Dai *et al.* (2017) highlighted the pH-responsive and glutathione (GSH)-sensitive T1-weighted MRI capabilities of MnO_x-functionalized Ta_4C_3 nanosheets. The MnO_x motifs on the surface of the nanosheets confer these unique imaging properties, allowing them to respond to the mildly acidic and reductive conditions of the tumor microenvironment. This responsiveness is due to the instability of Mn–O bonds in such conditions, releasing Mn^{2+} ions that enhance the interaction with water molecules, thus improving MRI contrast. This pH- and GSH-responsive MRI performance was validated through both *in vitro* and *in vivo* experiments, demonstrating significant MRI-signal enhancement in tumor tissues post-injection of the nanosheets.

PA imaging combines optical and ultrasound imaging, providing high spatial resolution and deep tissue penetration. It is particularly effective for imaging the distribution of nanosheets in tumors due to its sensitivity to optical absorption by contrast agents. In Dai *et al.*'s study, MnO_x/Ta_4C_3 composite nanosheets exhibited enhanced PA signals proportional to the concentration of tantalum. The *in vivo* experiments further confirmed the PA imaging capabilities of these nanosheets, where rapid heating and subsequent acoustic emission signals were observed in tumor tissues following laser pulse illumination. This demonstrated the potential of MnO_x/Ta_4C_3 nanosheets as effective PA contrast agents.

The integration of these three imaging modalities using MnO_x/Ta_4C_3 composite nanosheets offers a multifaceted approach to cancer diagnosis and monitoring. Each modality complements the others by providing unique and valuable information about the tumor. CT imaging offers high-resolution anatomical details, MRI provides soft tissue contrast and functional information related to the tumor microenvironment, and PA imaging adds another layer of detail regarding the distribution and dynamics of the contrast agent within the tumor.

The synergies among these imaging modalities enhance the overall diagnostic capability, allowing for a more comprehensive assessment of tumor characteristics and behaviour. This multimodal approach facilitates better localization and characterization of tumors, enabling precise and effective treatment planning. Furthermore, the ability to monitor treatment responses in real-time through these combined imaging techniques provides invaluable feedback for adjusting therapeutic strategies, thereby improving patient outcomes.

In summary, the study by Dai *et al.* (2017) exemplifies how the unique properties of tantalum-based nanomaterials can be harnessed to create multifunctional contrast agents that synergistically enhance CT, MRI, and PA imaging.[109] This comprehensive imaging capability holds significant promise for advancing cancer diagnosis, treatment planning, and monitoring, ultimately leading to more personalized and effective cancer care.

The study by Zaluzec *et al.* (2024) highlighted the promising potential of tantalum-based nanoparticles (TaO_x) as versatile contrast agents, particularly for their use in various imaging modalities for comprehensive cancer diagnosis and monitoring.[125] The results demonstrate that TaO_x nanoparticles offer superior imaging performance, high local retention, rapid systemic clearance, and low toxicity, positioning them as advantageous compared to traditional contrast agents like Omnipaque and other metal-based nanoparticles such as MVivo Au and Fenestra VC.

TaO_x nanoparticles showed exceptional imaging capabilities in microCT, providing clear and detailed visualization of the ductal tree immediately after infusion with minimal outward diffusion and high homogeneity. This is crucial for image-guided procedures, ensuring that the entire target area is accurately visualized, which is essential for effective treatment planning and execution. The ability of TaO_x to maintain high signal intensity and resolution in both stock PBS solution and 70% ethanol (EtOH) solutions makes it a robust agent for different clinical scenarios, including those requiring high contrast for intricate anatomical structures (Fig. 17).

Beyond microCT, the unique properties of TaO_x suggest its potential applicability in other imaging modalities such as fluoroscopy, MRI, and potentially hybrid imaging techniques. Fluoroscopy, known for its real-time imaging capability, could greatly benefit from the high retention and rapid visualization provided by TaO_x, allowing for precise guidance during interventional procedures. The persistent yet controlled presence of

TaO_x within the target area enhances the visibility of structures, facilitating accurate and timely interventions.

MRI, another critical modality in cancer diagnosis and monitoring, could also leverage the high atomic number and radiodensity of tantalum. Although primarily a CT contrast agent, the paramagnetic properties of tantalum could be explored for developing novel MRI contrast agents, providing enhanced contrast and improved delineation of soft tissues. This dual-modality approach, combining CT and MRI, could offer comprehensive imaging data, combining the high spatial resolution of CT with the superior soft-tissue contrast of MRI.

Moreover, the rapid systemic clearance of TaO_x nanoparticles, coupled with their low toxicity profile, supports their use in longitudinal studies and repeated imaging sessions. This is particularly beneficial for ongoing monitoring of cancer progression or response to therapy, where repeated imaging is necessary. The low toxicity and minimal long-term retention of TaO_x reduce the risk of cumulative side effects, making it a safer option for repeated use. The potential for integrating TaO_x nanoparticles with other imaging modalities, such as PET or SPECT, through functionalization with radioisotopes or other targeting ligands, could further expand their utility. This integration could enable functional imaging, providing insights into the metabolic and molecular characteristics of tumors, alongside the anatomical information provided by CT and MRI. Such multimodal imaging approaches could offer a more comprehensive understanding of cancer biology, aiding in more precise diagnosis, treatment planning, and monitoring.

The study's results showed that TaO_x nanoparticles provided the best imaging performance for nitid visualization of the ductal tree immediately after infusion, low outward diffusion, and high homogeneity. TaO_x had the highest local clearance rate and exhibited low toxicity. TaO_x-containing solutions provided consistent and clear imaging over extended periods, demonstrating significant potential for use in serial imaging sessions necessary for comprehensive cancer monitoring. These results collectively underscore the synergetic potential of TaO_x nanoparticles across multiple imaging modalities for enhanced cancer diagnosis and monitoring, ultimately improving patient outcomes.

5 Photothermal therapy (PTT) applications

5.1 Mechanisms underlying the photothermal effect of tantalum-based nanoparticles

In recent years, the field of cancer therapy has seen significant advancements driven by nanotechnology, particularly in the realm of photothermal therapy (PTT).[136,137] Tantalum-based nanoparticles (TaNPs) have emerged as a promising candidate for PTT due to their unique physical and chemical properties.[138–142] This comprehensive review explores the intricate mechanisms underlying the photothermal effect of TaNPs, highlighting their structural advantages, light interactions, biological effects, and optimization opportunities for cancer treatment.

5.2 Structural advantages of tantalum-based nanoparticles

TaNPs possess several structural advantages that make them well-suited for photothermal applications. Tantalum, a transition metal with a high atomic number, provides excellent X-ray attenuation properties, making TaNPs effective contrast agents for imaging modalities such as computed tomography (CT).[143] Additionally, their plasmonic properties allow TaNPs to efficiently absorb and convert light energy into heat, crucial for inducing the photothermal effect in cancer therapy.[144]

5.3 Interaction of TaNPs with light

Central to the photothermal effect of tantalum nanoparticles (TaNPs) is their interaction with near-infrared (NIR) electromagnetic radiation (700–1100 nm), which penetrates tissues more deeply and is less absorbed by biological components like water and hemoglobin.[145,146] When exposed to NIR light, several mechanisms enhance their photothermal efficacy.

5.3.1 Plasmon resonance. TaNPs exhibit plasmon resonance, where free electrons on their surfaces oscillate in response to incident light.[147] This phenomenon can be precisely tuned by altering the size, shape, and surface chemistry of the nanoparticles, optimizing their absorption efficiency at specific NIR wavelengths.[148,149]

Plasmon resonance occurs when the frequency of incident light aligns with the natural frequency of electron oscillations within the nanoparticle.[150] This alignment results in strong light absorption and enhanced electromagnetic fields near the nanoparticle surface, which is critical for applications in sensing, imaging, and photothermal therapy.[151,152] By modifying nanoparticle properties, the plasmon resonance wavelength can be tailored to desired NIR regions, maximizing performance in biomedical imaging and cancer therapy.[153,154] Additionally, engineering TaNPs with enhanced plasmonic properties could improve biomolecular sensing, solar energy conversion, and optical biosensor sensitivity.[155]

For example, Das and Singh (2021) explored the effects of tantalum pentoxide (Ta_2O_5) nanoparticles in photonic crystal fibers (PCFs) for refractive index (RI) sensing.[156] The integration of Ta_2O_5 nanoparticles significantly enhanced sensor performance due to their high refractive index and ability to facilitate surface plasmon resonance (SPR).

Ta_2O_5 nanoparticles improved phase matching and mode coupling between core-guided and SP modes, enabling effective energy transfer. As the operating wavelength increased, the effective indices of both modes converged, enhancing energy transfer and increasing the loss curve at the resonance wavelength. This was particularly notable at the phase matching condition (1.315 μm), where maximum energy transfer and a sharp loss peak were observed. The study showed that varying Ta_2O_5 layer thickness significantly affected loss spectra and resonance wavelengths. Thicker layers (20 nm to 40 nm) decreased loss values, indicating more efficient SPR due to Ta_2O_5's high refractive index, which required greater energy for the evanescent field to penetrate the layer. This resulted in a redshift of the resonance wavelength from 1.10 μm to 1.48 μm as thickness increased, with a fixed silver (Ag) layer of 50 nm.

Sensitivity was also influenced by Ta_2O_5 thickness, with thinner layers yielding higher sensitivity; the maximum reported sensitivity was 50 000 nm/RIU for a 20 nm Ta_2O_5 thickness. This high sensitivity was attributed to efficient surface plasmon excitation at lower thicknesses, enhancing the evanescent field's interaction with the analyte. Although sensitivity decreased slightly with increasing thickness, it remained superior to that of other materials. The variation in Ta_2O_5 thickness allowed for tuning the sensor's operational region to different analyte RI ranges, facilitating precise detection of refractive index changes in diverse environments. Increasing Ta_2O_5 thickness shifted the operational RI range toward lower values, making it suitable for detecting aqueous media.

In summary, tantalum-based nanoparticles, particularly Ta_2O_5, significantly enhance the plasmonic properties of photonic crystal fiber-based RI sensors. The high refractive index of Ta_2O_5 improves phase matching and mode coupling, resulting in advancements in sensor sensitivity and tunability. This positions Ta_2O_5 as a valuable material for advanced plasmonic sensing applications, delivering high performance and adaptability across various sensing environments.

5.3.2 Photon absorption and energy conversion. Upon absorbing near-infrared (NIR) photons, tantalum nanoparticles (TaNPs) experience electronic excitation, converting photon energy into localized heat. This process involves rapid non-radiative relaxation of the excited electrons within the nanoparticles, leading to a significant temperature increase in their immediate vicinity.[157]

The study by Allam *et al.* (2014) focused on the photon absorption and energy conversion characteristics of tantalum oxynitride (TaON) nanorod arrays for solar water splitting.[158] These nanorods were synthesized through a nitridation process of anodically fabricated tantalum oxide (Ta_2O_5) nanorod arrays, transforming them into TaON. This conversion significantly altered the material's optical properties, resulting in an optical bandgap energy of approximately 2.3 eV, aligning closely with theoretical predictions from density functional theory (DFT), which estimated the bandgap of TaON at around 2.08 eV.

The relatively narrow bandgap of TaON compared to Ta_2O_5 enables effective absorption of visible light, making it suitable for photoelectrochemical (PEC) applications. The study revealed that TaON nanorod films, when illuminated with simulated sunlight (AM 1.5G) in a 1 M KOH electrolyte with a 0.6 V DC bias, achieved visible-light incident photon conversion efficiencies (IPCE) as high as 7.5%. This indicates that TaON nanorods efficiently convert absorbed photons into electrical energy, which is crucial for effective solar water splitting.

The ordered, one-dimensional structure of the TaON nanorods enhances photon absorption and energy conversion. Their alignment promotes efficient charge carrier separation and transport, minimizing recombination losses and improving overall photocurrent generation. Furthermore, TaON's smaller electron effective mass, compared to Ta_2O_5, suggests higher electron mobility, contributing to improved PEC performance.

Incorporating nitrogen into the tantalum oxide lattice to form TaON shifts the valence band to higher energies due to the greater potential energy of the N 2p orbitals compared to O 2p orbitals. This shift results in a narrower bandgap, enhancing the material's ability to absorb visible light. Consequently, TaON nanorods exhibit superior photon absorption and energy conversion characteristics, making them promising candidates for solar energy conversion and PEC water splitting applications.

5.3.3 Heat generation and distribution. Tantalum nanoparticles (TaNPs) exhibit high photothermal conversion efficiency (PCE), making them highly effective in converting light energy into heat.[159] The generated heat induces hyperthermia (typically 42–45 °C), triggering various biological responses in the tumor microenvironment, such as cell membrane disruption, protein denaturation, and eventual cell death.

Landon *et al.* (2015) studied the thermal conductivity of amorphous tantalum oxide (TaO_x) films, revealing key insights for thermal management in memristive devices.[160] Their research focused on how oxygen content affects the thermal properties of these films, which are crucial for understanding heat generation and distribution in memristive applications. Thermal conductivity measurements of TaO_x films using time-domain thermoreflectance (TDTR) showed that the vibrational contribution to thermal conductivity remains constant at approximately 0.7 W mK^{-1}, regardless of oxygen concentration. However, total thermal conductivity varies significantly from 0.7 W mK^{-1} to nearly 5 W mK^{-1}, depending on the oxygen content. This variation is attributed to the electronic contribution, quantifiable using the Wiedemann–Franz law.

The study highlighted a switching mechanism for the dominant thermal carrier in TaO_x films, which can alternate between vibrations and electrons based on oxygen content. This has implications for memristive operation, suggesting that thermal conductivity can be dynamically tuned by adjusting oxygen levels during film deposition or inducing ion migration.

In photothermal applications, Landon *et al.* emphasize the importance of controlling thermal conductivity to manage heat generated by photothermal nanomaterials. Efficient heat generation and distribution are vital for achieving the desired hyperthermia effect in therapeutic applications like cancer treatment. Dynamically controlling the thermal properties of TaO_x films can optimize heat delivery to target areas, enhancing cell membrane disruption, protein denaturation, and cell death within the tumor microenvironment. The results underscore the potential of using TaO_x and other transition metal oxides in applications where thermal conductivity needs active management, not only in memristive devices but also in photothermal therapies that require efficient light-to-heat conversion and precise heat control.

Su *et al.* (2015) provided a comprehensive analysis of the heat generation and distribution characteristics of amorphous tantalum oxide (ATO) films, with significant implications for hyperthermia therapy in cancer treatment.[161] Their research highlighted the exceptional photothermal conversion efficiency of tantalum-based nanoparticles, capable of converting absorbed light energy into heat effectively. This characteristic is crucial for inducing hyperthermia, where controlled heating to temperatures between 42 °C and 45 °C elicits biological

responses, including cell membrane disruption, protein denaturation, and ultimately, cell death, exploiting cancer cells' higher sensitivity to elevated temperatures compared to normal cells.

Su *et al.* measured stress signals in ATO films during annealing at temperatures ranging from 100 °C to 500 °C over $5\frac{1}{2}$ hours.[161] Findings revealed that compressive stresses occurred during the ramp-up phase, while tensile stresses emerged during cooling periods, primarily due to thermal expansion mismatches between tantalum metal and quartz substrates. Notably, net tensile stress-thickness was observed in samples heated between 200 °C and 400 °C, attributed to oxide densification and the desorption of hydration species, confirmed by thermal desorption spectra indicating significant water release from the oxide structure.

At temperatures above 400 °C, net compressive stresses emerged, suggesting additional oxide formation from oxygen uptake from ambient air. The structural changes and stress evolution during heat treatments align well with effective hyperthermia induction requirements. Controlled and efficient heat generation by tantalum-based nanoparticles ensures precise targeting of tumor cells, minimizing collateral damage to surrounding healthy tissues. Moreover, maintaining uniform heat distribution within the tumor microenvironment enhances therapeutic efficacy, achieving the desired hyperthermia temperature range consistently.

In summary, Su *et al.*'s study provides valuable insights into the thermal behavior of tantalum-based materials, reinforcing their potential for photothermal cancer therapy.[161] The efficient heat generation and distribution properties of these nanoparticles, combined with the biological responses induced by hyperthermia, underscore their therapeutic benefits. This research advances our understanding of the material properties of tantalum oxides and highlighted their practical relevance in developing innovative cancer treatment modalities.

5.4 Biological effects of the photothermal effect

The photothermal effect induced by TaNPs exerts profound biological effects that contribute to their therapeutic efficacy in cancer treatment.

5.4.1 Selective tumor cell destruction. Selective tumor cell destruction using tantalum-based nanoparticles (TaNPs) relies on their ability to induce hyperthermia, a process where heat is generated and selectively damages cancer cells while sparing normal tissues.[162,163] This targeted cytotoxicity stems from several critical differences between cancerous and normal cells. Cancer cells typically exhibit higher metabolic rates and altered heat shock responses compared to their healthy counterparts. These factors make cancer cells more vulnerable to the damaging effects of heat.[164,165]

Metabolically active cancer cells have an increased demand for nutrients and energy, which can make them more susceptible to stressors like heat. Moreover, cancer cells often exhibit dysfunctional heat shock responses, which are cellular mechanisms designed to protect against temperature-induced damage.[166–168] When exposed to hyperthermia induced by TaNPs, these compromised heat shock responses in cancer cells fail to adequately mitigate the cellular stress caused by elevated temperatures. In contrast, normal cells with lower metabolic rates and intact heat shock responses are better equipped to maintain cellular homeostasis under thermal stress, thus experiencing less severe damage.[169,170]

This selective vulnerability of cancer cells to TaNP-induced hyperthermia is pivotal in therapeutic strategies aiming to minimize collateral damage to healthy tissues. By exploiting these biochemical differences, TaNPs can effectively target and destroy cancerous tissues while preserving surrounding normal cells, thereby enhancing the efficacy and safety of thermal-based cancer treatments.[171,172] The Figure below illustrates the active and passive uptake of nanoparticles, highlighting the enhanced permeability and retention (EPR) effect that facilitates the accumulation of TaNPs specifically within tumor tissues. This process is critical for the selective heating and subsequent destruction of cancer cells while sparing normal cells.[173] Fig. 18 underscores the importance of nanoparticle uptake mechanisms in achieving targeted cancer therapy through hyperthermia.

The passive uptake of TaNPs is largely governed by the EPR effect, which allows nanoparticles to accumulate more readily in tumor tissues than in normal tissues. Tumors often have leaky vasculature and poor lymphatic drainage, which enhance the permeability and retention of nanoparticles. This effect ensures that a higher concentration of TaNPs can be delivered to the tumor site, where they can be activated to induce hyperthermia.[175–177]

In addition to passive uptake, active targeting strategies can further improve the selective accumulation of TaNPs in tumors. Functionalizing the surface of TaNPs with targeting ligands such as antibodies, peptides, or small molecules can facilitate their binding to specific receptors that are overexpressed on cancer cells.[178,179] This active targeting approach enhances the specificity of TaNP delivery to tumor cells, minimizing off-target effects and further protecting normal tissues.[180]

The combined effects of passive and active targeting result in the effective delivery of TaNPs to tumor sites, where they can be activated to generate localized heat. The heat generated by TaNPs disrupts the tumor microenvironment, leading to the direct destruction of cancer cells through mechanisms such as protein denaturation, membrane disruption, and induction of apoptosis.[12] The localized hyperthermia also enhances the tumor's susceptibility to other therapeutic modalities, including chemotherapy and radiation therapy, by increasing drug uptake and sensitizing cancer cells to radiation-induced damage.[181,182]

Moreover, the hyperthermia induced by TaNPs can modulate the immune response within the tumor microenvironment. The heat can promote the release of tumor antigens, enhance antigen presentation, and stimulate the recruitment and activation of immune cells. These immunomodulatory effects contribute to the overall antitumor response, providing a multifaceted approach to cancer therapy that leverages both direct cytotoxicity and immune-mediated mechanisms.[174,183,184]

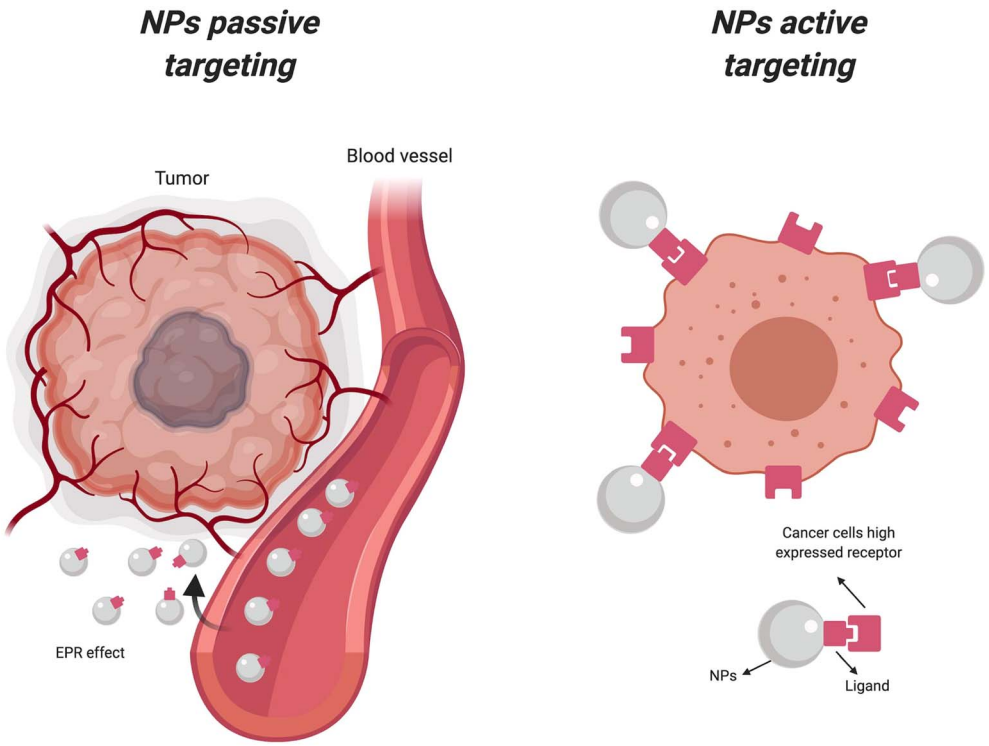

Fig. 18 Active and passive uptake of nanoparticles. NPs, nanoparticles; EPR, enhanced permeability retention (Reproduced from ref. 174 with permission from Portland Press copyright [2024]).

In summary, the use of TaNPs for selective tumor cell destruction through hyperthermia exploits the unique vulnerabilities of cancer cells while preserving normal tissues. The combination of passive and active targeting strategies ensures the effective delivery of TaNPs to tumor sites, where they can generate localized heat to induce direct cytotoxic effects and enhance the antitumor immune response. This multifaceted approach offers a promising avenue for the development of safer and more effective thermal-based cancer treatments.

The selective tumor cell destruction facilitated by hyperthermia generated from tantalum-based nanoparticles is a critical component of the study conducted by Peng *et al.* (2020). The unique properties of these nanoparticles make them particularly effective at targeting cancer cells, which are more susceptible to heat-induced damage compared to normal cells.[185] The hollow mesoporous TaO_x nanospheres, incorporated with ultrasmall CuS nanocrystals, exhibit excellent photothermal performance when exposed to near-infrared (NIR) laser irradiation. This exposure causes a significant increase in temperature specifically within the tumor microenvironment, leading to enhanced therapeutic effects.

Cancer cells, unlike their normal counterparts, often exhibit a higher metabolic rate and are more vulnerable to changes in temperature. The mild hyperthermia induced by the tantalum-based nanoparticles exploits this vulnerability. Upon NIR laser irradiation, the temperature in the tumor increases, resulting in the destruction of cancer cells while sparing normal cells. This selective destruction is a direct consequence of the higher susceptibility of cancer cells to heat, which disrupts their cellular functions and ultimately leads to cell death.

Additionally, the hyperthermia generated by the nanoparticles not only targets cancer cells directly but also enhanced the delivery and efficacy of radiotherapy. The increased temperature improves intratumoral blood flow, facilitating better oxygenation and reducing hypoxia, a common cause of resistance to radiotherapy. The presence of oxygen enhances the generation of reactive oxygen species (ROS) during radiotherapy, leading to increased DNA damage and further promoting the death of cancer cells.

In vivo studies demonstrated that the use of these nanoparticles in combination with radiotherapy almost completely inhibited tumor growth without significant side effects. The tantalum element in the nanoparticles effectively absorbs radiant energy, concentrating it within the tumor and maximizing the radiotherapeutic effect. This triple sensitization approach—combining the direct cytotoxic effects of hyperthermia, improved oxygenation, and enhanced radiotherapy—offers a promising strategy for cancer treatment.

Overall, the selective tumor cell destruction achieved through hyperthermia generated by tantalum-based nanoparticles represents a significant advancement in cancer therapy. The ability to specifically target cancer cells, reduce side effects, and improve the efficacy of existing treatments like radiotherapy underscores the potential of this innovative approach in clinical applications.

Jiao *et al.* (2023) explored the selective destruction of tumor cells through hyperthermia generated by mesoporous tantalum

oxide nanomaterials (PEG@mTa_2O_5).[186] The study demonstrated that the hyperthermia effect of PEG@mTa_2O_5 effectively targets cancer cells due to their heightened susceptibility to heat-induced damage compared to normal cells. This selective cytotoxicity arises from the higher metabolic activity and compromised heat shock response mechanisms of cancerous tissues, which make them more vulnerable to the increased temperatures induced by the nanoparticles.

The research detailed the structural and compositional characteristics of PEG@mTa_2O_5, noting their mesoporous spherical form, stability in various physiological fluids, and efficient uptake by human cardiac microvascular endothelial cells (HCMECs). This selective targeting is crucial because it allows the nanoparticles to focus their cytotoxic effects on malignant cells while sparing normal tissues, thereby reducing potential side effects.

Additionally, Jiao *et al.* observed that PEG@mTa_2O_5 induced significant apoptotic responses in HCMECs, characterized by cell shrinkage, loss of viability, and increased apoptosis markers.[186] The study linked these effects to mitochondrial dysfunction, evidenced by mitochondrial ROS production, $\Delta\Psi_m$ collapse, cytosolic Ca^{2+} overload, and ER stress. These findings underscore the role of mitochondrial and ER stress responses in mediating the cytotoxicity of PEG@mTa_2O_5.

The ability of PEG@mTa_2O_5 to selectively induce apoptosis in endothelial cells further supports its potential as a therapeutic agent in targeting cancer cells. By exploiting the inherent vulnerabilities of cancer cells, such as their altered metabolic states and weakened stress response pathways, PEG@mTa_2O_5 offers a promising strategy for enhancing the efficacy of hyperthermia-based cancer therapies. The study highlighted the dual role of PEG@mTa_2O_5 in providing both direct cytotoxic effects through hyperthermia and indirect effects by modulating cellular stress pathways, contributing to a comprehensive antitumor strategy.

5.4.2 Vascular effects and enhanced permeability. Localized heating by tantalum-based nanoparticles (TaNPs) induces significant vascular effects within tumors, primarily through vasodilation and increased vascular permeability. This process, often referred to as the enhanced permeability and retention (EPR) effect, plays a crucial role in enhancing the accumulation of TaNPs specifically within tumor tissues.[187–189] As described in Fig. 20, this process is similar to how antibody-drug conjugates (ADCs) or multifunctional nanoparticles interact with tumor-specific ligands on the cell surface, leading to receptor-mediated endocytosis and internalization of the nanoparticle or ADC complex. Once inside the cell, the nanoparticle or ADC linker is degraded within the *endo*-lysosomal system, resulting in the release of the therapeutic agent within the tumor cells.

Fig. 19 illustrates the enhanced permeability and retention (EPR) effect within tumors due to localized heating by TaNPs (tantalum-based nanoparticles). This process is crucial for improving the accumulation of TaNPs specifically within tumor tissues, which can enhance the efficacy of nanoparticle-based cancer therapies. Localized heating by TaNPs induces significant vascular effects within tumors. When TaNPs are introduced into tumor tissues and subjected to external stimuli like light or electromagnetic waves, they generate localized heat. This heat affects the surrounding tumor environment, particularly the blood vessels.[190–193]

One major effect of this localized heating is vasodilation, which is the widening of blood vessels. The heat generated by TaNPs causes the smooth muscle cells in the blood vessel walls to relax. This relaxation leads to an increase in the diameter of the blood vessels within the tumor.[194,195] Vasodilation is important because it enhances blood flow to the tumor area, allowing more TaNPs to be delivered to the tumor site. This increased blood flow can also improve the oxygen and nutrient supply to the tumor, which, paradoxically, can make the tumor more susceptible to certain treatments.[196]

Another important effect of localized heating by TaNPs is increased vascular permeability. Vascular permeability refers to the ability of blood vessel walls to allow the passage of substances. The heat from the TaNPs induces gaps between endothelial cells (cells lining the blood vessels), increasing the permeability of the blood vessels and allowing larger molecules, such as nanoparticles, to pass through more easily.[197,198] This increased permeability facilitates the entry of TaNPs into the tumor interstitial space. The ability of TaNPs to penetrate the tumor tissue is critical for their effectiveness, as it allows them to reach and interact with cancer cells directly.[199]

The combination of vasodilation and increased vascular permeability contributes to the EPR effect, which describes the preferential accumulation of nanoparticles in tumor tissue. The EPR effect is characterized by enhanced permeability and retention. Enhanced permeability allows the TaNPs to enter the tumor tissue more easily. Retention occurs because tumor tissues often have poor lymphatic drainage compared to normal tissues. This means that once the TaNPs enter the tumor, they tend to remain there. As a result, the concentration of TaNPs within the tumor tissue is significantly increased.[200–202]

This preferential accumulation of TaNPs within the tumor tissue is beneficial for several reasons. Firstly, it allows for higher concentrations of therapeutic agents at the tumor site, which can improve the effectiveness of treatments such as photothermal therapy, where the heat generated by the nanoparticles can directly damage cancer cells.[203,204] Secondly, by concentrating the therapeutic agents within the tumor, the EPR effect minimizes the impact on surrounding healthy tissues, thereby reducing potential side effects. This targeted delivery approach is a significant advantage in cancer therapy, as it can lead to better patient outcomes and a reduction in treatment-related toxicity.[205–208]

Localized heating by TaNPs induces significant vascular effects within tumors, primarily through vasodilation and increased vascular permeability. These effects enhance the EPR effect, leading to the preferential accumulation of TaNPs within tumor tissues. This process is crucial for improving the efficacy of nanoparticle-based cancer therapies by ensuring that therapeutic agents are concentrated in the tumor, reducing side effects, and improving patient outcomes.[209,210]

For example, Peng *et al.* (2020) also highlighted the significant role of hyperthermia and oxygen release in enhancing the permeability and vascular effects within tumor environments.[185]

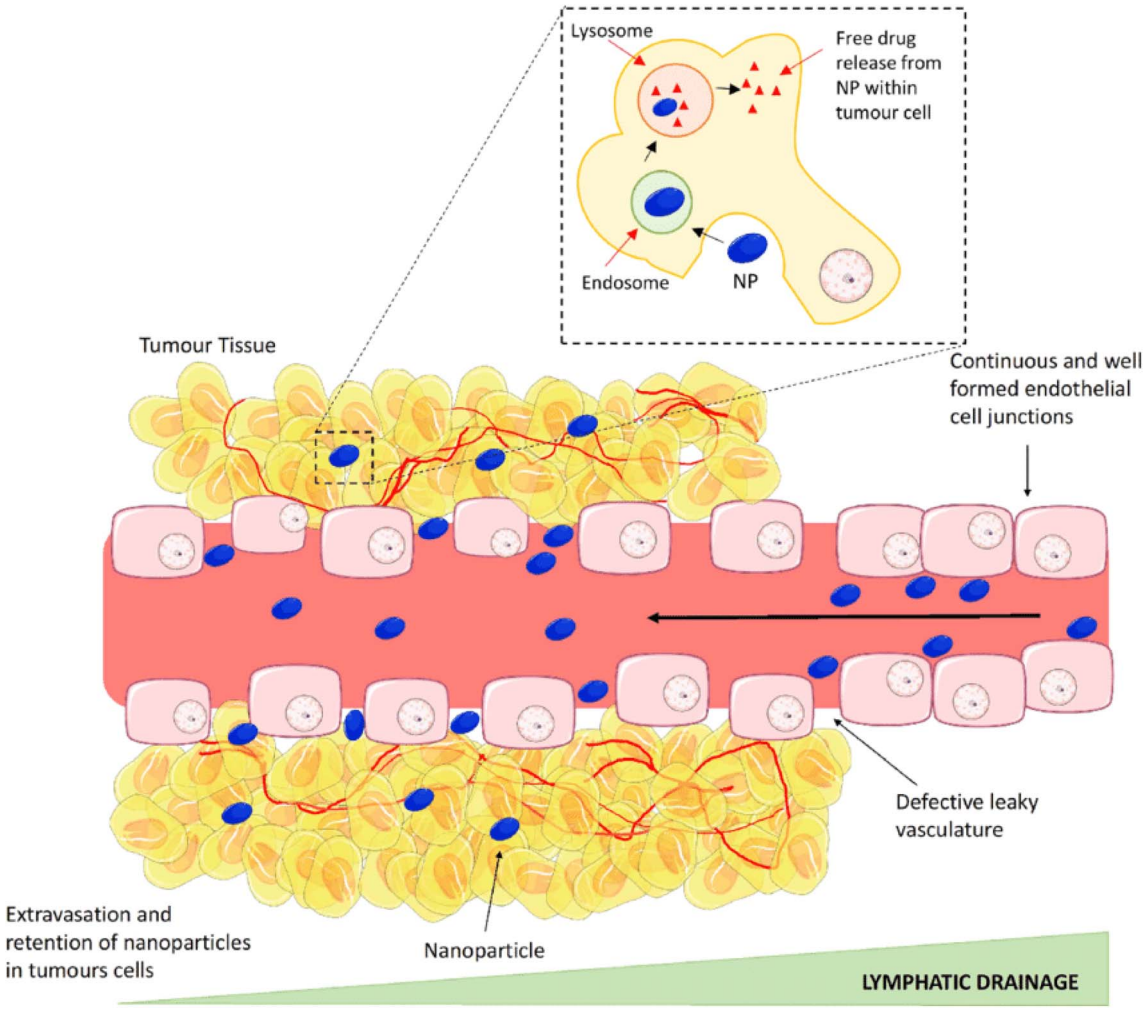

Fig. 19 The enhanced permeability and retention (EPR) effect (Reproduced from ref. 174 with permission from Portland Press copyright [2024]).

The utilization of PEGylated TaO_x-based oxygen-carrying nanoplatforms enables a multifaceted approach to sensitize tumors for radiotherapy, particularly through hyperthermia and improved vascular permeability.

The study demonstrates that near-infrared (NIR) laser-triggered mild hyperthermia results in increased intratumoral blood flow. This increase in blood flow is crucial as it aids in alleviating tumor hypoxia, a common challenge in effective cancer treatment. The mild hyperthermia induced by the NIR laser does not only cause a direct thermal effect but also facilitates the release of oxygen from the nanoplatforms. This oxygen release is mediated by the liquid–gas phase transition of perfluoropentane (PFP) encapsulated within the hollow TaO_x nanospheres. The released oxygen significantly improves the oxygenation of the tumor microenvironment, thereby mitigating the hypoxia-associated resistance to radiotherapy.

Additionally, the study illustrates that this enhanced permeability and retention (EPR) effect is further augmented by the structural properties of the nanospheres. The hollow, mesoporous structure of TaO_x nanospheres allows for efficient encapsulation and gradual release of therapeutic agents and gases. This design ensures a sustained therapeutic effect and improved delivery of oxygen directly to the tumor site, which is essential for overcoming hypoxia and enhancing radiotherapy efficiency.

Moreover, the enhanced vascular effects and permeability brought about by the mild hyperthermia improve the overall delivery and retention of the nanoplatforms within the tumor. This increased vascular permeability ensures that a higher concentration of the therapeutic agents reaches the tumor site, leading to a more effective treatment outcome. The results from the *in vivo* studies show that the combination of hyperthermia, enhanced permeability, and oxygen release from the nanoplatforms leads to almost total inhibition of tumor growth without significant side effects, highlighting the potential of this approach in multi-sensitizing tumor radiotherapy.

In summary, Peng *et al.* (2020) effectively showcases how the combination of hyperthermia and enhanced permeability *via* tantalum-based nanoparticles can significantly improve the efficacy of radiotherapy by increasing oxygenation and blood flow within tumors.[185] This strategy addresses the challenge of tumor hypoxia and enhances the delivery and retention of

therapeutic agents, paving the way for more effective cancer treatments.

Jiao *et al.* (2023) investigated the localized heating effects of mesoporous tantalum oxide nanoparticles (PEG@mTa_2O_5) and their implications for vascular dynamics within tumors.[186] Their study revealed that the hyperthermia generated by PEG@mTa_2O_5 induces significant vascular effects, including vasodilation and increased vascular permeability. This phenomenon is critical as it contributes to the enhanced permeability and retention (EPR) effect, a well-established mechanism in oncology.

The EPR effect describes how nanoparticles, such as PEG@mTa_2O_5, preferentially accumulate in tumor tissues due to their leaky vasculature and impaired lymphatic drainage, characteristics commonly found in solid tumors. By inducing vasodilation and increasing vascular permeability, PEG@mTa_2O_5 facilitates greater nanoparticle extravasation from blood vessels into the tumor interstitium. This accumulation enhances the local concentration of therapeutic agents delivered *via* nanoparticles, thereby improving treatment efficacy while minimizing systemic toxicity.

Jiao *et al.* demonstrated that PEG@mTa_2O_5's ability to locally heat tumor tissues not only targets cancer cells directly through hyperthermia but also enhances the overall therapeutic effect by promoting nanoparticle accumulation within the tumor microenvironment.[186] This dual mechanism of action underscores the potential of PEG@mTa_2O_5 as a promising strategy for enhancing the delivery and efficacy of cancer treatments, leveraging the EPR effect to maximize therapeutic outcomes while reducing adverse effects on healthy tissues.

5.5 Immunomodulatory effects

The photothermal effect of tantalum-based nanoparticles (TaNPs) extends beyond direct tumor cell destruction; it significantly modulates the tumor microenvironment to enhance antitumor immune responses. TaNPs convert light energy into heat, inducing localized hyperthermia within tumors.[211,212] This localized heating leads to notable vascular effects, primarily vasodilation and increased vascular permeability, contributing to the enhanced permeability and retention (EPR) effect. This effect facilitates the accumulation of TaNPs in tumor tissues, as illustrated in Fig. 20.[213,214] When TaNPs are introduced into tumors and activated by external stimuli, they generate heat that impacts the surrounding blood vessels.[215–217]

One critical outcome of this heating is vasodilation, which widens blood vessels by relaxing smooth muscle cells in their walls. This increase in vessel diameter enhances blood flow to the tumor, allowing more TaNPs to reach the site. Improved blood flow can also supply more oxygen and nutrients to the tumor, potentially increasing its susceptibility to treatments.[218–221] Increased vascular permeability is another effect of localized heating. The heat causes gaps between endothelial cells, allowing larger molecules, including nanoparticles, to pass more easily into the tumor interstitial space. This penetration is vital for the effectiveness of TaNPs, enabling direct interaction with cancer cells.[222–225]

The combination of vasodilation and increased permeability enhances the EPR effect, characterized by preferential accumulation of nanoparticles in tumor tissues. Enhanced permeability allows TaNPs to enter easily, while poor lymphatic drainage in tumors results in their retention, leading to significantly increased concentrations of TaNPs.[226–229] This preferential accumulation has several advantages: it increases the concentration of therapeutic agents at the tumor site, improving the effectiveness of treatments like photothermal therapy, and minimizes impacts on surrounding healthy tissues, thereby reducing side effects. This targeted delivery is crucial for better patient outcomes and lower treatment-related toxicity.[230–232]

In summary, localized heating by TaNPs induces vascular effects—primarily vasodilation and increased permeability—enhancing the EPR effect and improving nanoparticle-based cancer therapies. This mechanism ensures that therapeutic agents are concentrated in tumors, reducing side effects and improving patient outcomes.[233–235]

The photothermal effect of TaNPs also promotes immunogenic cell death (ICD), characterized by the release of damage-associated molecular patterns (DAMPs) and tumor-associated antigens (TAAs) from dying tumor cells.[236] The heat generated by TaNPs exposes these immunostimulatory signals, such as calreticulin, which alert the immune system to recognize and attack tumor cells more effectively.[237,238] Moreover, heat-induced changes stimulate innate immune cells, like dendritic cells (DCs) and macrophages, enhancing their capacity to present TAAs to T cells and initiate adaptive immune responses.[239–241] Fig. 21 illustrates the migration of activated CD_4^+ and CD_8^+ T cells to lymph nodes, priming them to attack tumor cells.[242–245] Increased vascular permeability also facilitates TaNP entry into tumors, critical for their effectiveness.[246,247] The combined effects of vasodilation and increased permeability contribute to the EPR effect, allowing TaNPs to preferentially accumulate in tumors, where they can remain due to poor lymphatic drainage.[248–250]

The immunomodulatory effects of TaNPs can synergize with immunotherapy strategies. For example, TaNP-induced hyperthermia may enhance the efficacy of immune checkpoint inhibitors by creating a more favorable immune landscape, promoting ICD, and improving antigen presentation. This approach could help overcome tumor immune evasion mechanisms and boost the effectiveness of therapies aimed at enhancing antitumor immune responses.[248,249] Overall, the immunomodulatory effects of TaNPs through photothermal properties present promising opportunities for improving long-term antitumor immunity. By leveraging these effects, researchers aim to develop innovative therapeutic strategies that target tumor cells while also engaging the immune system's ability to eradicate cancer cells.

In a nutshell, Fig. 21 illustrates the interplay between photothermal therapy with TaNPs and the immune system.[136] The conversion of light energy into heat induces localized hyperthermia, leading to ICD and the release of immunostimulatory signals, activating both innate and adaptive immune responses. This enhances the overall antitumor immune response and

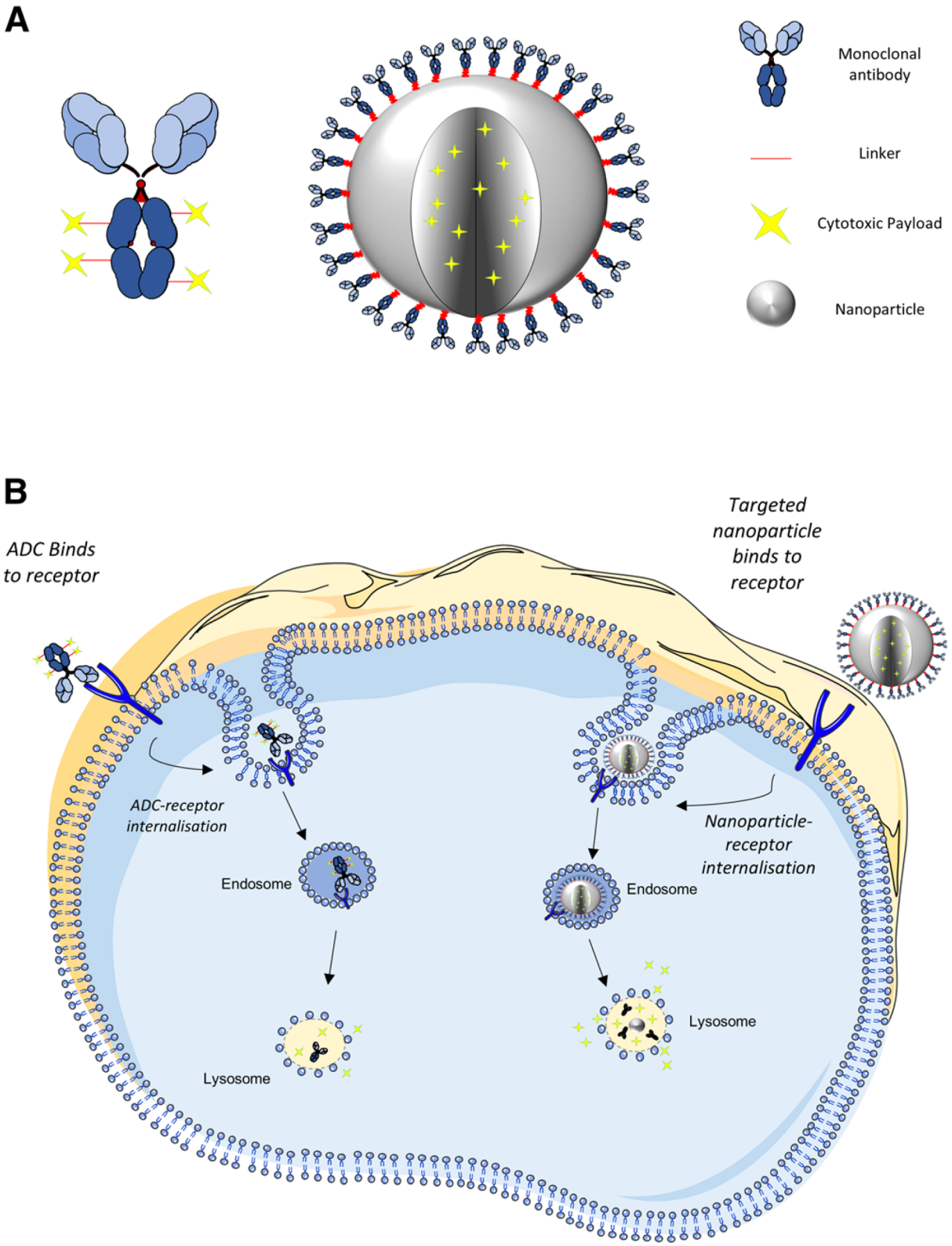

Fig. 20 Schematic representation highlighting (A) the conceptual structure of an ADC and a multifunctional antibody conjugated nanoparticle and (B) internalisation, breakdown, and drug release within the cell. The tumour-specific ligand of the ADC or nanoparticle interacts with and binds to the cell surface expressed antigen. Upon binding, the antigen–protein complex becomes internalised *via* receptor mediated endocytosis. The nanoparticle or ADC linker is degraded within the *endo*-lysosomal system, resulting in drug release within the cell (Reproduced from ref. 174 with permission from Portland Press copyright [2024]).

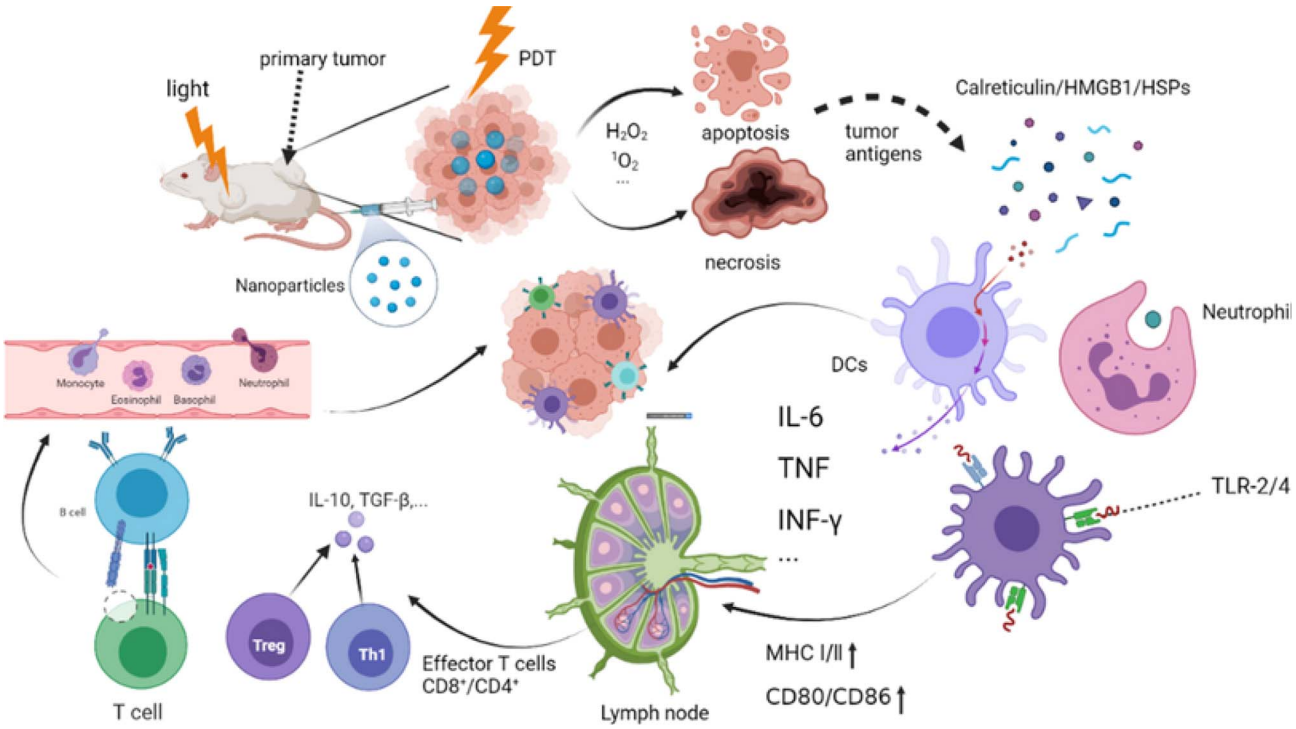

Fig. 21 The mechanism of photodynamic triggering immunotherapy. Photodynamic therapy tumor cell apoptosis and necrosis, releasing tumor antigens and injury-related molecular patterns, including CRT, HSPs, and HMGB1. Activated CD_4^+ and CD_8^+ T cells are gathered in the lymph nodes and kill the tumor cells by inherent immunity and adaptive immunity. TLR-2/4: toll-like receptor on the surface of the mononuclear macrophages; MHC I/II: Major histocompatibility class I/II (Reproduced from ref. 136 with permission from Wiley online Library copyright [2024]).

provides a basis for potential synergistic effects with existing immunotherapy strategies.

The study by Peng *et al.* (2020) highlighted the immunomodulatory effects of their PEGylated TaO_x-based oxygen-carrying nanoplatform.[185] The photothermal effect of these tantalum-based nanoparticles (TaNPs) was shown to significantly modulate the tumor microenvironment. This modulation was particularly evident through the promotion of immunogenic cell death, a process wherein dying tumor cells release signals that attract and activate immune cells. This form of cell death is crucial because it transforms the tumor into an *in situ* vaccine, stimulating the immune system to recognize and attack residual cancer cells.

This immunogenic cell death led to an enhanced infiltration of immune cells, particularly cytotoxic T lymphocytes, into the tumor site. The presence of these immune cells is essential for mounting an effective and sustained antitumor response. By converting the tumor into an environment that promotes immune activation, the TaNPs not only targeted the tumor cells directly but also provided a long-term immunological memory against the cancer. Additionally, this immunomodulatory effect was found to potentially synergize with existing immunotherapy strategies. By improving the immune system's ability to detect and respond to cancer cells, the nanoplatform could enhance the efficacy of immunotherapies, which rely on a robust immune response to eliminate tumors. The combination of TaNP-induced immunogenic cell death and immunotherapy could therefore offer a powerful strategy for achieving long-term antitumor immunity.

Overall, Peng *et al.* (2020) demonstrated that their PEGylated TaO_x nanoplatform could effectively reprogram the tumor microenvironment to support immune-mediated tumor eradication.[185] This dual action, combining direct photothermal therapy with the stimulation of an antitumor immune response, highlighted the potential of their approach to contribute significantly to cancer treatment.

A separate study conducted by Sun *et al.* (2022), investigated the multifaceted effects of tantalum-based nanoparticles (TaNPs), particularly focusing on their immunomodulatory potential and photothermal properties within the context of cancer therapy.[205] The photothermal effect of TaNPs extends beyond mere tumor cell destruction; it serves as a pivotal mechanism in reshaping the tumor microenvironment to enhance antitumor immune responses. This capability arises from TaNPs' ability to convert light energy into localized heat, inducing hyperthermia specifically within the tumor site.

Furthermore, Sun *et al.* (2022) highlighted that the localized hyperthermia induced by TaNPs can lead to the release of tumor-associated antigens and damage-associated molecular patterns (DAMPs).[205] These molecular signals are crucial in promoting dendritic cell maturation and antigen presentation, thereby facilitating the activation of cytotoxic T lymphocytes (CTLs) and other effector immune cells. This process effectively

primes the immune system to recognize and target tumor cells beyond the immediate vicinity of TaNPs' photothermal action.

Moreover, the immunomodulatory effects of TaNPs include their impact on regulatory T cells (Tregs) and myeloid-derived suppressor cells (MDSCs). Sun *et al.* (2022) discussed how hyperthermia induced by TaNPs can selectively inhibit Tregs while promoting the polarization of MDSCs towards an anti-tumor phenotype.[205] This dual effect helps to alleviate immunosuppression within the tumor microenvironment, further enhancing the efficacy of antitumor immune responses.

In summary, Sun *et al.* (2022) underscores the transformative potential of TaNPs not only as agents for direct tumor ablation *via* photothermal therapy but also as potent tools for reprogramming the tumor immune landscape.[205] Their findings advocate for TaNPs as promising candidates in synergistic cancer therapies that harness both photothermal effects and immunomodulation to combat tumor progression effectively.

5.5.1 Optimization of TaNPs for photothermal therapy. Optimizing TaNPs for effective photothermal therapy involves several critical considerations aimed at maximizing their therapeutic potential and minimizing off-target effects.

5.5.1.1 Surface functionalization. Functionalizing tantalum-based nanoparticles (TaNPs) with targeting ligands significantly enhances their specificity for cancer cells, thereby improving tumor uptake and reducing systemic clearance. Targeting ligands, such as antibodies, peptides, or small molecules, can be designed to recognize and bind to specific markers or receptors that are overexpressed on the surface of cancer cells. This targeted approach ensures that the nanoparticles are more efficiently taken up by the cancer cells, leading to higher concentrations of the therapeutic agent at the tumor site. Consequently, this targeted delivery minimizes the exposure of non-cancerous tissues to the nanoparticles, thereby reducing systemic clearance and potential side effects.[105–107]

Surface modifications of TaNPs also play a crucial role in enhancing their biocompatibility and stability in physiological environments. By attaching hydrophilic polymers like polyethylene glycol (PEG) or other stabilizing agents to the surface of the nanoparticles, researchers can create a "stealth" effect that helps evade the immune system, prolonging the circulation time of the nanoparticles in the bloodstream.[249,250] These modifications can also prevent protein adsorption and aggregation, which are common challenges that nanoparticles face in the complex biological environment of the human body. Enhanced biocompatibility ensures that the nanoparticles do not induce adverse immune responses or toxicity, while improved stability ensures that the nanoparticles maintain their structural integrity and functional properties until they reach their target site.[251,252] Together, these surface modifications make TaNPs more effective and safer for use in medical applications, particularly in targeted cancer therapy.[253,254] In line with this, the study by Song *et al.* (2017) highlighted the impact of surface modification on the effectiveness of tantalum oxide (TaO_x) nanoparticles.[255]

Song *et al.* (2017) reported on the surface modification of nanoparticles with the radiosensitizer tantalum oxide (TaO_x) and further functionalized these nanoplatforms with polyethylene glycol (PEG).[255] This modification strategy aimed to enhance the therapeutic efficacy and biocompatibility of the nanoparticles. The designed nanoparticles demonstrated a significant improvement in tumor cell oxygenation, which is crucial for effective radiotherapy (RT). By solving the issues associated with RT in *in vivo* models, these modifications ensured better treatment outcomes.

The study emphasized the role of hemoglobin, a component rich in red blood cells (RBCs), as an O_2 carrier due to its excellent oxygen-carrying capability. Hemoglobin's ability to enhance tumor oxygenation was leveraged by incorporating it into the design of the nanoparticles. This approach helped to overcome the hypoxic conditions commonly found in tumors, which often hinder the effectiveness of RT. By improving the oxygenation of tumor cells, the TaO_x nanoparticles facilitated more effective radiation-induced damage to cancer cells.

PEGylation, or the attachment of PEG chains to nanoparticles, is a well-known strategy to enhance the biocompatibility and stability of nanoparticles in physiological environments. In Song *et al.*'s study, PEGylation played a crucial role in reducing the systemic clearance of the nanoparticles, thereby prolonging their circulation time in the bloodstream.[255] This increased circulation time allowed for greater accumulation of the nanoparticles within the tumor site, improving their therapeutic efficacy.

Moreover, the surface modification with TaO_x not only enhanced the radiosensitizing properties of the nanoparticles but also improved their stability and biocompatibility. The functionalization of the nanoparticles ensured that they remained stable in the physiological environment and interacted favorably with biological systems. This stability is essential for maintaining the therapeutic efficacy of the nanoparticles throughout the treatment process.

In summary, the study by Song *et al.* demonstrates the importance of surface modifications in enhancing the therapeutic potential of TaO_x nanoparticles.[255] By functionalizing these nanoparticles with PEG and utilizing hemoglobin for improved oxygenation, the researchers were able to enhance tumor uptake, improve biocompatibility, and increase the stability of the nanoparticles in physiological environments. These modifications address critical challenges in cancer therapy, paving the way for more effective and targeted treatments.

In the study by Jin *et al.* (2015) on the cellular uptake of HA-functionalized TaO_x nanoparticles (NPs), the research focuses on how modifying these nanoparticles with hyaluronic acid (HA) enhances their specificity for cancer cells, particularly MDA-MB-231 breast cancer cells.[107] Fluorescence microscopy images showed that MDA-MB-231 cells incubated with TaO_x@Cy7-PEG-HA NPs at varying concentrations exhibited increased fluorescence intensity with higher nanoparticle concentrations, indicating enhanced cellular uptake. Quantitative analysis through a microplate reader further confirmed that the cellular uptake efficiency of HA-functionalized NPs was significantly higher than that of non-functionalized NPs at lower concentrations.

The study demonstrated that the higher uptake of HA-functionalized NPs was mediated through HA receptors on the cancer cells. This was confirmed by using HA as a competitive inhibitor, which significantly reduced the uptake of HA-functionalized NPs, thereby proving that the increased uptake was due to HA receptor-mediated endocytosis. Additionally, the research highlighted that cellular uptake efficiency increased with both nanoparticle concentration and incubation time, with the uptake efficiency plateauing after 4 hours, suggesting an optimal incubation period for maximum uptake.

These findings imply that HA-functionalized TaO_x NPs can serve as effective drug delivery carriers, facilitating higher intracellular accumulation of therapeutic agents. This targeted approach minimizes systemic clearance and potentially reduces side effects, thereby enhancing therapeutic efficacy. The HA functionalization of TaO_x NPs significantly improves their specificity and uptake by MDA-MB-231 cells, making these nanoparticles promising for targeted cancer therapy and drug delivery systems.

5.5.1.2 Size and shape control. The size and shape of Tantalum-based Nanoparticles (TaNPs) play critical roles in determining their optical and photothermal properties, which are essential for their performance in applications such as photothermal therapy (PTT) and imaging. Smaller TaNPs have a higher surface area-to-volume ratio compared to larger particles. This increased surface area enhances the light absorption capabilities of the nanoparticles, leading to higher efficiency in converting absorbed light into heat. Consequently, more photons interact with the surface of the nanoparticles, which is particularly beneficial for photothermal applications where the goal is to maximize heat generation upon light irradiation. The enhanced light absorption due to the high surface area-to-volume ratio of smaller TaNPs translates directly into more efficient heat generation. This efficiency is crucial for applications like PTT, where the localized heating effect induced by the nanoparticles can be used to ablate cancer cells.[256–259]

Nanoparticles with anisotropic shapes, such as rods, shells, or other non-spherical geometries, exhibit unique optical properties due to their shape. These shapes can be engineered to tune the plasmonic resonance of the nanoparticles, which is the collective oscillation of electrons in response to light. By adjusting the shape, it is possible to shift the plasmonic resonance to the NIR region, which is particularly useful for biomedical applications due to the deep tissue penetration of NIR light. The ability to tune the plasmonic resonance of TaNPs through shape control is pivotal for optimizing their performance in specific applications.[260–263]

The integration of size and shape effects is exemplified in the work of Jin *et al.* (2014), where TaO_x nanoparticles (NPs) were synthesized with an average diameter of 7 nm. These uniformly small nanoparticles exhibit significant photothermal effects under near-infrared (NIR) laser irradiation.[106] The study demonstrated that the small size of TaO_x NPs allowed for excellent light absorption and efficient heat generation, crucial for their application in PTT. The spherical shape of these nanoparticles also contributed to their uniform optical properties, enhancing their overall photothermal efficiency. Jin *et al.* highlighted that the uniformity in size and shape of TaO_x NPs resulted in stable and reproducible photothermal effects, underscoring the importance of controlling these parameters in the synthesis of TaNPs for biomedical applications.

In summary, the size and shape of TaNPs significantly influence their optical and photothermal properties. Smaller nanoparticles with higher surface area-to-volume ratios exhibit enhanced light absorption and heat generation, while specific shapes can be engineered to tune plasmonic resonance for optimal NIR absorption. The work of Jin *et al.* (2014) exemplifies how controlling these parameters can lead to the development of TaNPs with superior photothermal properties for effective biomedical applications.[106]

Although the investigation by Tiwari *et al.* (2020) primarily focuses on the glass transition and Kauzmann temperatures of silver (Ag) and tantalum (Ta) nanoparticles, certain aspects of their findings can be linked to the significant roles that the size and shape of Tantalum-based Nanoparticles (TaNPs) play in determining their optical and photothermal properties, which are crucial for applications such as photothermal therapy (PTT) and imaging.[264] Their study demonstrates that the thermal properties of nanoparticles, including TaNPs, are highly dependent on their size and shape. For instance, the authors reported that the Kauzmann temperature decreases significantly with a decrease in nanoparticle size, especially for dimensions below 5 nm. This size dependency is attributed to the increased surface-to-volume ratio at smaller scales, which alters the material's thermodynamic properties.

In the context of TaNPs, the shape also plays a critical role. Tiwari *et al.* (2020) found that different shapes of nanoparticles (*e.g.*, icosahedral, spherical, octahedral, tetrahedral) exhibit distinct glass transition temperatures, with icosahedral shapes generally showing the highest glass transition temperature and tetrahedral shapes the lowest for a constant size.[264] This variation is due to the different coordination numbers and surface atom distributions in various shapes, which affect the nanoparticles' overall stability and properties.

Linking these results to the optical and photothermal properties of TaNPs, it can be inferred that the shape-dependent thermal stability observed by Tiwari *et al.* could influence the nanoparticles' performance in photothermal applications.[264] For example, nanoparticles with higher thermal stability (like icosahedral shapes) might maintain their structure better under the high temperatures generated during photothermal therapy, potentially improving their efficacy in cancer treatment.[265] Similarly, the significant impact of size on the thermal properties suggests that smaller TaNPs, with their higher surface-to-volume ratios, might have enhanced optical absorption and heat generation capabilities, making them more effective for PTT.

Moreover, the study's observation that the thermal properties of TaNPs change with size and shape supports the idea that these parameters can be tuned to optimize the nanoparticles for specific biomedical applications. By carefully selecting the size and shape of TaNPs, researchers could potentially develop nanoparticles with superior optical and photothermal properties tailored for targeted cancer therapies.

Therefore, the insights from Tiwari *et al.* (2020) on the size and shape-dependent thermal properties of TaNPs align with the understanding that these physical characteristics are crucial for determining the nanoparticles' optical and photothermal performance, highlighting their potential usefulness in medical applications involving the treatment of cancer cells.

6 Biocompatibility and safety

Ensuring the biocompatibility and safety of TaNPs is essential for clinical translation. Surface coatings, such as polyethylene glycol (PEG) and silica, play a pivotal role in enhancing stability, reducing immunogenicity, and prolonging the circulation time of TaNPs *in vivo*. This, in turn, enhances the overall therapeutic efficacy and safety profile of TaNP-based photothermal therapy (PTT).[174,266]

Surface coatings on nanoparticles create a barrier that prevents direct contact between the nanoparticles and biological tissues, significantly reducing the potential for toxic interactions. PEGylation, or coating nanoparticles with polyethylene glycol, is one of the most widely used methods to improve biocompatibility. PEG is known for its ability to create a "stealth" effect, which reduces protein adsorption and subsequent recognition by the immune system. This not only prolongs the circulation time of the nanoparticles but also reduces the likelihood of an immune response, thereby enhancing the therapeutic window for treatments like PTT.[174,256,266]

Ji *et al.* (2022) provided an illustrative example of how these principles are applied. Their research focuses on the use of poly(vinylpyrrolidone) (PVP)-coated tantalum-based nanoparticles (Ta@PVP NPs) for the combined treatment of primary tumors and metastatic sentinel lymph nodes (SLNs) in breast cancer. The study highlighted several key benefits of using surface-coated TaNPs.[267]

The PVP coating on TaNPs helps in maintaining the stability of the nanoparticles in the biological environment. This coating prevents the aggregation of nanoparticles and ensures that they remain in a dispersed state, which is critical for effective delivery to the target sites. Additionally, the PVP coating minimizes the immune system's recognition of the TaNPs. This reduction in immunogenicity is crucial for preventing adverse immune responses that could lead to rapid clearance of the nanoparticles from the body and potential side effects.

By utilizing PVP coating, Ji *et al.* (2022) achieved significant advancements in improving the biocompatibility and safety of TaNPs, which is critical for their potential use in clinical applications.[267] This research underscores the importance of surface modifications in translating TaNPs into viable therapeutic agents.

The study by Leng *et al.* (2006) explores the biocompatibility of tantalum and tantalum oxide films synthesized through pulsed metal vacuum arc source deposition and subsequent heat oxidation.[266] Tantalum films were prepared on silicon wafers and oxidized in air at 700 °C to form tantalum oxide films. These films were subjected to biocompatibility using using human umbilical vein endothelial cells (HUVEC).

In vitro tests demonstrated that the adherence, growth, morphology, and proliferation of endothelial cells on tantalum and tantalum oxide films were significantly better than on 316L stainless steel and commercially pure titanium (CP-Ti). The endothelial cells on the tantalum and tantalum oxide films formed a perfect monolayer and maintained their natural cobblestone shape, indicating excellent biocompatibility. In contrast, the cells on 316L stainless steel and CP-Ti showed deformation and lower cell density.

The findings indicated that tantalum and tantalum oxide films meet the requirements for use as coatings on blood-contacting devices, such as stents. The excellent endothelialization properties of these films suggest they could help reduce restenosis by promoting rapid re-endothelialization and vascular healing.

These biocompatibility results have significant implications for the application of tantalum oxide nanoparticles in photothermal therapy (PTT) for cancer treatment. The high biocompatibility of tantalum oxide means that when these nanoparticles are used for PTT, they are less likely to cause adverse reactions or toxicity in the body. This enhances the safety profile of the nanoparticles, making them suitable for clinical applications.

Moreover, the ability of tantalum oxide films to support endothelial cell growth and proliferation indicates that tantalum oxide nanoparticles could potentially be used to target tumor vasculature. In PTT, these nanoparticles can be directed to the tumor site, where they absorb near-infrared light and convert it into heat, effectively ablating cancer cells without harming surrounding healthy tissue.

The biocompatibility of tantalum oxide nanoparticles, as demonstrated by Leng *et al.* (2006), supports their use in PTT by ensuring that the treatment is not only effective in destroying cancer cells but also safe for the patient. This dual benefit of efficacy and safety is crucial for the successful clinical translation of nanoparticle-based cancer therapies.

Yang *et al.* (2019) conducted an extensive biocompatibility evaluation of tantalum (Ta) nanofilms both *in vitro* and *in vivo*.[268] The *in vitro* studies utilized RAW 264.7 and MC3T3-E1 cells to assess the cellular response to the Ta nanofilms. The CCK-8 assay results indicated a significant increase in cell viability for the Ta groups compared to the titanium (Ti) control group, with nearly 30% more cell growth on the Ta-III surface after seven days. This enhanced proliferation was further confirmed through fluorescence staining, which demonstrated better cell-sample surface interactions in the Ta groups. These results suggest that the Ta nanofilms provide a more conducive environment for the proliferation of osteoblasts and macrophages compared to Ti, underscoring their superior biocompatibility *in vitro*.

To ensure that the Ta nanofilms were biocompatible *in vivo*, a mouse subcutaneous implantation model was employed. After 30 days, the study involved preparing pathological sections of major organs and performing routine blood tests and biochemical analyses. The results showed no significant differences in the morphologies of major organs, nor were there any discrepancies in blood or biochemical test outcomes among

the groups. This indicates that the Ta nanofilms did not exert long-term toxicity on the major organs, confirming their biocompatibility in a living organism.

The observed biocompatibility of Ta nanofilms has important implications for their use in photothermal ablation (PTA) of cancer cells. PTA relies on the conversion of light energy into heat to selectively destroy cancer cells, necessitating materials that can efficiently convert energy while being biocompatible to avoid adverse reactions in the body. The favorable *in vitro* and *in vivo* biocompatibility of Ta nanofilms, as demonstrated by Yang *et al.*, indicates that they are likely to be well-tolerated when used in biomedical applications such as PTA. Their ability to promote cell proliferation without causing long-term toxicity makes them promising candidates for medical treatments that require both high efficacy and safety.

Moreover, the enhanced biocompatibility of Ta nanofilms over Ti surfaces suggests that Ta-based materials could reduce potential complications associated with implant rejection or inflammation. This aspect is crucial for cancer therapies, where the primary goal is to eradicate cancer cells without compromising the patient's overall health. The Ta nanofilms' biocompatibility supports their potential use in PTA by ensuring that the material can be safely integrated into the body, providing a stable platform for effective cancer treatment without eliciting significant adverse biological responses.

The study by Kang *et al.* (2021) focuses on exploring the biocompatibility of tantalum-based nanoparticles (Ta-NPs) and their role in promoting osteoblast proliferation through autophagy induction.[269] The MC3T3-E1 osteoblast cells were treated with 20 μg per mL Ta-NPs, with or without pretreatment with PI3K/Akt/mTOR pathway inhibitors (LY294002, Triciribine, Rapamycin).

The findings suggest that Ta-NPs promote osteoblast proliferation by activating autophagy. When pretreated with pathway inhibitors, significant changes in protein expressions were observed, particularly the downregulation of the p-Akt/Akt ratio and upregulation of autophagy protein LC3-II/LC3-I. This indicates that the PI3K/Akt/mTOR signalling pathway plays a crucial role in Ta-NPs-induced autophagy and proliferation. The inhibitors also increased apoptosis and arrested the G1 phase of the cell cycle, further highlighting the involvement of this pathway.

In terms of biocompatibility, Ta-NPs exhibit excellent potential in medical applications, particularly in promoting bone formation and healing. Their ability to induce osteoblast proliferation at low concentrations, while maintaining cell viability, underscores their utility in biomedical contexts. However, at higher concentrations, Ta-NPs may inhibit proliferation due to increased autophagy and oxidative stress. This study reinforces the biocompatibility of Ta-NPs, showing that they can be effectively used to enhance cellular functions critical for bone health, especially when modulating the PI3K/Akt/mTOR pathway. Further research is needed to fully understand the signalling mechanisms and optimize the concentrations for therapeutic applications.

The photothermal effect of tantalum-based nanoparticles represents a sophisticated yet promising approach in the landscape of cancer therapy. By harnessing their unique physicochemical properties, particularly their ability to convert light energy into localized heat, TaNPs offer a targeted and minimally invasive strategy for treating solid tumors. Ongoing advancements in nanoparticle design, including surface functionalization, size optimization, and biocompatibility enhancement, hold tremendous potential for further improving the efficacy and clinical applicability of TaNP-based photothermal therapy. As research progresses, TaNPs are poised to play a pivotal role in the future of personalized cancer treatment, integrating seamlessly with existing therapeutic modalities to achieve comprehensive and effective management of malignancies.

7 Studies demonstrating the efficacy of tantalum-based nanoparticles in PTT for cancer treatment

The application of nanotechnology in cancer treatment has revolutionized therapeutic approaches, offering novel strategies that target tumors with precision while minimizing damage to healthy tissues. Among these advancements, tantalum-based nanoparticles (TaNPs) have emerged as promising candidates for photothermal therapy (PTT), a non-invasive treatment modality that utilizes light-absorbing nanoparticles to selectively ablate cancerous cells through localized heating.[266,269]

Tantalum, a biocompatible and chemically stable metal, exhibits unique properties that are particularly advantageous for PTT. TaNPs possess a high atomic number, enabling efficient absorption of near-infrared (NIR) light—a wavelength that can penetrate deep into tissues without causing harm. Upon exposure to NIR light, TaNPs rapidly convert light energy into heat through the photothermal effect. This process leads to localized hyperthermia within the tumor microenvironment, ultimately inducing thermal damage to cancer cells while sparing surrounding healthy tissues.[17,267,268]

Numerous preclinical studies have provided compelling evidence of TaNPs' efficacy in PTT for various types of cancer. These studies have demonstrated that TaNPs can accumulate selectively within tumors due to their small size and surface modifications, which facilitate enhanced permeability and retention (EPR) in tumor tissues. Once accumulated, TaNPs efficiently convert NIR light into heat, achieving temperatures sufficient to induce coagulative necrosis and apoptosis of cancer cells.[106,109,110]

The efficacy of TaNPs in PTT has been validated across different cancer models, showcasing their potential as versatile therapeutic agents. Researchers have investigated the synergistic benefits of combining TaNPs with conventional therapies such as chemotherapy or immunotherapy, aiming to enhance treatment outcomes through complementary mechanisms. This integrated approach not only improves therapeutic efficacy but also reduces systemic toxicity associated with traditional cancer treatments.[116,138]

Research investigating the efficacy of tantalum-based nanoparticles in photothermal therapy (PTT) for cancer treatment highlighted their potential as a revolutionary approach.

Tantalum-based nanoparticles (TaNPs) demonstrate the capability to target tumors precisely, leveraging their localized photothermal effect, thereby presenting a promising avenue for personalized cancer therapy.[139,140] Below are examples of several studies that have explored the effectiveness of tantalum-based nanoparticles in PTT for cancer treatment:

Jin *et al.* (2017) conducted *in vivo* antitumor experiments to determine the optimal combination of photothermal therapy (PTT) and chemotherapy using PPy&DOX@TaO$_x$-NIRDye800-PEG nanoparticles.[135] Tumor-bearing mice were divided into seven groups: PBS control, laser only, free DOX, PPy@TaO$_x$-NIRDye800-PEG nanoparticles, PPy&DOX@TaO$_x$-NIRDye800-PEG nanoparticles, PPy@TaO$_x$-NIRDye800-PEGu nanoparticles with laser, and PPy&DOX@TaO$_x$-NIRDye800-PEG nanoparticles with laser. Each group received 100 μL of either PBS, free DOX solution, PPy@TaO$_x$-NIRDye800-PEG nanoparticles, or PPy&DOX@TaO$_x$-NIRDye800-PEG nanoparticles (DOX 5 mg kg^{-1} or nanoparticles 25 mg kg^{-1}) *via* tail vein injection when the tumors reached approximately 100 mm^3 in size. After 24 hours, tumors were exposed to an 808 nm laser at 0.6 W cm^{-2} for 10 minutes or received no laser treatment.

The *in vivo* photothermal effect of PPy&DOX@TaO$_x$-NIRDye800-PEG nanoparticles was monitored using an IR thermal camera, which tracked temperature changes in the tumor areas before and after NIR laser irradiation. Tumors injected with PBS showed no significant temperature increase (<42 °C) during the 10 minutes of laser irradiation. In contrast, tumors injected with PPy@TaO$_x$-NIRDye800-PEG or PPy&DOX@TaO$_x$-NIRDye800-PEG nanoparticles exhibited significant temperature increases, indicating the strong photothermal performance of the nanoparticles *in vivo*.

Jin *et al.* (2017) also carried out another study focusing on photothermal ablation, MnO$_x$/Ta$_4$C$_3$-SP composite nanosheets were investigated for their therapeutic efficiency in 4T1 breast tumor-bearing mouse xenografts.[135] When tumor volumes reached approximately 60 mm^3, the mice were divided into four groups: control, NIR laser only, MnO$_x$/Ta$_4$C$_3$-SP composite nanosheets only, and MnO$_x$/Ta$_4$C$_3$-SP composite nanosheets with NIR laser irradiation. Following a 4-hours injection period, NIR laser irradiation (808 nm) was performed at 2 W cm^{-2} for 10 minutes. Whole-body thermal images showed that the surface temperature of tumors treated with MnO$_x$/Ta$_4$C$_3$-SP nanosheets increased to ~55 °C within 10 minutes, sufficient for tumor ablation. In contrast, tumors in mice not treated with MnO$_x$/Ta$_4$C$_3$-SP only increased by 5 °C under the same laser conditions.

Over the 21-days monitoring period, the PPy&DOX@TaO$_x$-NIRDye800-PEG nanoparticles plus laser group achieved complete tumor eradication without recurrence. Tumor growth inhibition rates were 35.1 ± 12.6% for free DOX, 55.6 ± 4.1% for PPy&DOX@TaO$_x$-NIRDye800-PEG nanoparticles, and 89.1 ± 12.8% for PPy@TaO$_x$-NIRDye800-PEG plus NIR laser groups. Although the PPy@TaO$_x$-NIRDye800-PEG plus NIR laser group showed complete tumor eradication by day 3, tumor regrowth occurred by day 6. These results indicated that the combination of PPy&DOX@TaO$_x$-NIRDye800-PEG nanoparticles with NIR laser effectively combined PTT and chemotherapy, achieving superior therapeutic efficacy without tumor recurrence. This synergistic effect offers greater potential for tumor therapy compared to PTT or chemotherapy alone.

The study by Dai *et al.* (2017) provides a comprehensive investigation into the photothermal therapy (PTT) applications of MnO$_x$/Ta$_4$C$_3$-SP composite nanosheets.[109] This research specifically focuses on the ability of these nanosheets to act as efficient agents for *in vivo* photothermal hyperthermia, which involves the use of near-infrared (NIR) laser irradiation to generate localized heat for the ablation of tumor cells.

In the experimental setup, male Balb/c nude mice were injected subcutaneously with 4T1 tumor cells. Once the tumors reached a size of approximately 50 mm^3, the mice were divided into four groups: a control group with no treatment, a group exposed only to NIR laser irradiation, a group injected with MnO$_x$/Ta$_4$C$_3$-SP nanosheets without laser exposure, and a group that received both the nanosheets and NIR laser irradiation.

The results demonstrated that the MnO$_x$/Ta$_4$C$_3$-SP nanosheets, when combined with NIR laser irradiation, significantly enhanced the photothermal effect. The mice in the MnO$_x$/Ta$_4$C$_3$-SP + NIR laser group exhibited a rapid increase in tumor temperature upon irradiation, as captured by infrared thermal imaging. This elevated temperature was sufficient to induce hyperthermia, leading to the effective ablation of tumor cells.

The study employed an 808 nm laser with a power density of 2 W cm^{-2} for 10 minutes, following an 8-hours post-injection period to allow for optimal distribution and accumulation of the nanosheets in the tumor tissues. The infrared thermal imaging recorded significant temperature rises in the tumors treated with both MnO$_x$/Ta$_4$C$_3$-SP nanosheets and NIR laser, compared to minimal temperature changes in the other groups.

Following the treatment, tumor volumes were measured every two days for two weeks. The MnO$_x$/Ta$_4$C$_3$-SP + NIR laser group showed a substantial reduction in tumor growth compared to the other groups, indicating the high efficacy of this combined treatment approach. The control group, as expected, showed continuous tumor growth, while the groups with either NIR laser or MnO$_x$/Ta$_4$C$_3$-SP nanosheets alone did not exhibit significant tumor suppression, highlighting the necessity of both components for effective PTT. The MnO$_x$/Ta$_4$C$_3$-SP composite nanosheets were synthesized through a detailed procedure involving HF etching, sonication exfoliation, *in situ* redox reaction with KMnO$_4$, and subsequent surface modification. This synthesis resulted in two-dimensional nanosheets with high photothermal conversion efficiency, enabling effective PTT.

Moreover, the theranostic functions of these nanosheets were illustrated, emphasizing their capability for MR/CT/PA imaging-guided PTT. This multifunctionality allows for precise imaging and localization of the tumor, ensuring that the laser irradiation is accurately targeted, thereby maximizing the therapeutic outcome while minimizing damage to surrounding healthy tissues. Fig. 22 presented an illustration of the theranostic capabilities of MnO$_x$/Ta$_4$C$_3$-SP composite nanosheets, specifically highlighting their use in MR/CT/PA imaging-guided efficient PTT ablation of cancer.

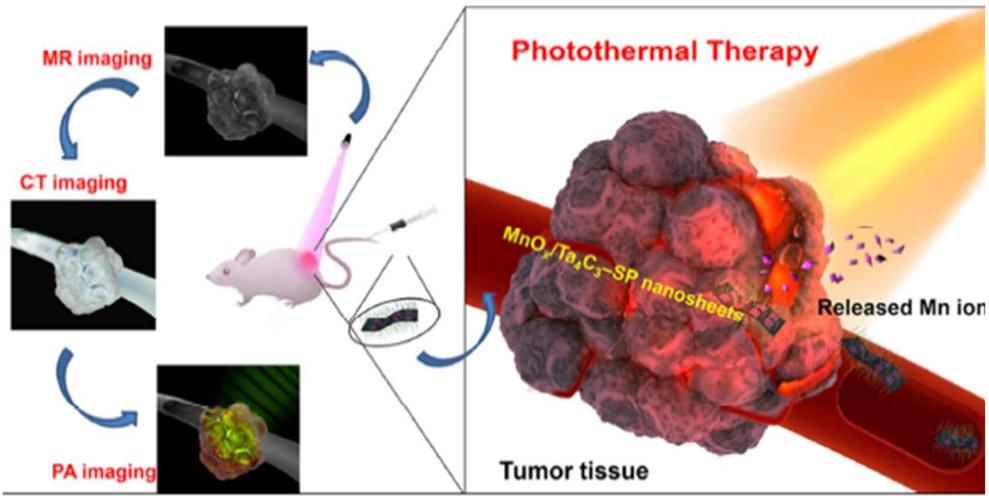

Fig. 22 Illustration of theranostic functions of MnO_x/Ta4C_3-SP composite nanosheets, *i.e.*, MR/CT/PA imaging-guided efficient PTT ablation of cancer.[109]

In summary, Dai *et al.* (2017) demonstrated that MnO_x/Ta_4C_3-SP composite nanosheets are highly effective for photothermal hyperthermia of tumors when combined with NIR laser irradiation.[109] The study underscores the potential of these nanosheets not only for efficient heat generation and tumor ablation but also for their integration with imaging modalities to guide and monitor the therapeutic process, paving the way for advanced cancer treatment strategies.

In a study, Miao *et al.* (2019) investigated the photothermal effects of tantalum-based nanoparticles (TaNPs) and demonstrated their potential for cancer treatment.[256] This research primarily focused on the ability of these nanoparticles to convert photon energy into heat energy, making them effective agents for both photoacoustic (PA) imaging and photothermal therapy.

To illustrate the photothermal capabilities of TaNPs, *in vitro* experiments were conducted using HeLa cancer cells. These cells were incubated with PEGylated TaNPs for 4 h and then subjected to near-infrared (NIR) laser irradiation (808 nm, 4 W cm^{-2}). The results showed that the combined treatment of TaNPs and laser irradiation effectively killed the cancer cells, as evidenced by the calcein acetoxymethyl ester (calcein AM) and propidium iodide (PI) staining, which distinguished between live and dead cells. Notably, there was almost no cell death when the cells were treated with either the NPs or laser alone, underscoring the necessity of both components for effective photothermal ablation. Moreover, the extent of cell death increased with higher concentrations of TaNPs (0–2 mg mL^{-1}) under laser irradiation due to greater heat generation from the photothermal effect (Fig. 23a).

A standard MTT assay was performed to quantitatively evaluate the photothermal ablation's efficacy. The assay revealed that less than 10% of HeLa cells remained alive after incubation with PEGylated TaNPs (2 mg mL^{-1}) followed by 10 minutes of laser irradiation, indicating a high efficiency in ablating cancer cells through the photothermal effect (Fig. 23b). Additionally, similar experiments with pristine TaNPs showed slightly lower ablation efficiency compared to PEGylated TaNPs, aligning with their respective photothermal performances.

To further assess the *in vivo* potential of PEGylated TaNPs, photothermal therapy experiments were conducted on 4T1 tumor-bearing mice. When the tumors reached approximately 150 mm^3 in volume, PBS or PEGylated TaNPs (0.05 mL, 5 mg mL^{-1}) were injected intratumorally. Upon irradiation with an 808 nm laser (1 W cm^{-2}), a significant temperature increases from 34.2 °C to 55.4 °C within 2 minutes was observed in tumors treated with PEGylated TaNPs. In contrast, only a slight temperature change was noted for PBS-treated tumors even after 10 minutes of irradiation, highlighting the high photothermal conversion efficiency of PEGylated TaNPs *in vivo*. Histological analysis of tumor tissues confirmed severe damage in the laser-irradiated regions treated with PEGylated TaNPs, as indicated by hematoxylin and eosin (H&E) staining results, which showed broken, smaller, or fewer nuclei in the affected areas.

The study also evaluated the biocompatibility of PEGylated TaNPs *in vivo*. Histological sections of major organs (heart, liver, spleen, lung, and kidney) from mice treated with PEGylated TaNPs displayed no detectable signs of damage or inflammatory lesions, similar to the PBS group, indicating the nanoparticles' suitability for biomedical applications. The inherent biocompatibility of elemental Ta, coupled with negligible cytotoxicity and reactive oxygen species (ROS) scavenging properties of PEGylated TaNPs, further ensures their safety for clinical use.

This research demonstrates that PEGylated TaNPs are effective photothermal agents capable of efficiently ablating cancer cells both *in vitro* and *in vivo*. Their high biocompatibility and strong photothermal conversion ability make them promising candidates for cancer diagnosis and therapy. The study highlighted the potential of TaNPs not only for photothermal therapy but also as contrast agents for PA imaging, thereby broadening their application scope in the biomedical field.

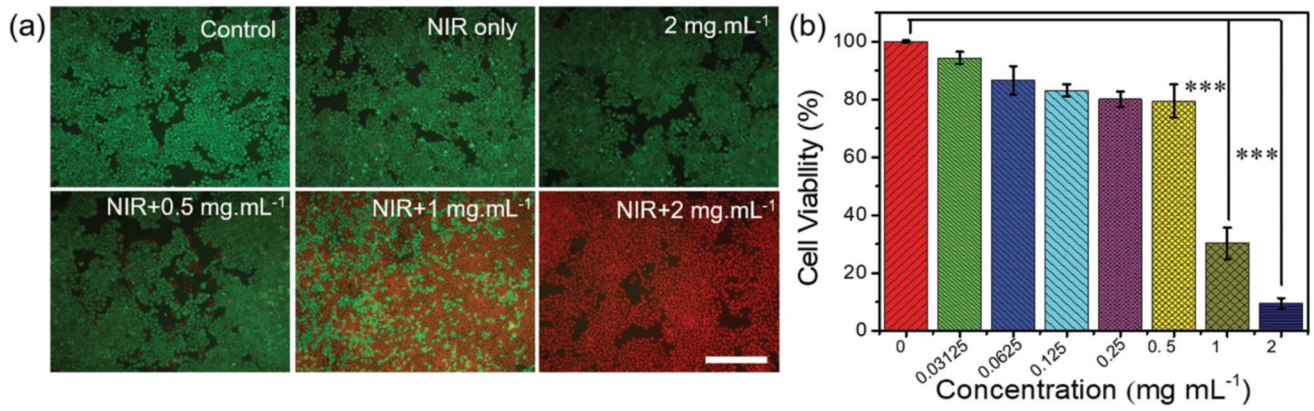

Fig. 23 Photothermal ablation of HeLa cancer cells *in vitro*. (a) Fluorescence microscopy images of HeLa cells treated differently as indicated. Scale bar is 1 mm. (b) Cell viability of HeLa cells after incubation with PEGylated TaNPs as well as laser irradiation (808 nm, 4 W cm^{-2}) for 10 min, $p < 0.001$ (***) (Reproduced from ref. 256 with permission from Wiley online Library copyright [2024]).

The study by Yi *et al.* (2023) delves into the photothermal effect of tantalum-based nanoparticles (TaN-PVP NPs) in the context of cancer therapy, focusing on their application for photothermal therapy (PTT).[270] The researchers utilized TaN-PVP NPs due to their notable absorption capacity in the near-infrared second window (NIR-II), which is pivotal for effective PTT.

The photothermal performance of TaN-PVP NPs was rigorously evaluated using various concentrations of nanoparticle dispersions irradiated with a 1064 nm laser. The temperature increase was directly proportional to both the duration of irradiation and the concentration of the nanoparticles. Specifically, at a concentration of 300 μg mL^{-1}, the temperature of the TaN-PVP NP solution rose from 28.0 °C to 56.4 °C within 5 minutes under 1064 nm laser irradiation at a power density of 0.8 W cm^{-2}. In contrast, the temperature of ultrapure water under the same conditions only increased by 2.5 °C. This substantial temperature rise underscores the superior photothermal properties of the TaN-PVP NPs (Fig. 24).

The study also reported a photothermal conversion efficiency of 33.1% for the TaN-PVP NPs, which was calculated using a previously established method. This high efficiency is crucial for maximizing the therapeutic effects of PTT. Furthermore, the photostability of TaN-PVP NPs was demonstrated through repeated irradiation cycles, showing consistent temperature changes and stable absorption spectra, indicating their reliability for continuous use in biomedical applications.

In terms of cytotoxicity, TaN-PVP NPs exhibited minimal toxicity to both normal (HEK293T) and cancer (4T1) cells in the absence of laser irradiation. However, under NIR-II laser exposure, a significant reduction in cell viability was observed, particularly in the 4T1 cancer cells. For instance, at a concentration of 200 μg mL^{-1} of TaN-PVP NPs with laser irradiation, the survival rate of 4T1 cells dropped below 10%. Live/dead staining assays further corroborated these findings, showing abundant red fluorescence (indicative of dead cells) in the PTT-treated groups compared to negligible fluorescence in the control groups.

The study extended these findings to *in vivo* experiments using mice bearing 4T1 tumors. The results were compelling: tumors in the PTT group were completely eradicated, whereas the control groups (treated with either NIR-II or TaN-PVP alone) showed no significant tumor inhibition. Histological analyses supported these outcomes, with hematoxylin and eosin (H&E) staining revealing a marked decrease in cell density in the tumors from the PTT group. Additionally, Ki67 staining indicated a significant reduction in the proliferative capacity of tumor cells in the PTT-treated group.

These comprehensive results highlighted the potent photothermal therapeutic effect of TaN-PVP NPs, demonstrating their capability to efficiently convert photon energy into heat, thereby killing cancer cells effectively both *in vitro* and *in vivo*. The study concludes that TaN-PVP NPs, with their excellent photothermal conversion efficiency and stability, hold significant promise for future applications in photoacoustic imaging and photothermal cancer therapy.

The study by Ding *et al.* (2021) explores the efficacy of tantalum-based nanoparticles in photothermal therapy (PTT) for cancer treatment by examining the photothermal conversion properties of tantalum coatings subjected to thermal oxidation at different temperatures.[271] Tantalum coatings were deposited on titanium implants *via* plasma spraying to enhance their biocompatibility, followed by thermal oxidation to achieve tantalum oxide coatings. The impact of this thermal treatment on the morphology, composition, and structure of the coatings was thoroughly investigated. The study compared UV-vis-NIR spectra, cancer therapy effects *in vitro*, and photothermal conversion properties among tantalum oxide coatings under varying thermal treatment conditions.

The findings indicate that tantalum coatings treated at 200 °C (VT200) exhibited the most substantial near-infrared (NIR) absorption, highest photothermal conversion efficiency, and most effective photothermal ablation effect *in vitro*. This superior performance is attributed to incomplete oxidation at the low temperature, which results in the formation of oxygen vacancies that narrow the band gap and enhance photothermal conversion.

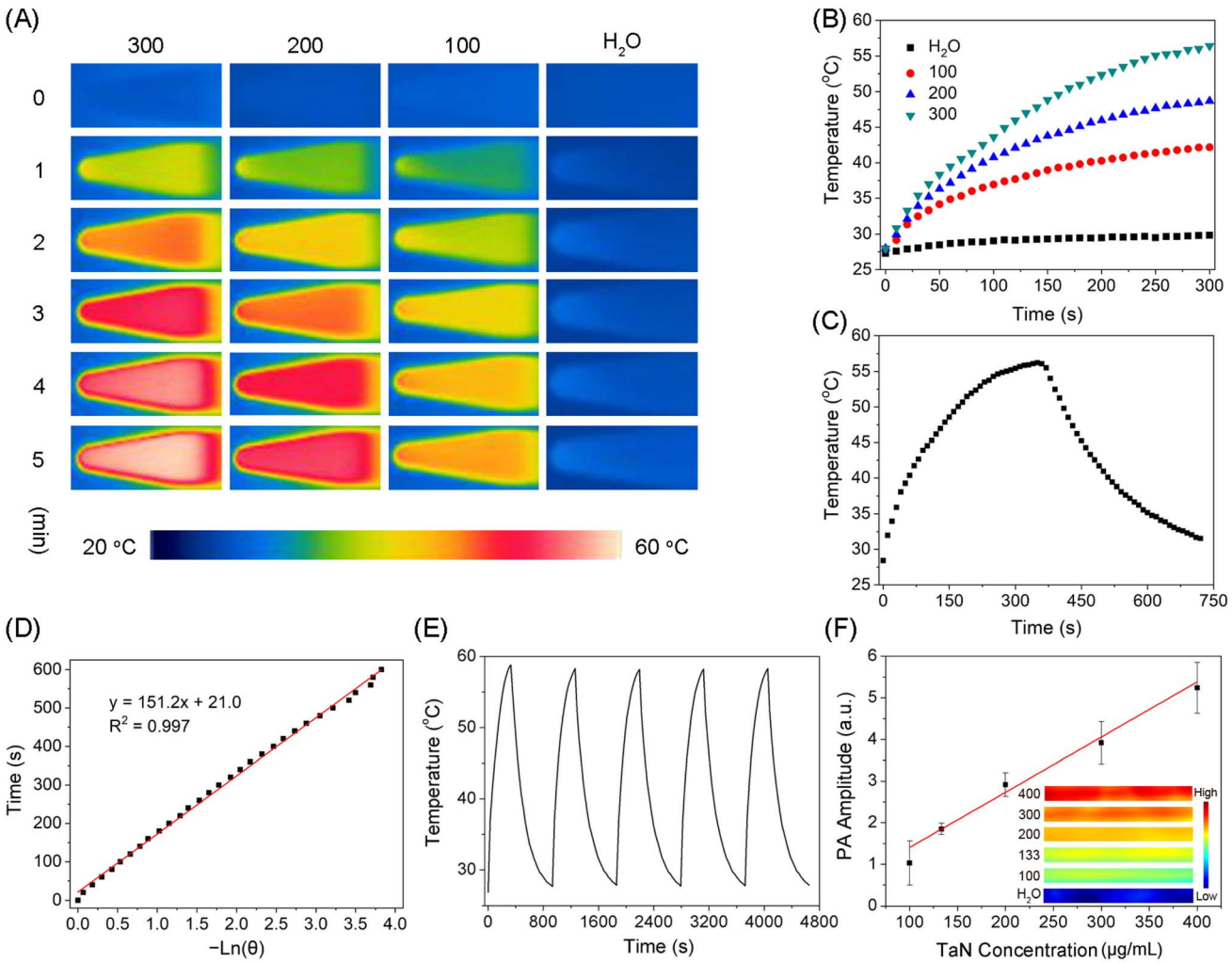

Fig. 24 (A) Thermal images and (B) photothermal curves of TaN-PVP dispersions at varying concentrations (100–300 μg mL^{-1}), with ultrapure water serving as the control. (C) Photothermal response of a 300 μg mL^{-1} TaN-PVP solution under 1064 nm laser irradiation, followed by cooling. (D) Cooling time plotted against the negative natural logarithmF of the temperature driving force. (E) Evaluation of photothermal stability through five consecutive laser on/off cycles. (F) PA signal intensity and images of TaN-PVP dispersions at specified concentrations (Reproduced from ref. 270 with permission from MDPI copyright [2024]).

In contrast, the sample treated at 600 °C (VT600) lost its porous structure, beneficial for cell adhesion and proliferation, leading to its exclusion from subsequent analyses.

Photothermal conversion properties were evaluated using an 808 nm laser in PBS solutions, with VT200 demonstrating the highest temperature increase, from 25 °C to 47 °C within 600 seconds of irradiation. This was significantly higher compared to the VT (untreated) and VT400 samples. The study also assessed the photothermal effect on MG-63 bone-tumor cells, revealing a drastic reduction in cell viability post-irradiation, especially for VT200, which showed the most substantial photothermal ablation effect.

Confocal imaging confirmed these results, showing a significant decrease in living cells on VT200 and VT400 after laser treatment (Fig. 25). The presence of oxygen vacancies in the tantalum coatings treated at lower temperatures (200 °C and 400 °C) was found to be crucial in enhancing photothermal therapy abilities. Therefore, the study concludes that tantalum coatings treated at lower temperatures exhibit enhanced photothermal conversion properties and are more effective in PTT for cancer treatment due to the formation of oxygen vacancies that facilitate better photothermal performance.

8 Future directions and challenges in the development and application of tantalum-based nanoparticles for cancer imaging and therapy

The utilization of tantalum-based nanoparticles (TaNPs) in cancer imaging and therapy represents a promising frontier in nanomedicine, offering significant potential for improving diagnostic accuracy and therapeutic efficacy. Despite considerable progress, several research gaps and challenges remain that

need to be addressed to fully realize the clinical potential of TaNPs. This discussion explored key research gaps, potential strategies to overcome existing limitations, and emerging trends and technologies that are poised to shape the future of nanoparticle-based contrast agents in oncology.[272,273]

8.1 Identification of key research gaps and challenges

8.1.1 Biocompatibility and toxicity. The use of tantalum-based nanoparticles (TaNPs) in biomedical applications shows promise due to their high biocompatibility and stability. However, a major challenge lies in the limited understanding of their long-term toxicity and biodegradability.[273,274] Current research focuses primarily on short-term evaluations, such as cytotoxicity, inflammatory responses, and acute biodistribution, providing valuable but incomplete insights.[275,276]

Addressing this gap requires comprehensive longitudinal studies to assess the chronic toxicity of TaNPs over extended periods, potentially spanning months to years. These studies should explore long-term interactions with tissues and organs, including potential accumulation, chronic inflammation, immune responses, and organ-specific toxicities. Moreover, investigating the biodegradability of TaNPs is essential to prevent potential long-term health risks associated with non-degradable particles. By conducting such studies, researchers can better assess the safety of TaNPs, supporting their future clinical use.

8.1.2 Targeting efficiency. Achieving precise targeting of cancer cells using tantalum-based nanoparticles (TaNPs) remains a major challenge in biomedical research. Effective cancer therapy depends on ensuring that TaNPs selectively target malignant cells while minimizing damage to healthy tissues. However, the current efficiency of targeting ligands, such as antibodies, peptides, and small molecules, needs further optimization to improve specificity and efficacy in clinical applications.[277,278]

A significant research gap exists in understanding how various targeting ligands interact with TaNPs. Detailed investigations into the binding affinities of these ligands to cancer cell receptors or biomarkers are critical. Additionally, studies should focus on the internalization mechanisms by which TaNPs, coupled with targeting ligands, enter cancer cells. This knowledge would help design TaNPs capable of delivering therapeutic agents specifically to cancerous tissues while minimizing exposure to healthy cells. Furthermore, the stability of targeting ligands on TaNPs under physiological conditions is crucial to maintaining targeting specificity during circulation and within the tumor microenvironment. Addressing these gaps will improve the precision and effectiveness of TaNPs in targeted cancer therapies, potentially enhancing therapeutic outcomes and reducing side effects, thereby advancing nanoparticle-based cancer treatment toward safer, more efficient clinical applications.

8.1.3 Photothermal conversion efficiency. Tantalum-based nanoparticles (TaNPs) show great potential for photothermal therapy (PTT) due to their capacity to convert light energy into heat, enabling the selective ablation of cancerous tissues. However, optimizing the photothermal conversion efficiency of TaNPs remains a key challenge, as this efficiency directly influences the effectiveness of tumor ablation and overall therapeutic outcomes.[231] To address this challenge, research must focus on filling critical gaps related to the structural and compositional optimization of TaNPs. Studies should explore synthesis methods that allow precise control over the size, shape, and crystal structure of the nanoparticles. Additionally, surface modifications are essential for improving the interaction between TaNPs and incident light, which enhances their photothermal properties.

Investigations into how structural parameters, such as nanoparticle size and morphology, affect light absorption and heat generation are crucial. Moreover, novel surface

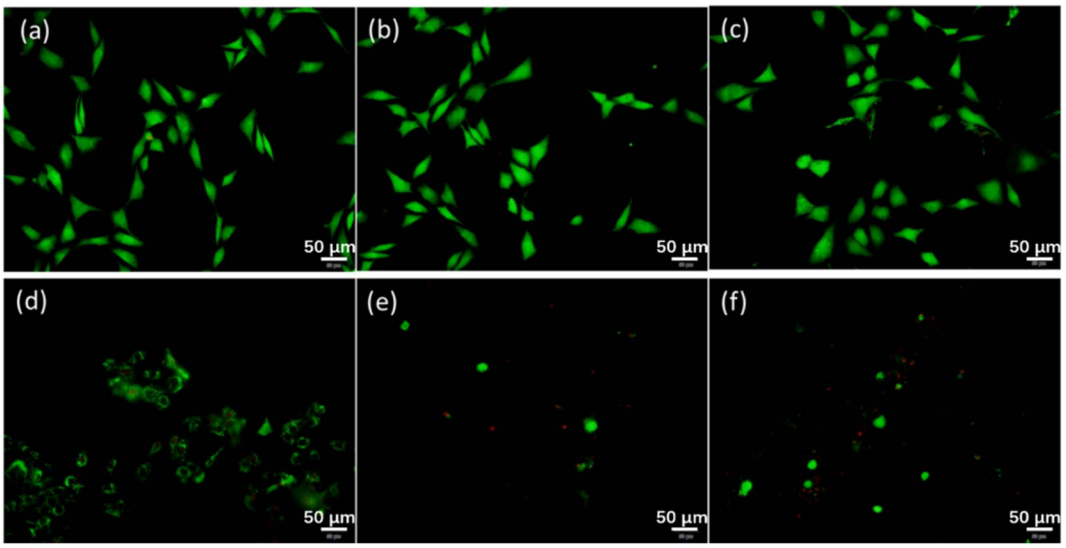

Fig. 25 Confocal images of cells on VT, VT200, and VT400 before ((a–c) respectively) and after ((d–f) respectively) irradiation (Reproduced from ref. 271 with permission from MDPI copyright [2024]).

engineering approaches, including functionalizing TaNPs with plasmonic materials or biocompatible coatings, could further improve their photothermal performance. By addressing these research gaps and improving our understanding of the factors influencing photothermal conversion efficiency in TaNPs, researchers can develop more effective PTT agents. These optimized nanoparticles hold the potential to deliver precise, targeted cancer treatment while minimizing damage to healthy tissues, thereby advancing nanomedicine in cancer therapy.

8.1.4 Clinical translation. Transitioning tantalum-based nanoparticles (TaNPs) from preclinical research to clinical use faces key challenges, including meeting regulatory requirements and ensuring reproducibility across labs and clinical settings.[199,279–281] A major gap is the lack of standardized protocols for synthesis, characterization, and testing. Establishing these guidelines is crucial for consistency in nanoparticle properties and for streamlining regulatory approval.

Scaling up production to meet clinical demands without compromising quality is another challenge. Current methods are suited for small-scale production, so developing scalable techniques is essential for clinical translation. Addressing these gaps through interdisciplinary collaboration will accelerate TaNP clinical adoption, enabling their use in cancer therapy, imaging, and drug delivery, ultimately improving patient outcomes.

8.1.5 Multifunctionality. Incorporating multiple functionalities into a single tantalum-based nanoparticle (TaNP) holds great potential for advancing nanomedicine by enabling simultaneous imaging, therapy, and drug delivery. However, achieving this integration without compromising each function remains a major challenge.[116,282] The primary research gap lies in developing strategies to ensure the stability, biocompatibility, and efficacy of multifunctional TaNPs. Researchers must explore innovative design and synthesis techniques that enable the seamless integration of various components, such as imaging agents, therapeutic drugs, and targeting ligands. This requires understanding how these components interact and affect the nanoparticle's overall performance, ensuring effective delivery, precise imaging, and controlled release of therapeutics.

By addressing these challenges, multifunctional TaNPs could improve cancer diagnosis and treatment by offering targeted therapy, real-time imaging, and controlled drug delivery in a single platform. This would enhance treatment efficiency, reduce the need for multiple interventions, and lead to more streamlined clinical procedures, ultimately improving patient outcomes.

8.1.6 *In vivo* distribution and pharmacokinetics. Understanding the *in vivo* distribution, clearance mechanisms, and pharmacokinetics of tantalum-based nanoparticles (TaNPs) is essential for predicting their behaviour in the human body and ensuring safe, effective medical use.[101,283–286] Key challenges involve tracking how TaNPs circulate, accumulate in tissues, and are cleared, which is critical for assessing toxicity, therapeutic efficacy, and biocompatibility.

A major research gap exists in developing advanced imaging and analytical techniques to monitor TaNPs in real-time within living organisms. Traditional methods often lack the precision needed to observe nanoparticles at the cellular level. Innovative approaches such as high-resolution fluorescence imaging, MRI, and PET, combined with cutting-edge analytical methods, can offer detailed insights into nanoparticle biodistribution and clearance pathways. Real-time tracking also provides valuable pharmacokinetic data on absorption, distribution, metabolism, and excretion, informing dosage and safety guidelines for TaNP-based therapies. Addressing these gaps will enhance the understanding of TaNPs' *in vivo* behaviour, enabling better design and optimization of nanoparticle-based drug delivery systems. This progress will help translate TaNPs from preclinical research to safe and effective clinical applications.

9 Potential strategies to address limitations and enhance performance

9.1 Surface functionalization

Understanding the *in vivo* distribution, clearance, and pharmacokinetics of tantalum-based nanoparticles (TaNPs) is essential for predicting their behavior and ensuring safe, effective use in medical applications. A major challenge lies in developing advanced imaging techniques and analytical methods to accurately track TaNPs in real-time, as traditional methods lack the sensitivity to monitor their movement at cellular and subcellular levels.[101,286]

Advanced tools like high-resolution fluorescence imaging, MRI, and PET offer detailed insights into how TaNPs interact with tissues, where they accumulate, and their clearance pathways. This real-time tracking is crucial for evaluating nanoparticle pharmacokinetics—absorption, distribution, metabolism, and excretion—and optimizing their design for safer, more effective drug delivery systems. By addressing these research gaps, scientists can enhance the clinical translation of TaNPs, ensuring their performance in complex biological environments and paving the way for more precise, targeted therapies in nanomedicine.

9.2 Size and shape control

To optimize the optical and photothermal properties of tantalum-based nanoparticles (TaNPs) for applications like photothermal therapy (PTT), precise control over their size and shape is essential. Smaller nanoparticles with high surface area-to-volume ratios are more efficient at converting light into heat, crucial for effective tumor ablation. Consistency in size and shape also enhances the reliability of their performance in biomedical applications.[109,110,135] Advanced synthesis techniques can facilitate this control. Seed-mediated growth, for example, uses small nanoparticle seeds as nucleation sites, allowing fine-tuning of size and shape by adjusting material deposition and growth conditions. This method can produce nanoparticles of various shapes by modifying the initial seeds. Microemulsion techniques also allow for uniform size and shape control. By synthesizing nanoparticles in microemulsions—tiny droplets of one liquid dispersed in another—researchers can precisely manage droplet size, resulting in

uniform nanoparticles with specific compositions and surface properties.

Template-assisted methods utilize pre-formed templates to guide nanoparticle synthesis, leading to highly uniform sizes and shapes. By depositing material in confined template spaces, complex shapes and hierarchical structures can be achieved, with the template removed afterward. By leveraging these advanced techniques, researchers can produce TaNPs with optimized properties for PTT, maximizing light absorption and heat generation. Uniform nanoparticles also enhance predictability in biological interactions, contributing to consistent therapeutic outcomes. Overall, precise control over the size and shape of TaNPs through these advanced synthesis methods is critical for enhancing their effectiveness in PTT and advancing nanomedicine, ultimately improving patient care.

9.3 Biodegradability

Developing biodegradable tantalum-based nanoparticles (TaNPs) is a promising strategy to ensure their safe breakdown and clearance from the body after therapeutic use, addressing long-term toxicity and accumulation issues associated with non-degradable nanoparticles.[287–289] To implement this, researchers should explore biodegradable polymers and hybrid nanoparticles. One effective approach is coating TaNPs with biodegradable polymers like poly(lactic-*co*-glycolic acid) (PLGA), polycaprolactone (PCL), or chitosan, known for their biocompatibility. Encapsulating TaNPs in these polymers can create a stable nanoparticle system that degrades safely in the body over time while retaining the therapeutic properties of tantalum. Hybrid nanoparticles combining tantalum's stability with biodegradable components offer another avenue. By integrating biodegradable materials like calcium phosphate into the TaNP structure, composite nanoparticles can be designed to maintain the beneficial properties of TaNPs while ensuring safe degradation and clearance.

Various synthesis techniques, such as co-precipitation, solvent evaporation, or emulsion methods, can create these biodegradable or hybrid TaNPs. These methods allow precise control over the composition and structure, ensuring uniform distribution of biodegradable components. Detailed studies on the degradation kinetics and byproducts of these biodegradable TaNPs are essential. Research should focus on how these nanoparticles break down in biological environments, identify degradation products, and confirm their non-toxicity for safe clearance from the body. This requires comprehensive *in vitro* and *in vivo* studies to monitor degradation and evaluate the biocompatibility of byproducts. By developing biodegradable TaNPs, researchers can create systems that offer the therapeutic benefits of tantalum while minimizing long-term risks. This strategy enhances the safety of TaNP-based therapies and broadens their applications in biomedicine, contributing to more effective and safer treatments for patients.

9.4 Combination therapies

Combining tantalum-based nanoparticles (TaNPs) with therapeutic modalities like chemotherapy, immunotherapy, or radiotherapy enhances treatment outcomes through synergistic effects. Leveraging TaNPs' photothermal capabilities and imaging potential allows for multifunctional treatment strategies.[290–296] To implement this, researchers can design multifunctional TaNPs that co-deliver therapeutic agents while providing photothermal therapy and imaging. Chemotherapeutic drugs can be encapsulated in biodegradable coatings or conjugated to TaNP surfaces for targeted delivery, enhancing efficacy and minimizing side effects. TaNPs can also serve as photothermal agents by absorbing near-infrared light and converting it to heat, selectively destroying cancer cells and promoting drug release. Additionally, functionalizing TaNPs with imaging agents enables real-time visualization of nanoparticle distribution and therapeutic response, allowing clinicians to monitor treatment progress.

Successful implementation requires interdisciplinary collaboration to optimize nanoparticle synthesis and conduct preclinical studies evaluating safety and efficacy. By integrating TaNPs with complementary therapies and imaging capabilities, researchers can develop advanced systems that improve treatment outcomes, maximize efficacy, and enable personalized approaches tailored to individual patient needs.

9.5 Advanced imaging techniques

Utilizing advanced imaging techniques such as photoacoustic imaging, magnetic resonance imaging (MRI), and computed tomography (CT) to monitor tantalum-based nanoparticles (TaNPs) *in vivo* enhances their application in biomedical research and clinical settings. These methods provide critical insights into the biodistribution, pharmacokinetics, and therapeutic effects of TaNPs within living organisms.[297–304]

To effectively implement this strategy, researchers can create hybrid nanoparticles that combine imaging agents with TaNPs.[305] These systems facilitate simultaneous imaging and therapeutic functions, enabling comprehensive evaluation of nanoparticle-based treatments. Photoacoustic imaging uses laser pulses to produce acoustic waves from TaNPs, yielding high-resolution images based on their light absorption, while incorporating contrast agents improves visibility for deep tissue detection. MRI offers excellent soft tissue contrast and spatial resolution for non-invasive imaging of TaNPs. Hybrid TaNPs can be designed with paramagnetic materials to serve as MRI contrast agents, allowing precise localization and tracking. CT employs X-rays to generate cross-sectional images, and functionalizing TaNPs with high atomic number elements like gold or iodine enhances X-ray attenuation, providing strong contrast for accurate monitoring of TaNP distribution.

Optimizing nanoparticle synthesis for stability, biocompatibility, and imaging functionality is essential, along with preclinical validation to ensure sensitivity, specificity, and safety in relevant disease models. By developing hybrid nanoparticles that merge therapeutic functions with advanced imaging capabilities, researchers can advance nanomedicine, enabling real-time tracking of TaNPs and personalized treatment strategies, ultimately improving outcomes in nanoparticle-based therapies.

9.6 Personalized medicine

Tailoring tantalum-based nanoparticles (TaNPs) therapies to individual patient profiles enhances treatment efficacy and minimizes side effects. This personalized medicine approach utilizes biomarkers and genetic profiling to create nanoparticle formulations and treatment protocols that meet each patient's unique needs.

By incorporating biomarkers, such as specific molecular signatures or protein expression levels in cancer cells, researchers can identify targets for TaNP therapies. This allows for the selection of appropriate targeting ligands or surface modifications to improve nanoparticle accumulation in diseased tissues while reducing off-target effects on healthy cells. Genetic profiling is also critical, as it reveals genetic variations that may affect an individual's treatment response. Understanding factors related to drug metabolism, immune response, or disease susceptibility helps customize TaNP formulations to optimize therapeutic efficacy and safety. Implementing this strategy requires integrating biomarker and genetic information into TaNP design and optimization. Researchers can develop systems that selectively deliver therapeutic payloads, such as chemotherapeutic drugs or immunomodulatory agents, based on the patient's biomolecular profile. This not only improves treatment outcomes but also reduces adverse reactions and enhances patient compliance and satisfaction. Validation of personalized nanoparticle formulations through preclinical and clinical studies is essential to assess their efficacy and safety. Close collaboration among researchers, clinicians, and bioinformaticians is crucial to effectively translate personalized TaNP therapies from bench to bedside. By tailoring TaNP-based therapies to individual profiles, researchers can advance nanomedicine toward more precise treatments. This personalized approach promises improved patient outcomes, optimized therapeutic benefits, and a pathway for personalized medicine in oncology and other disease areas.

10 Conclusion

The study of tantalum-based nanoparticles (TaNPs) presents a compelling narrative of innovation and potential in biomedical research and clinical applications. TaNPs offer a unique combination of biocompatibility, photothermal properties, and multifunctionality that positions them as promising candidates for advanced therapies and imaging modalities, particularly in oncology. Throughout this exploration, significant challenges and research gaps have been identified. These include the need for deeper understanding of TaNPs' long-term biocompatibility, strategies to optimize their therapeutic efficacy through precise surface functionalization and hybridization with other therapeutic agents, and the development of advanced imaging techniques for real-time monitoring and precise localization within the body. Strategic approaches have been proposed to address these challenges. These include enhancing biocompatibility through tailored surface modifications like PEGylation, optimizing nanoparticle size and shape to maximize photothermal conversion efficiency for effective cancer therapy, and innovating biodegradable TaNPs to ensure safe degradation and clearance post-therapy. Integration of advanced imaging technologies such as photoacoustic imaging, MRI, and CT holds promise for real-time tracking and monitoring of TaNPs' biodistribution and therapeutic responses, thus advancing their clinical application. Moreover, the concept of personalized medicine emerges as a transformative strategy, leveraging biomarkers and genetic profiling to customize TaNP-based therapies according to individual patient profiles. This approach not only enhances treatment efficacy by targeting specific molecular signatures but also minimizes adverse effects, potentially revolutionizing patient care in oncology and beyond. In a nutshell, TaNPs represent a frontier in nanomedicine with the potential to redefine cancer treatment paradigms. Continued interdisciplinary research, collaboration across scientific disciplines, and rigorous clinical validation are essential to harnessing the full therapeutic potential of TaNPs and translating these advancements into clinical practice. By addressing current challenges and expanding upon promising strategies, TaNPs hold promise as versatile tools in personalized and precision medicine, paving the way for more effective and tailored treatments that improve patient outcomes and quality of life.

Data availability

The data and materials used in this study are available upon request.

Author contributions

Ikhazuagbe H. Ifijen drafted the initial version of the manuscript. All other authors—Awoyemi Taiwo Christopher, Ogunnaike Korede Lekan, Omowunmi Rebecca Aworinde, Emmanuel Faderin, Oluwafunke Obembe, Tawakalitu Folashade Abdulsalam_Akanji, Juliet C. Igboanugo, Uzochukwu Udogu, Godwin Onogwu Ogidi, Terungwa H. Iorkula and Osasere Jude-Kelly Osayawe—revised the manuscript and provided additional writeups as needed. Each author contributed significantly to the development and refinement of the review, ensuring its comprehensiveness and accuracy.

Conflicts of interest

On behalf of all authors, the corresponding author states that there is no conflict of interest.

References

1 I. H. Ifijen, E. U. Ikhuoria, S. O. Omorogbe, *et al.*, Chemical, plant and microbial mediated synthesis of tin oxide nanoparticles: antimicrobial and anticancer potency, *Braz. J. Chem. Eng.*, 2023, **40**, 965–991, DOI: 10.1007/s43153-023-00315-0.
2 I. H. Ifijen, M. Maliki, I. J. Odiachi, *et al.*, Performance of metallic-based nanomaterials doped with strontium in biomedical and supercapacitor electrodes: a review, *Biomed. Mater. Devices*, 2023, **1**, 402–418, DOI: 10.1007/s44174-022-00006-3.

3 I. H. Ifijen and M. Maliki, A comprehensive review on the synthesis and photothermal cancer therapy of titanium nitride nanostructures, *Inorg. Nano-Met. Chem.*, 2022, **53**(4), 366–387, DOI: 10.1080/24701556.2022.2068596.
4 S. I. Omonmhenle and I. H. Ifijen, Advancements in layered double hydroxide-based chemotherapeutic nanosystems for cancer treatment, *J. Appl. Sci. Environ. Manage.*, 2023, **27**(4), 24, DOI: 10.4314/jasem.v27i4.24.
5 A. P. Onivefu, A. Efunnuga, A. Efunnuga, *et al.*, Photoresist performance: an exploration of synthesis, surface modification techniques, properties tailoring, and challenges navigation in copper/copper oxide nanoparticle applications, *Biomed. Mater. Devices*, 2024, 1–31, DOI: 10.1007/s44174-024-00167-3.
6 E. U. Ikhuoria, I. E. Uwidia, G. O. Otabor, *et al.*, Comparative analysis of magnesium oxide nanoparticles biosynthesized from rubber seed shell and rubber leaf extracts, *Biomed. Mater. Devices*, 2024, **2**, 1078–1088, DOI: 10.1007/s44174-023-00139-z.
7 I. Ifijen, E. Ikhuoria, I. Uwidia, R. Okojie and I. Chikaodili, Fe-Ag-V ternary oxide nanoparticles synthesized from Ganoderma lucidum extract: antioxidant and antibacterial proficiency in focus, *Nanomed. Res. J.*, 2024, 131–154, DOI: 10.22034/nmrj.2024.2022657.1629.
8 E. M. Jonathan, I. H. Ifijen, K. E. Mokobia, *et al.*, A review on the heightened mechanical features of nanosilica-based concrete and the response of human fibroblasts to nanosilica, *Biomed. Mater. Devices*, 2023, **1**, 286–300, DOI: 10.1007/s44174-022-00013-4.
9 I. E. Uwidia, E. U. Ikhuoria, R. O. Okojie, *et al.*, Antibacterial properties of rod-like vanadium oxide nanostructures *via* Ganoderma lucidum plant extract approach, *Chem. Afr.*, 2024, **7**, 1951–1961, DOI: 10.1007/s42250-023-00854-6.
10 Y. Dang and J. Guan, Nanoparticle-based drug delivery systems for cancer therapy, *Smart Mater. Med.*, 2020, **1**, 10–19, DOI: 10.1016/j.smaim.2020.04.001.
11 N. Muhamad, T. Plengsuriyakarn and K. Na-Bangchang, Application of active targeting nanoparticle delivery system for chemotherapeutic drugs and traditional/herbal medicines in cancer therapy: a systematic review, *Int. J. Nanomed.*, 2018, **13**, 3921–3935, DOI: 10.2147/IJN.S165210.
12 R. Bazak, M. Houri, S. Achy, S. Kamel and T. Refaat, Cancer active targeting by nanoparticles: a comprehensive review of literature, *J. Cancer Res. Clin. Oncol.*, 2015, **141**, 769–784, DOI: 10.1007/s00432-014-1767-3.
13 A. Khorasani, D. Shahbazi-Gahrouei and A. Safari, Recent metal nanotheranostics for cancer diagnosis and therapy: a review, *Diagnostics*, 2023, **13**, 833, DOI: 10.3390/diagnostics13050833.
14 E. Koshevaya, E. Krivoshapkina and P. Krivoshapkin, Tantalum oxide nanoparticles as an advanced platform for cancer diagnostics: a review and perspective, *J. Mater. Chem. B*, 2021, 5008–5024, DOI: 10.1039/d1tb00570g.
15 R. Li, W. Zhao, T. Wu, A. Wang, Q. Li, Y. Liu and H. Xiong, Tantalum-carbon-integrated nanozymes as a nano-radiosensitizer for radiotherapy enhancement, *Front. Bioeng. Biotechnol.*, 2022, **10**, 1042646, DOI: 10.3389/fbioe.2022.1042646.
16 K. Bogusz, M. Zuchora, V. Sencadas, M. Tehei, M. Lerch, N. Thorpe, *et al.*, Synthesis of methotrexate-loaded tantalum pentoxide–poly(acrylic acid) nanoparticles for controlled drug release applications, *J. Colloid Interface Sci.*, 2019, **538**, 286–296, DOI: 10.1016/j.jcis.2018.11.097.
17 M. Zhao, C. Ji, H. Dai, C. Wang, R. Liu, J. Xie, *et al.*, Mussel-inspired tantalum nanocomposite hydrogels for *in situ* oral cancer treatment, *ACS Appl. Mater. Interfaces*, 2023, **15**(4), 4984–4995, DOI: 10.1021/acsami.2c20467.
18 U. Ulusoy, A review of particle shape effects on material properties for various engineering applications: from macro to nanoscale, *Minerals*, 2023, 81, DOI: 10.3390/min13010091.
19 T. Seidu, P. Kutoka, D. Asante, M. Farooq, R. Alolga and W. Bo, Functionalization of nanoparticulate drug delivery systems and its influence in cancer therapy, *Pharmaceutics*, 2022, **14**, 1113, DOI: 10.3390/pharmaceutics14051113.
20 S. I. Omonmhenle and I. H. Ifijen, Advancements in Layered Double Hydroxide-Based Chemotherapeutic Nanosystems for Cancer Treatment, *J. Appl. Sci. Environ. Manag.*, 2023, **27**(4), 815–821, DOI: 10.4314/jasem.v27i4.24.
21 A. Attama, P. Nnamani, O. Onokala, A. Ugwu and A. Onugwu, Nanogels as target drug delivery systems in cancer therapy: A review of the last decade, *Front. Pharmacol*, 2022, **13**, 874510, DOI: 10.3389/fphar.2022.874510.
22 T. Yang, J. Zhai, D. Hu, R. Yang, G. Wang, Y. Li, *et al.*, "Targeting design" of nanoparticles in tumor therapy, *Pharmaceutics*, 2022, **14**, 1919, DOI: 10.3390/pharmaceutics14091919.
23 K. Pawelec, E. Tu, S. Chakravarty, J. Hix, L. Buchanan, L. Kenney, *et al.*, Incorporating tantalum oxide nanoparticles into implantable polymeric biomedical devices for radiological monitoring, *Adv. Healthcare Mater.*, 2023, **12**, e2203167, DOI: 10.1002/adhm.202203167.
24 C. Badea, D. Clark, A. Alphin, J. Ramirez-Giraldo, P. Bhandari, Y. Mowery, *et al.*, Co-clinical photon counting CT research for multi-contrast imaging, *Proc. SPIE*, 2022, **12304**, 123040G, DOI: 10.1117/12.2646399.
25 Z. Jiang, M. Zhang, P. Li, Y. Wang and Q. Fu, Nanomaterial-based CT contrast agents and their applications in image-guided therapy, *Theranostics*, 2023, **13**, 483–509, DOI: 10.7150/thno.79625.
26 M. Sivasubramanian, C. Chu, S. Cheng, N. Chen, C. Chen, C. Yao, *et al.*, Multimodal magnetic resonance and photoacoustic imaging of tumor-specific enzyme-responsive hybrid nanoparticles for oxygen modulation, *Front. Bioeng. Biotechnol.*, 2022, **10**, 910902, DOI: 10.3389/fbioe.2022.910902.
27 S. Chen, L. Huang, B. Huang, M. Zhang, H. Li, D. Pang, *et al.*, Ultrasmall MnSe nanoparticles as T1-MRI contrast agents for *in vivo* tumor imaging, *ACS Appl. Mater. Interfaces*, 2022, 11167–11176, DOI: 10.1021/acsami.1c25101.

28 D. Gupta, P. Roy, R. Sharma, R. Kasana, P. Rathore and T. K. Gupta, Recent nanotheranostic approaches in cancer research, *Clin. Exp. Med.*, 2024, **24**, 8, DOI: **10.1007/s10238-023-01262-3**.

29 S. Sharma, S. Sharma, S. Vashist, G. Kaur, S. Arora and S. Suchet, Metallic nanoparticles as antimicrobials and radiosensitizers: a review, *Asian Pac. J. Health Sci.*, 2022, 171–174, DOI: **10.21276/apjhs.2022.9.4s.34**.

30 X. Mo, B. Fabre, N. Herlin-Boime and E. Tse, Rapid laser synthesis of surfactantless tantalum-based nanomaterials as bifunctional catalysts for direct peroxide–peroxide fuel cells, *SmartMat*, 2023, **4**, e1181, DOI: **10.1002/smm2.1181**.

31 C. Kayser, L. Mueller, L. Soares, D. Volz, A. Ziulkoski, E. Schneider, *et al.*, Organic-inorganic films with anticorrosive and bactericidal properties for titanium implants, *Mater. Res.*, 2023, e20230218, DOI: **10.1590/1980-5373-mr-2023-0218**.

32 K. Xie, X. Wei, L. Ye, M. Wan, S. Li and J. Wu, Recovery and preparation of potassium fluorotantalate from high-tantalum-bearing waste slag by pressure alkaline decomposition, *Metals*, 2022, 648, DOI: **10.3390/met12040648**.

33 J. Carbó, M. Gómez, C. Hernández-Prieto, A. Hernán-Gómez, A. Martín, M. Mena, *et al.*, Reductive hydrogenation of sulfido-bridged tantalum alkyl complexes: A mechanistic insight, *Inorg. Chem.*, 2023, **62**, 10100–10109, DOI: **10.1021/acs.inorgchem.3c00043**.

34 Y. Sebti, T. Chauveau, M. Chalal, Y. Lalatonne, C. Lefebvre and L. Motte, Assessment of the morphological, optical, and photoluminescence properties of HfO2 nanoparticles synthesized by a sol-gel method assisted by microwave irradiation, *Inorg. Chem.*, 2022, 6508–6518, DOI: **10.1021/acs.inorgchem.2c00277**.

35 U. Utari, H. Maulidina, R. Arilasita, H. Widiyandari and S. Purnama B, Citric acid concentration tune of structural and magnetic properties in hematite (α−Fe2O3) nanoparticles synthesized by sol−gel method, *Mater. Res. Express*, 2023, **10**, 036101, DOI: **10.1088/2053-1591/acbf0c**.

36 S. C and R. Meda U, Synthesis of silicon dioxide nanoparticles by sol-gel method for applications in geopolymer composites, *ECS Trans.*, 2022, 5533–5541, DOI: **10.1149/10701.5533ecst**.

37 P. Bogdanov, L. Sokura, A. Kremleva and V. Vitkin, Sol-gel synthesis of uniform arrays of Ag and Au nanoparticles, *Rev. Adv. Mater. Technol.*, 2023, **5**(1), 39–44, DOI: **10.17586/2687-0568-2023-5-1-39-44**.

38 P. Imoisili and T. Jen, Microwave-assisted sol–gel template-free synthesis and characterization of silica nanoparticles obtained from South African coal fly ash, *Nanotechnol. Rev.*, 2022, **11**, 3042–3052, DOI: **10.1515/ntrev-2022-0476**.

39 A. Nyabadza, É. McCarthy, M. Makhesana, S. Heidarinassab, A. Plouze, M. Vazquez, *et al.*, A review of physical, chemical, and biological synthesis methods of bimetallic nanoparticles and applications in sensing, water treatment, biomedicine, catalysis, and hydrogen storage, *Adv. Colloid Interface Sci.*, 2023, **321**, 103010, DOI: **10.1016/j.cis.2023.103010**.

40 G. Dantelle, S. Beauquis, R. Le Dantec, V. Monnier, C. Galez and Y. Mugnier, Solution-based synthesis routes for the preparation of noncentrosymmetric 0-D oxide nanocrystals with perovskite and nonperovskite structures, *Small*, 2022, **18**(30), 2200992, DOI: **10.1002/smll.202200992**.

41 H. Nayebzadeh, A. Rohani, A. Sistani, A. Hassanpour and J. Gardy, Modelling and optimisation of the sol-gel conditions for synthesis of semi-hexagonal titania-based nano-catalyst for esterification reaction, *Catalysts*, 2022, 239, DOI: **10.3390/catal12020239**.

42 W. Latif and M. AL-Owaidi, Review article: Sol-gel method, "synthesis and applications.", *World J. Adv. Eng. Technol. Sci.*, 2023, 160–166, DOI: **10.30574/wjaets.2023.8.2.0071**.

43 R. Georgiev, B. Georgieva, K. Lazarova, M. Vasileva and T. Babeva, Sol-gel tantalum pentoxide thin films with tunable refractive index for optical sensing applications, *Opt. Quantum Electron.*, 2020, **52**, 437, DOI: **10.1007/s11082-020-02540-0**.

44 T. Ohishi, M. Sachiko and A. Katoh, Synthesis and properties of tantalum oxide films prepared by the sol-gel method using photo-irradiation, *J. Non-Cryst. Solids*, 1992, 493–498, DOI: **10.1016/S0022-3093(05)80665-9**.

45 C. Gül, S. Albayrak and H. Çinici, Characterization of tantalum oxide sol-gel-coated AZ91 Mg alloys, *Trans. Indian Inst. Met.*, 2020, **73**, 1249–1256, DOI: **10.1007/s12666-020-01976-y**.

46 C. Liu, W. Wang, Q. He, A. Wang, J. Wu, H. Wang, J. Zhang and Z. Fu, Synthesis of ultra-fine tantalum carbide powders by a combinational method of sol-gel and spark plasma sintering, *Ceram. Int.*, 2018, 19106–19112, DOI: **10.1016/J.CERAMINT.2018.05.258**.

47 A. Phani and S. Santucci, Structural characterization of nickel tantalum oxide synthesized by sol-gel spin coating technique, *Mater. Lett.*, 2001, **47**, 20–24, DOI: **10.1016/s0167-577x(00)00205-6**.

48 M. Oubaha, R. Copperwhite, A. Gorin, V. Purlys, C. Boothman, M. O'Sullivan, R. Gadonas, C. McDonagh and B. MacCraith, Novel tantalum-based photocurable hybrid sol-gel material employed in the fabrication of channel optical waveguides and three-dimensional structures, *Appl. Surf. Sci.*, 2011, **257**, 2995–2999, DOI: **10.1016/J.APSUSC.2010.10.106**.

49 D. Richard, M. Romero and R. Faccio, Experimental and theoretical study on the structural, electrical and optical properties of tantalum-doped ZnO nanoparticles prepared *via* sol-gel acetate route, *Ceram. Int.*, 2018, **44**, 703–711, DOI: **10.1016/J.CERAMINT.2017.09.232**.

50 E. Koshevaya, E. Khramov, R. Svetogorov, A. Krasnov, I. Martakov, I. Shishkin, E. Krivoshapkina and P. Krivoshapkin, Stokes and anti-Stokes luminescent rare-earth-doped tantalum oxide nanoparticles, *Inorg. Chem.*, 2023, 10369–10381, DOI: **10.1021/acs.inorgchem.3c01231**.

51 D. Blanc, W. Zhang, C. Massard and J. Mugnier, Synthesis and characterisation of tantalum-incorporating silica hybrid sol gel thin films for optical applications, *Opt.*

Mater., 2006, **28**(3), 331–335, DOI: 10.1016/J.OPTMAT.2005.01.020.

52 E. Simonenko, N. Simonenko, Y. Ezhov, V. Sevastyanov and N. Kuznetsov, Study of the synthesis of nanocrystalline mixed tantalum–zirconium carbide, *Phys. At. Nucl.*, 2015, **78**(10), 1357–1365, DOI: 10.1134/S106377881512011X.

53 X. Zhou, C. Heinrich, M. Kluenker, S. Dolique, D. Mull and C. Lind, Non-hydrolytic sol–gel synthesis of tantalum sulfides, *J. Sol-Gel Sci. Technol.*, 2014, **69**(3), 596–604, DOI: 10.1007/s10971-013-3262-8.

54 Ö. Çelikbıçak, M. Atakay, Ü. Güler and B. Salih, A novel tantalum-based sol-gel packed microextraction syringe for highly specific enrichment of phosphopeptides in MALDI-MS applications, *Analyst*, 2013, **138**(15), 4403–4410, DOI: 10.1039/c3an00021d.

55 F. Rechberger, E. Tervoort and M. Niederberger, Nonaqueous sol–gel synthesis of InTaO4 nanoparticles and their assembly into macroscopic aerogels, *J. Am. Ceram. Soc.*, 2017, **100**(12), 4483–4490, DOI: 10.1111/JACE.15018.

56 N. Wei, D. Zhang, X. Han, F. Yang, Z. Zhong and K. Zheng, Synthesis and mechanism of ferroelectric potassium tantalate niobate nanoparticles by the solvothermal and hydrothermal processes, *J. Am. Ceram. Soc.*, 2007, **90**(5), 1434–1437, DOI: 10.1111/J.1551-2916.2007.01628.X.

57 J. Kelly and O. Graeve, Statistical experimental design approach for the solvothermal synthesis of nanostructured tantalum carbide powders, *J. Am. Ceram. Soc.*, 2011, **94**(5), 1706–1715, DOI: 10.1111/J.1551-2916.2010.04304.X.

58 J. Buha, D. Arčon, M. Niederberger and I. Djerdj, Solvothermal and surfactant-free synthesis of crystalline Nb2O5, Ta2O5, HfO2, and Co-doped HfO2 nanoparticles, *Phys. Chem. Chem. Phys.*, 2010, **12**(47), 15537–15543, DOI: 10.1039/c0cp01298j.

59 H. Kominami, M. Miyakawa, S. Murakami, T. Yasuda, M. Kohno, S. Onoue, Y. Kera and B. Ohtani, Solvothermal synthesis of tantalum(V) oxide nanoparticles and their photocatalytic activities in aqueous suspension systems, *Phys. Chem. Chem. Phys.*, 2001, **3**(14), 2697–2703, DOI: 10.1039/B101313K.

60 D. Gömpel, M. Tahir, M. Panthöfer, E. Mugnaioli, R. Brandscheid, U. Kolb and W. Tremel, Facile hydrothermal synthesis of crystalline Ta2O5 nanorods, MTaO3 (M = H, Na, K, Rb) nanoparticles, and their photocatalytic behaviour, *J. Mater. Chem. A*, 2014, **2**(24), 8033–8040, DOI: 10.1039/C4TA00183D.

61 D. Das and A. Ganguli, Design of nanostructured cadmium tantalate and niobate and their photocatalytic properties, *RSC Adv.*, 2013, **3**, 21697–21705, DOI: 10.1039/C3RA42667J.

62 J. Li, W. Dai, J. Yan, G. Wu, L. Li and N. Guan, Hydrothermal synthesis and photocatalytic properties of tantalum pentoxide nanorods, *Chin. J. Catal.*, 2015, **36**, 432–438, DOI: 10.1016/S1872-2067(14)60215-1.

63 M. Hsieh, G. Wu, W. Liu, W. Goddard and C. Yang, Nanocomposites of tantalum-based pyrochlore and indium hydroxide showing high and stable photocatalytic activities for overall water splitting and carbon dioxide reduction, *Angew. Chem.*, 2014, **53**(51), 14216–14220, DOI: 10.1002/anie.201408868.

64 R. Rafique, S. Baek, L. Phan, S. Chang, A. Gul and T. Park, A facile hydrothermal synthesis of highly luminescent NaYF4+/Er3+ upconversion nanoparticles and their biomonitoring capability, *Mater. Sci. Eng., C*, 2019, **99**, 1067–1074, DOI: 10.1016/j.msec.2019.02.046.

65 V. Luzanov, A. Vedeneev, V. Ryl'kov, M. Temiryazeva, A. Kozlov, M. Dukhnovskii and A. Bugaev, Synthesis of thin tantalum films by magnetron sputtering, *J. Commun. Technol. Electron.*, 2015, **60**, 1325–1327, DOI: 10.1134/S1064226915110133.

66 D. Singh, P. Grammatikopoulos, C. Cassidy, M. Benelmekki, M. Bohra, Z. Hawash, K. Baughman and M. Sowwan, Assembly of tantalum porous films with graded oxidation profile from size-selected nanoparticles, *J. Nanopart. Res.*, 2014, **16**, 1–10, DOI: 10.1007/s11051-014-2373-7.

67 Y. Horiuchi, S. Mine, M. Moriyasu, M. Anpo, T. Kim and M. Matsuoka, Preparation of tantalum oxynitride thin film photocatalysts by reactive magnetron sputtering deposition under high substrate temperature, *Res. Chem. Intermed.*, 2017, **43**, 5123–5136, DOI: 10.1007/s11164-017-3040-2.

68 T. Lertvanithphol, W. Rakreungdet, C. Chananonnawathorn, P. Eiamchai, S. Limwichean, N. Nuntawong, V. Patthanasettakul, A. Klamchuen, N. Khemasiri, J. Nukeaw, K. Seawsakul, C. Songsiriritthigul, N. Chanlek, H. Nakajima, P. Songsiriritthigul and M. Horprathum, Spectroscopic study on amorphous tantalum oxynitride thin films prepared by reactive gas-timing RF magnetron sputtering, *Appl. Surf. Sci.*, 2019, **490**, 100–106, DOI: 10.1016/J.APSUSC.2019.06.199.

69 J. Vlček, J. Rezek, J. Houška, R. Čerstvý and R. Bugyi, Process stabilization and a significant enhancement of the deposition rate in reactive high-power impulse magnetron sputtering of ZrO2 and Ta2O5 films, *Surf. Coat. Technol.*, 2013, **236**, 550–556, DOI: 10.1016/J.SURFCOAT.2013.10.052.

70 S. Chandra, S. Uthanna and G. Rao, Effect of substrate temperature on the structural, optical and electrical properties of dc magnetron sputtered tantalum oxide films, *Appl. Surf. Sci.*, 2008, **254**, 1953–1960, DOI: 10.1016/J.APSUSC.2007.08.005.

71 E. Hollands and D. Campbell, The mechanism of reactive sputtering, *J. Mater. Sci.*, 1968, **3**, 544–552, DOI: 10.1007/BF00549739.

72 M. Fekete, K. Bernátová, P. Klein, J. Hnilica and P. Vašina, Evolution of discharge parameters and sputtered species ionization in reactive HiPIMS with oxygen, nitrogen and acetylene, *Plasma Sources Sci. Technol.*, 2019, **28**, 025011, DOI: 10.1088/1361-6595/ab0363.

73 M. Renner, J. Fischer, H. Hajihoseini, J. Gudmundsson, M. Rudolph and D. Lundin, Angular distribution of titanium ions and neutrals in high-power impulse

magnetron sputtering discharges, *J. Vac. Sci. Technol., A*, 2023, 033009, DOI: 10.1116/6.0002555.

74 R. Arnell, P. Kelly and J. Bradley, Recent developments in pulsed magnetron sputtering, *Surf. Coat. Technol.*, 2004, **188**, 158–163, DOI: 10.1016/J.SURFCOAT.2004.08.010.

75 K. Patel, A. Sergievskaya, S. Chauhan and S. Konstantinidis, Heating of liquid substrate by low-pressure sputtering plasma, *J. Appl. Phys.*, 2022, 203301, DOI: 10.1063/5.0089214.

76 P. Cormier, A. Balhamri, A. Thomann, R. Dussart, N. Semmar, J. Mathias, R. Snyders and S. Konstantinidis, Measuring the energy flux at the substrate position during magnetron sputter deposition processes, *J. Appl. Phys.*, 2013, **113**, 013305, DOI: 10.1063/1.4773103.

77 H. Cook, An investigation of sputtered tantalum thin films, *Vacuum*, 1967, 80–86, DOI: 10.1116/1.1492526.

78 J. Alexander and H. Wirth, Preparation of tantalum targets of known thicknesses, *Nucl. Instrum. Methods Phys. Res., Sect. A*, 1985, **236**, 545–548, DOI: 10.1016/0168-9002(85)90958-1.

79 V. Shapovalov, Physicochemical model for reactive sputtering of a sandwich target, *J. Appl. Phys.*, 2023, 085301, DOI: 10.1063/5.0128399.

80 A. Baker, A. Engwall, L. Bayu-Aji, J. Bae, S. Shin, J. Moody and S. Kucheyev, Tantalum suboxide films with tunable composition and electrical resistivity deposited by reactive magnetron sputtering, *Coatings*, 2022, **12**, 917, DOI: 10.3390/coatings12070917.

81 D. Cristea, I. Velicu, L. Cunha, N. Barradas, E. Alves and V. Craciun, Tantalum-titanium oxynitride thin films deposited by DC reactive magnetron co-sputtering: Mechanical, optical, and electrical characterization, *Coatings*, 2021, **12**, 36, DOI: 10.3390/coatings12010036.

82 T. Beline, J. Silva, A. Matos, N. Neto, A. Almeida, F. Júnior, D. Leite, E. Rangel and V. Barão, Tailoring the synthesis of tantalum-based thin films for biomedical application: Characterization and biological response, *Mater. Sci. Eng. C*, 2019, **101**, 111–119, DOI: 10.1016/j.msec.2019.03.072.

83 M. Rudolph, A. Demeter, E. Foy, V. Tiron, L. Sirghi, T. Minea, B. Bouchet-Fabre and M. Hugon, Improving the degree of crystallinity of magnetron-sputtered Ta3N5 thin films by augmenting the ion flux onto the substrate, *Thin Solid Films*, 2017, **636**, 48–53, DOI: 10.1016/J.TSF.2017.05.033.

84 Y. Carvajal-Campos, L. Ceballos-Mendivil, F. Baldenebro-Lopez, C. Pérez-Rábago and C. Estrada, Synthesis and characterization of tantalum carbide nanoparticles using concentrated solar energy, *Adv. Powder Technol.*, 2019, **30**, 898–906, DOI: 10.1016/J.APT.2019.08.004.

85 Q. Gao, C. Giordano and M. Antonietti, Controlled synthesis of tantalum oxynitride and nitride nanoparticles, *Small*, 2011, **7**, 3334–3340, DOI: 10.1002/smll.201101207.

86 A. Egeberg, L. Faden, A. Zimina, J. Grunwaldt, D. Gerthsen and C. Feldmann, Liquid-phase synthesis of highly oxophilic zerovalent niobium and tantalum nanoparticles, *Chem. Commun.*, 2021, **57**, 3648–3651, DOI: 10.1039/d1cc00681a.

87 M. Jalaly, F. Gotor and M. Sayagués, Mechanochemical combustion synthesis of vanadium carbide (VC), niobium carbide (NbC) and tantalum carbide (TaC) nanoparticles, *J. Refract. Met. Hard Mater.*, 2019, **81**, 146–154, DOI: 10.1016/J.IJRMHM.2018.12.011.

88 P. Pleskunov, T. Košutová, M. Vaidulych, D. Nikitin, Z. Krtouš, S. Ali-Ogly, K. Kishenina, R. Tafiichuk, H. Biederman, I. Gordeev, J. Drewes, I. Barg, F. Faupel, M. Cieslar, R. Yatskiv, Y. Pihosh, V. Nandal, K. Seki, K. Domen and A. Choukourov, The sputter-based synthesis of tantalum oxynitride nanoparticles with architecture and bandgap controlled by design, *Appl. Surf. Sci.*, 2021, **559**, 149974, DOI: 10.1016/J.APSUSC.2021.149974.

89 A. Jo, Y. Lee and C. Lee, Electrodeposition of tantalum on carbon black in non-aqueous solution and its electrocatalytic properties, *Anal. Chim. Acta*, 2016, **933**, 59–65, DOI: 10.1016/j.aca.2016.05.030.

90 H. Hajibabaei and T. Hamann, Selective Electrodeposition of Tantalum(V) Oxide Electrodes, *Langmuir*, 2017, **33**, 10800–10806, DOI: 10.1021/acs.langmuir.7b02414.

91 H. Simunkova, T. Lednický, A. Whitehead, L. Kalina, P. Šimůnek and J. Hubálek, Tantalum-based nanotube arrays *via* porous-alumina-assisted electrodeposition from ionic liquid: Formation and electrical characterization, *Appl. Surf. Sci.*, 2021, **548**, 149264, DOI: 10.1016/J.APSUSC.2021.149264.

92 Y. Wang, Z. Cui and Z. Zhang, Synthesis and phase structure of tantalum nanoparticles, *Mater. Lett.*, 2004, **58**, 3017–3020, DOI: 10.1016/J.MATLET.2004.05.031.

93 C. Ho, K. Low, R. Klie, K. Maeda, K. Domen, R. Meyer and P. Snee, Synthesis and characterization of semiconductor tantalum nitride nanoparticles, *J. Phys. Chem. C*, 2011, **115**, 647–652, DOI: 10.1021/JP110105U.

94 J. Kim, A. Silva, J. Hsu, P. Maidment, N. Shapira, P. Noël and D. Cormode, Radioprotective garment-inspired biodegradable polymetal nanoparticles for enhanced CT contrast production, *Chem. Mater.*, 2019, **32**(1), 381–391, DOI: 10.1021/acs.chemmater.9b03931.

95 N. Lee, S. Choi and T. Hyeon, Nano-sized CT contrast agents, *Adv. Mater.*, 2013, **25**, 2641–2660, DOI: 10.1002/adma.201300081.

96 M. Shilo, T. Reuveni, M. Motiei and R. Popovtzer, Nanoparticles as computed tomography contrast agents: current status and future perspectives, *Nanomedicine*, 2012, **7**(2), 257–269, DOI: 10.2217/nnm.11.190.

97 I. Steinberg, D. Huland, O. Vermesh, H. Frostig, W. Tummers and S. Gambhir, Photoacoustic clinical imaging, *Photoacoustics*, 2019, **14**, 77–98, DOI: 10.1016/j.pacs.2019.05.001.

98 J. Weber, P. Beard and S. Bohndiek, Contrast agents for molecular photoacoustic imaging, *Nat. Methods*, 2016, **13**, 639–650, DOI: 10.1038/nmeth.3929.

99 P. Beard, Biomedical photoacoustic imaging, *Interface Focus*, 2011, **1**, 602–631, DOI: 10.1098/rsfs.2011.0028.

100 W. Vogt, C. Jia, K. Wear, B. Garra, T. Pfefer and J. Pfefer, Biologically relevant photoacoustic imaging phantoms with tunable optical and acoustic properties, *J. Biomed. Opt.*, 2016, **21**, 101405, DOI: 10.1117/1.JBO.21.10.101405.

101 P. Bonitatibus, A. Torres, G. Goddard, P. Fitzgerald and A. Kulkarni, Synthesis, characterization, and computed tomography imaging of a tantalum oxide nanoparticle imaging agent, *Chem. Commun.*, 2010, **46**(47), 8956–8958, DOI: 10.1039/c0cc03302b.

102 M. Oh, N. Lee, H. Kim, S. Park, Y. Piao, J. Lee, S. Jun, W. Moon, S. Choi and T. Hyeon, Large-scale synthesis of bioinert tantalum oxide nanoparticles for X-ray computed tomography imaging and bimodal image-guided sentinel lymph node mapping, *J. Am. Chem. Soc.*, 2011, **133**(14), 5508–5515, DOI: 10.1021/ja200120k.

103 A. Torres, P. Bonitatibus, R. Colborn, G. Goddard, P. Fitzgerald, B. Lee and M. Marino, Biological performance of a size-fractionated core-shell tantalum oxide nanoparticle X-ray contrast agent, *Investig. Radiol.*, 2012, **47**, 578–587, DOI: 10.1097/RLI.0b013e318260fc40.

104 X. Wang, C. Wang, S. Anderson and X. Zhang, Fabrication of hydrogel particles with tantalum oxide nanoparticle payloads as computed tomography contrast agents, *2013 Transducers & Eurosensors XXVII: the 17th International Conference on Solid-State Sensors, Actuators and Microsystems (TRANSDUCERS & EUROSENSORS XXVII)*, 2013, pp. 426–429, DOI: 10.1109/TRANSDUCERS.2013.6626794.

105 J. Freedman, H. Lusic, B. Snyder and M. Grinstaff, Tantalum oxide nanoparticles for the imaging of articular cartilage using X-ray computed tomography: visualization of ex vivo/in vivo murine tibia and ex vivo human index finger cartilage, *Angew. Chem. Int. Ed.*, 2014, **53**(32), 8406–8410, DOI: 10.1002/anie.201404519.

106 Y. Jin, Y. Li, X. Ma, Z. Zha, L. Shi, J. Tian and Z. Dai, Encapsulating tantalum oxide into polypyrrole nanoparticles for X-ray CT/photoacoustic bimodal imaging-guided photothermal ablation of cancer, *Biomaterials*, 2014, **35**(22), 5795–5804, DOI: 10.1016/j.biomaterials.2014.03.086.

107 Y. Jin, X. Ma, S. Feng, X. Liang, Z. Dai, J. Tian and X. Yue, Hyaluronic Acid Modified Tantalum Oxide Nanoparticles Conjugating Doxorubicin for Targeted Cancer Theranostics, *Bioconjugate Chem.*, 2015, **26**(12), 2530–2541, DOI: 10.1021/acs.bioconjchem.5b00551.

108 P. Fitzgerald, M. Butts, J. Roberts, R. Colborn, A. Torres, B. Lee, B. Yeh and P. Bonitatibus, A Proposed Computed Tomography Contrast Agent Using Carboxybetaine Zwitterionic Tantalum Oxide Nanoparticles: Imaging, Biological, and Physicochemical Performance, *Invest. Radiol.*, 2016, **51**, 786–796, DOI: 10.1097/RLI.0000000000000279.

109 C. Dai, Y. Chen, X. Jing, L. Xiang, D. Yang, H. Lin, Z. Liu, X. Han and R. Wu, Two-Dimensional Tantalum Carbide (MXenes) Composite Nanosheets for Multiple Imaging-Guided Photothermal Tumor Ablation, *ACS Nano*, 2017, **11**(12), 12696–12712, DOI: 10.1021/acsnano.7b07241.

110 Y. Liu, X. Ji, J. Liu, W. Tong, D. Askhatova and J. Shi, Tantalum Sulfide Nanosheets as a Theranostic Nanoplatform for Computed Tomography Imaging-Guided Combinatorial Chemo-Photothermal Therapy, *Adv. Funct. Mater.*, 2017, **27**, 1703261, DOI: 10.1002/adfm.201703261.

111 E. Koshevaya, D. Nazarovskaia, M. Simakov, A. Belousov, V. Morozov, E. Gandalipov, E. Krivoshapkina and P. Krivoshapkin, Surfactant-free tantalum oxide nanoparticles: synthesis, colloidal properties, and application as a contrast agent for computed tomography, *J. Mater. Chem. B*, 2020, **8**, 7763–7774, DOI: 10.1039/d0tb01204a.

112 S. Chakravarty, J. Hix, K. Wiewiora, M. Volk, E. Kenyon, D. Shuboni-Mulligan, B. Blanco-Fernandez, M. Kiupel, J. Thomas, L. Sempere and E. Shapiro, Tantalum oxide nanoparticles as versatile contrast agents for X-ray computed tomography, *Nanoscale*, 2020, **12**, 17026–17035, DOI: 10.26434/chemrxiv.11845572.

113 T. Lawson, A. Joenathan, A. Patwa, B. Snyder and M. Grinstaff, Tantalum Oxide Nanoparticles for the Quantitative Contrast-Enhanced Computed Tomography of Ex Vivo Human Cartilage: Assessment of Biochemical Composition and Biomechanics, *ACS Nano*, 2021, **15**(8), 13243–13255, DOI: 10.1021/acsnano.1c03375.

114 A. Narasimhan, S. Balasubramanian and G. Krishnamurthi, Influence of europium (Eu) doped tantalum oxide nanoparticles (TaOx NPs): A potential contrast agent, *Mater. Lett.*, 2021, **300**, 130214, DOI: 10.1016/J.MATLET.2021.130214.

115 N. Lee, H. Cho, M. Oh, S. Lee, K. Kim, B. Kim, K. Shin, T. Ahn, J. Choi, Y. Kim, S. Choi and T. Hyeon, Multifunctional Fe3O4/TaO(x) core/shell nanoparticles for simultaneous magnetic resonance imaging and X-ray computed tomography, *J. Am. Chem. Soc.*, 2012, **134**(25), 10309–10312, DOI: 10.1021/ja3016582.

116 L. Feng, C. Wang, C. Li, S. Gai, F. He, R. Li, G. An, C. Zhong, Y. Dai, Z. Yang and P. Yang, Multifunctional Theranostic Nanoplatform Based on Fe-mTa2O5@CuS-ZnPc/PCM for Bimodal Imaging and Synergistically Enhanced Phototherapy, *Inorg. Chem.*, 2018, **57**(9), 4864–4876, DOI: 10.1021/acs.inorgchem.7b02959.

117 E. Ehlerding, P. Grodzinski, W. Cai and C. Liu, Big Potential from Small Agents: Nanoparticles for Imaging-Based Companion Diagnostics, *ACS Nano*, 2018, **12**(3), 2106–2121, DOI: 10.1021/acsnano.7b07252.

118 L. Manen, J. Dijkstra, C. Boccara, E. Benoit, A. Vahrmeijer, M. Gora and J. Mieog, The clinical usefulness of optical coherence tomography during cancer interventions, *J. Cancer Res. Clin. Oncol.*, 2018, **144**, 1967–1990, DOI: 10.1007/s00432-018-2690-9.

119 M. Unterrainer, M. Unterrainer, C. Eze, H. Ilhan, S. Marschner, O. Roengvoraphoj, N. Schmidt-Hegemann, F. Walter, W. Kunz, P. Rosenschöld, R. Jeraj, N. Albert, A. Grosu, M. Niyazi, P. Bartenstein and C. Belka, Recent advances of PET imaging in clinical radiation oncology,

Radiat. Oncol., 2020, **15**, 1–8, DOI: **10.1186/s13014-020-01519-1**.

120 S. Curran, A. Muellner and L. Schwartz, Imaging response assessment in oncology, *Cancer Imag.*, 2006, **6**(Spec No A), 126–130, DOI: **10.1102/1470-7330.2006.9039**.

121 J. Lambert, Y. Sun, C. Stillson, Z. Li, R. Kumar, S. Wang, P. Fitzgerald, P. Bonitatibus, R. Colborn, J. Roberts, P. Edic, M. Marino and B. Yeh, An intravascular tantalum oxide-based CT contrast agent: preclinical evaluation emulating overweight and obese patient size, *Radiology*, 2018, **289**(1), 103–110, DOI: **10.1148/radiol.2018172381**.

122 Q. Xiao, W. Bu, Q. Ren, S. Zhang, H. Xing, F. Chen, M. Li, X. Zheng, Y. Hua, L. Zhou, W. Peng, H. Qu, Z. Wang, K. Zhao and J. Shi, Radiopaque fluorescence-transparent TaOx decorated upconversion nanophosphors for *in vivo* CT/MR/UCL trimodal imaging, *Biomaterials*, 2012, **33**(30), 7530–7539, DOI: **10.1016/j.biomaterials.2012.06.028**.

123 Q. Xiao, W. Bu, Q. Ren, S. Zhang, H. Xing, F. Chen, M. Li, X. Zheng, Y. Hua, L. Zhou, W. Peng, H. Qu, Z. Wang, K. Zhao and J. Shi, Radiopaque fluorescence-transparent TaOx decorated upconversion nanophosphors for *in vivo* CT/MR/UCL trimodal imaging, *Biomaterials*, 2012, **33**(30), 7530–7539, DOI: **10.1016/j.biomaterials.2012.06.028**.

124 S. Mouli, P. Tyler, J. Mcdevitt, A. Eifler, Y. Guo, J. Nicolai, R. Lewandowski, W. Li, D. Procissi, R. Ryu, Y. Wang, R. Salem, A. Larson and R. Omary, Image-guided local delivery strategies enhance therapeutic nanoparticle uptake in solid tumors, *ACS Nano*, 2013, **7**(9), 7724–7733, DOI: **10.1021/nn4023119**.

125 E. K. Zaluzec, E. Kenyon, M. Volk, *et al.*, Tantalum oxide nanoparticles as versatile and high-resolution X-ray contrast agents for intraductal image-guided ablative procedures in rodent models of breast cancer, *npj Imaging*, 2024, **2**, 3, DOI: **10.1038/s44303-024-00007-5**.

126 H. Na, I. Song and T. Hyeon, Inorganic nanoparticles for MRI contrast agents, *Adv. Mater.*, 2009, **21**, 2133–2148, DOI: **10.1002/adma.200802366**.

127 S. Ahn, N. Lee, C. Choi, S. Shin, Y. Han and H. Park, Feasibility study of Fe3O4/TaOx nanoparticles as a radiosensitizer for proton therapy, *Phys. Med. Biol.*, 2018, **63**, 114001, DOI: **10.1088/1361-6560/aac27b**.

128 J. C. De La Vega and U. O. Häfeli, Utilization of nanoparticles as X-ray contrast agents for diagnostic imaging applications, *Contrast Media Mol. Imaging*, 2014, **10**(2), 81–95, DOI: **10.1002/cmmi.1613**.

129 C. F. C. G. Geraldes, Rational design of magnetic nanoparticles as T1–T2 dual-mode MRI contrast agents, *Molecules*, 2024, **29**, 1352, DOI: **10.3390/molecules29061352**.

130 Y. Qin, H. Peng, X. He, W. Li and Y. Zhang, pH-responsive polymer-stabilized ZIF-8 nanocomposite for fluorescence and magnetic resonance dual-modal imaging-guided chemo/photodynamic combinational cancer therapy, *ACS Appl. Mater. Interfaces*, 2019, 34268–34281, DOI: **10.1021/acsami.9b12641**.

131 T. Beyer, L. S. Freudenberg, D. W. Townsend and J. Czernin, The future of hybrid imaging-part 1: hybrid imaging technologies and SPECT/CT, *Insights Imaging*, 2011, **2**(2), 161–169, DOI: **10.1007/s13244-010-0063-2**.

132 G. Crișan, N. S. Moldovean-Cioroianu, D. G. Timaru, G. Andrieș, C. Căinap and V. Chiș, Radiopharmaceuticals for PET and SPECT imaging: a literature review over the last decade, *Int. J. Mol. Sci.*, 2022, **23**(9), 5023, DOI: **10.3390/ijms23095023**.

133 J. Cal-Gonzalez, I. Rausch, L. K. Shiyam Sundar, M. L. Lassen, O. Muzik, E. Moser, L. Papp and T. Beyer, Hybrid imaging: instrumentation and data processing updated, *Front. Phys.*, 2018, **6**, 47, DOI: **10.3389/fphy.2018.00047**.

134 G. Song, Y. Chao, Y. Chen, C. Liang, X. Yi, G. Yang, K. Yang, L. Cheng, Q. Zhang and Z. Liu, All-in-one theranostic nanoplatform based on hollow TaOx for chelator-free labeling imaging, drug delivery, and synergistically enhanced radiotherapy, *Adv. Funct. Mater.*, 2016, 8243–8254, DOI: **10.1002/adfm.201603845**.

135 Y. Jin, X. Ma, S. Zhang, H. Meng, M. Xu, X. Yang, W. Xu and J. Tian, A tantalum oxide-based core/shell nanoparticle for triple-modality image-guided chemo-thermal synergetic therapy of esophageal carcinoma, *Cancer Lett.*, 2017, **397**, 61–71, DOI: **10.1016/j.canlet.2017.03.030**.

136 D. Cormode, P. Naha and Z. Fayad, Nanoparticle contrast agents for computed tomography: a focus on micelles, *Contrast Media Mol. Imaging*, 2014, **9**(1), 37–52, DOI: **10.1002/cmmi.1551**.

137 M. Galper, M. Saung, V. Fuster, E. Roessl, A. Thran, R. Proksa, Z. Fayad and D. Cormode, Effect of computed tomography scanning parameters on gold nanoparticle and iodine contrast, *Investig. Radiol.*, 2012, **47**, 475–481, DOI: **10.1097/RLI.0b013e3182562ab9**.

138 S. Rajasekar, E. Martin, S. Kuppusamy and C. Vetrivel, Chitosan coated molybdenum sulphide nanosheet incorporated with tantalum oxide nanomaterials for improving cancer photothermal therapy, *Arabian J. Chem.*, 2020, **13**, 4741–4750, DOI: **10.1016/j.arabjc.2019.11.005**.

139 N. Fernandes, C. Rodrigues, A. Moreira and I. Correia, Overview of the application of inorganic nanomaterials in cancer photothermal therapy, *Biomater. Sci.*, 2020, 2990–3020, DOI: **10.1039/d0bm00222d**.

140 Z. Zhou, Y. Yan, L. Wang, Q. Zhang and Y. Cheng, Melanin-like nanoparticles decorated with an autophagy-inducing peptide for efficient targeted photothermal therapy, *Biomaterials*, 2019, **203**, 63–72, DOI: **10.1016/j.biomaterials.2019.02.023**.

141 H. Sun, Q. Zhang, J. Li, S. Peng, X. Wang and R. Cai, Near-infrared photoactivated nanomedicines for photothermal synergistic cancer therapy, *Nano Today*, 2021, **37**, 101073, DOI: **10.1016/J.NANTOD.2020.101073**.

142 S. Kumari, N. Sharma and S. Sahi, Advances in Cancer Therapeutics: Conventional Thermal Therapy to Nanotechnology-Based Photothermal Therapy, *Pharmaceutics*, 2021, **13**, 1174, DOI: **10.3390/pharmaceutics13081174**.

143 Q. Chen, L. Xu, C. Liang, C. Wang, R. Peng and Z. Liu, Photothermal therapy with immune-adjuvant

nanoparticles together with checkpoint blockade for effective cancer immunotherapy, *Nat. Commun.*, 2016, **7**, 13193, DOI: 10.1038/ncomms13193.

144 M. Salimi, S. Mosca, B. Gardner, F. Palombo, P. Matousek and N. Stone, Nanoparticle-Mediated Photothermal Therapy Limitation in Clinical Applications Regarding Pain Management, *Nanomaterials*, 2022, **12**, 922, DOI: 10.3390/nano12060922.

145 L. Amornkitbamrung, S. Srisaard, C. Jubsilp, C. Bielawski, S. Um and S. Rimdusit, Near-infrared light responsive shape memory polymers from bio-based benzoxazine/epoxy copolymers produced without using photothermal filler, *Polymer*, 2020, **209**, 122986, DOI: 10.1016/j.polymer.2020.122986.

146 A. Agrawal, S. Cho, O. Zandi, S. Ghosh, R. Johns and D. Milliron, Localized Surface Plasmon Resonance in Semiconductor Nanocrystals, *Chem. Rev.*, 2018, **118**(6), 3121–3207, DOI: 10.1021/acs.chemrev.7b00613.

147 S. Kumar and S. Seo, Plasmonic sensors: A new frontier in nanotechnology, *Biosensors*, 2023, **13**(3), 385, DOI: 10.3390/bios13030385.

148 T. I. Shabatina, O. I. Vernaya, N. L. Shimanovskiy and M. Y. Melnikov, Metal and metal oxides nanoparticles and nanosystems in anticancer and antiviral theragnostic agents, *Pharmaceutics*, 2023, **15**(4), 1181, DOI: 10.3390/pharmaceutics15041181.

149 X. Ding, C. H. Liow, Z. Mengxin, R. Huang, C. Li, H. Shen, M. Liu, Y. Zou, N. Gao, Z. Zhang, Y. Li, Q. Wang, S. Li and J. Jiang, Surface plasmon resonance enhanced light absorption and photothermal therapy in the second near-infrared window, *J. Am. Chem. Soc.*, 2014, **136**(44), 15350–15358, DOI: 10.1021/ja508641z.

150 A. R. Indhu, L. Keerthana and G. Dharmalingam, Plasmonic nanotechnology for photothermal applications—An evaluation, *Beilstein J. Nanotechnol.*, 2023, **14**, 380–419, DOI: 10.3762/bjnano.14.33.

151 E. Petryayeva and U. J. Krull, Localized surface plasmon resonance: Nanostructures, bioassays, and biosensing—A review, *Anal. Chim. Acta*, 2011, **706**(1), 8–24, DOI: 10.1016/j.aca.2011.08.020.

152 J. Liu, H. He, D. Xiao, S. Yin, W. Ji, S. Jiang, D. Luo, B. Wang and Y. Liu, Recent advances of plasmonic nanoparticles and their applications, *Materials*, 2018, **11**(10), 1833, DOI: 10.3390/ma11101833.

153 N. Khlebtsov, L. A. Trachuk and A. G. Mel'nikov, The effect of the size, shape, and structure of metal nanoparticles on the dependence of their optical properties on the refractive index of a disperse medium, *Opt Spectrosc.*, 2005, **98**(1), 77–83, DOI: 10.1134/1.1858043.

154 S. Schelm, G. H. Smith, P. D. Garrett and W. K. Fisher, Tuning the surface-plasmon resonance in nanoparticles for glazing applications, *J. Appl. Phys.*, 2005, **97**(12), 124314, DOI: 10.1063/1.1924873.

155 J. Fernandes and S. Kang, Numerical study on the surface plasmon resonance tunability of spherical and non-spherical core-shell dimer nanostructures, *Nanomaterials*, 2021, **11**(7), 1728, DOI: 10.3390/nano11071728.

156 S. Das and V. K. Singh, The role of Ta2O5 thin film on a plasmonic refractive index sensor based on photonic crystal fiber, *Photon. Nanostruct: Fundam. Appl.*, 2021, **44**, 100904, DOI: 10.1016/j.photonics.2021.100904.

157 M. K. Mahata, R. De and K. T. Lee, Near-infrared-triggered upconverting nanoparticles for biomedicine applications, *Biomedicines*, 2021, **9**(7), 756, DOI: 10.3390/biomedicines9070756.

158 N. K. Allam, B. S. Shaheen and A. M. Hafez, Layered tantalum oxynitride nanorod array carpets for efficient photoelectrochemical conversion of solar energy: Experimental and DFT insights, *ACS Appl. Mater. Interfaces*, 2014, **6**(7), 4609–4615, DOI: 10.1021/am500286n.

159 X. Cui, Q. Ruan, X. Zhuo, X. Xia, J. Hu, R. Fu, Y. Li, J. Wang and H. Xu, Photothermal nanomaterials: A powerful light-to-heat converter, *Chem. Rev.*, 2023, **123**(11), 6891–6952, DOI: 10.1021/acs.chemrev.3c00159.

160 C. D. Landon, M. T. Brumbach, G. L. Brennecka, M. Blea-Kirby, J. F. Ihlefeld, M. Marinella, *et al.*, Thermal transport in tantalum oxide films for memristive applications, *Appl. Phys. Lett.*, 2015, **107**(5), 059902, DOI: 10.1063/1.4928532.

161 X. Su, M. Viste, J. H. Schott, L. Yang and B. W. Sheldon, In-situ stress measurement during heat treatment of amorphous tantalum oxide, *ECS J. Solid State Sci. Technol.*, 2015, **4**(7), N64–N69, DOI: 10.1149/2.0091507jss.

162 T. Kagawa, Y. Matsumi, H. Aono, T. Ohara, H. Tazawa, K. Shigeyasu, *et al.*, Immuno-hyperthermia effected by antibody-conjugated nanoparticles selectively targets and eradicates individual cancer cells, *Cell Cycle*, 2021, **20**, 1221–1230, DOI: 10.1080/15384101.2021.1915604.

163 A. Bettaieb, P. K. Wrzal and D. A. Averill-Bates, *Hyperthermia: Cancer Treatment and beyond*, InTech, 2013, DOI: 10.5772/55795.

164 D. Liu, Y. Hong, Y. Li, C. Hu, T. C. Yip, W. K. Yu, *et al.*, Targeted destruction of cancer stem cells using multifunctional magnetic nanoparticles that enable combined hyperthermia and chemotherapy, *Theranostics*, 2020, **10**(3), 1181–1196, DOI: 10.7150/thno.38989.

165 V. M. Bala, D. I. Lampropoulou, S. Grammatikaki, V. Kouloulias, N. Lagopati, G. Aravantinos, *et al.*, Nanoparticle-mediated hyperthermia and cytotoxicity mechanisms in cancer, *Int. J. Mol. Sci.*, 2024, **25**(1), 296, DOI: 10.3390/ijms25010296.

166 M. Szwed and A. Marczak, Application of nanoparticles for magnetic hyperthermia for cancer treatment—The current state of knowledge, *Cancers*, 2024, **16**(6), 1156, DOI: 10.3390/cancers16061156.

167 D. Chang, M. Lim, J. A. C. M. Goos, R. Qiao, Y. Y. Ng, F. M. Mansfeld, *et al.*, Biologically targeted magnetic hyperthermia: Potential and limitations, *Front. Pharmacol*, 2018, **9**, 831, DOI: 10.3389/fphar.2018.00831.

168 T. Grimmig, R. Thumm, R. Moench, E. Moll, C. Germer, A. Waaga-Gasser, *et al.*, Hyperthermia and chemotherapy mediated effects on tumor cell proliferation and heat shock protein expression in human colon cancer, *Cancer Res.*, 2015, **75**, 1244, DOI: 10.1158/1538-7445.AM2015-1244.

169 F. Lin, C. Hsu and Y. Lin, Nano-therapeutic cancer immunotherapy using hyperthermia-induced heat shock proteins: Insights from mathematical modeling, *Int. J. Nanomed.*, 2018, **13**, 3529–3539, DOI: 10.2147/IJN.S166000.

170 M. Rylander, Y. Feng, J. Bass and K. Diller, Thermally induced injury and heat-shock protein expression in cells and tissues, *Ann. N. Y. Acad. Sci.*, 2005, **1066**, 249–262, DOI: 10.1196/annals.1363.009.

171 N. Larson, A. Gormley, N. Frazier and H. Ghandehari, Synergistic enhancement of cancer therapy using a combination of heat shock protein targeted HPMA copolymer-drug conjugates and gold nanorod induced hyperthermia, *J. Controlled Release*, 2013, **170**(1), 41–50, DOI: 10.1016/j.jconrel.2013.04.006.

172 R. Ishii, T. Kamiya, H. Hara and T. Adachi, Hyperthermia synergistically enhances cancer cell death by plasma-activated acetated Ringer's solution, *Arch. Biochem. Biophys.*, 2020, 108565, DOI: 10.1016/j.abb.2020.108565.

173 A. Burke, R. Singh, D. Carroll, J. Wood, R. D'Agostino, P. Ajayan, *et al.*, The resistance of breast cancer stem cells to conventional hyperthermia and their sensitivity to nanoparticle-mediated photothermal therapy, *Biomaterials*, 2012, **33**(10), 2961–2970, DOI: 10.1016/j.biomaterials.2011.12.052.

174 G. Sanità, B. Carrese and A. Lamberti, Nanoparticle surface functionalization: How to improve biocompatibility and cellular internalization, *Front. Mol. Biosci.*, 2020, **7**, 587012, DOI: 10.3389/fmolb.2020.587012.

175 H. Maeda, H. Nakamura and J. Fang, The EPR effect for macromolecular drug delivery to solid tumors: Improvement of tumor uptake, lowering of systemic toxicity, and distinct tumor imaging in vivo, *Adv. Drug Delivery Rev.*, 2013, **65**(1), 71–79, DOI: 10.1016/j.addr.2012.10.002.

176 H. Kang, S. Rho, W. Stiles, S. Hu, Y. Baek, D. Hwang, *et al.*, Size-dependent EPR effect of polymeric nanoparticles on tumor targeting, *Adv. Healthcare Mater.*, 2019, **9**(16), 1901223, DOI: 10.1002/adhm.201901223.

177 M. Yu and J. Zheng, Clearance pathways and tumor targeting of imaging nanoparticles, *ACS Nano*, 2015, **9**(7), 6655–6674, DOI: 10.1021/acsnano.5b01320.

178 D. Vyas, M. Patel and S. Wairkar, Strategies for active tumor targeting—An update, *Eur. J. Pharmacol.*, 2021, **895**, 174512, DOI: 10.1016/j.ejphar.2021.174512.

179 M. Masucci, M. Minopoli and M. Carriero, Tumor-associated neutrophils: Their role in tumorigenesis, metastasis, prognosis, and therapy, *Front. Oncol.*, 2019, **9**, 1146, DOI: 10.3389/fonc.2019.01146.

180 T. Lammers, F. Kiessling, W. Hennink and G. Storm, Drug targeting to tumors: Principles, pitfalls, and (pre-)clinical progress, *J. Controlled Release*, 2012, **161**(2), 175–187, DOI: 10.1016/j.jconrel.2011.09.063.

181 F. Danhier, O. Féron and V. Préat, To exploit the tumor microenvironment: Passive and active tumor targeting of nanocarriers for anti-cancer drug delivery, *J. Controlled Release*, 2010, **148**(2), 135–146, DOI: 10.1016/j.jconrel.2010.08.027.

182 R. Wakaskar, Passive and Active Targeting in Tumor Microenvironment, *Int. J. Drug Dev. Res.*, 2017, **9**, 37.

183 P. Schildkopf, B. Frey, O. Ott, Y. Rubner, G. Multhoff, R. Sauer, *et al.*, Radiation combined with hyperthermia induces HSP70-dependent maturation of dendritic cells and release of pro-inflammatory cytokines by dendritic cells and macrophages, *Radiother. Oncol.*, 2011, **101**(1), 109–115, DOI: 10.1016/j.radonc.2011.05.056.

184 A. Ito, F. Matsuoka, H. Honda and T. Kobayashi, Antitumor effects of combined therapy of recombinant heat shock protein 70 and hyperthermia using magnetic nanoparticles in an experimental subcutaneous murine melanoma, *Cancer Immunol. Immunother.*, 2003, **53**, 26–32, DOI: 10.1007/s00262-003-0416-5.

185 C. Peng, Y. Liang, Y. Chen, X. Qian, W. Luo, S. Chen, *et al.*, Hollow mesoporous tantalum oxide based nanospheres for triple sensitization of radiotherapy, *ACS Appl. Mater. Interfaces*, 2020, **12**(5), 5520–5530, DOI: 10.1021/acsami.9b20053.

186 Y. Jiao, X. Zhang, H. Yang, H. Ma and J. Zou, Mesoporous tantalum oxide nanomaterials induced cardiovascular endothelial cell apoptosis *via* mitochondrial-endoplasmic reticulum stress apoptotic pathway, *Drug Deliv.*, 2023, **30**(1), 108–120, DOI: 10.1080/10717544.2022.2147251.

187 V. Deepagan, H. Ko, S. Kwon, N. Rao, S. Kim, W. Um, *et al.*, Intracellularly Activatable Nanovasodilators to Enhance Passive Cancer Targeting Regime, *Nano Lett.*, 2018, **18**(4), 2637–2644, DOI: 10.1021/acs.nanolett.8b00495.

188 M. Kettering, H. Richter, F. Wiekhorst, S. Bremer-Streck, L. Trahms, W. Kaiser, *et al.*, Minimal-invasive magnetic heating of tumors does not alter intra-tumoral nanoparticle accumulation, allowing for repeated therapy sessions: an *in vivo* study in mice, *Nanotechnology*, 2011, **22**, 505102, DOI: 10.1088/0957-4484/22/50/505102.

189 A. Nel, E. Ruoslahti and H. Meng, New Insights into "Permeability" as in the Enhanced Permeability and Retention Effect of Cancer Nanotherapeutics, *ACS Nano*, 2017, **11**(10), 9567–9569, DOI: 10.1021/acsnano.7b07214.

190 R. Shannon, P. Tracey, P. Smyth, C. J. Barelle and C. J. Scott, Development of next generation nanomedicine-based approaches for the treatment of cancer: We've barely scratched the surface, *Biochem. Soc. Trans.*, 2021, **49**(5), 2253–2269, DOI: 10.1042/BST20210343.

191 D. Kalyane, N. Raval, R. Maheshwari, V. Tambe, K. Kalia and R. Tekade, Employment of enhanced permeability and retention effect (EPR): Nanoparticle-based precision tools for targeting of therapeutic and diagnostic agent in cancer, *Mater. Sci. Eng. C*, 2019, **98**, 1252–1276, DOI: 10.1016/j.msec.2019.01.066.

192 U. Prabhakar, H. Maeda, R. K. Jain, E. Sevick-Muraca, W. A. Zamboni, O. C. Farokhzad, *et al.*, Challenges and key considerations of the enhanced permeability and retention effect for nanomedicine drug delivery in oncology, *Cancer Res.*, 2013, **73**(8), 2412–2417, DOI: 10.1158/0008-5472.CAN-12-4561.

193 M. Izci, C. Maksoudian, B. Manshian and S. J. Soenen, The Use of Alternative Strategies for Enhanced Nanoparticle

Delivery to Solid Tumors, *Chem. Rev.*, 2021, **121**, 1746–1803, DOI: 10.1021/acs.chemrev.0c00779.

194 C. Babbs, D. DeWitt, W. Voorhees, J. McCaw and R. Chan, Theoretical feasibility of vasodilator-enhanced local tumor heating, *Eur. J. Cancer Clin. Oncol.*, 1982, **18**(11), 1137–1146, DOI: 10.1016/0277-5379(82)90095-5.

195 P. Vaupel, H. Piazena, M. Notter, A. Thomsen, A. Grosu, F. Scholkmann, *et al.*, From Localized Mild Hyperthermia to Improved Tumor Oxygenation: Physiological Mechanisms Critically Involved in Oncologic Thermo-Radio-Immunotherapy, *Cancers*, 2023, **15**, 1394, DOI: 10.3390/cancers15051394.

196 Ş. Bayram and N. Çalışkan, Effects of local heat application before intravenous catheter insertion in chemotherapy patients, *J. Clin. Nurs.*, 2016, **25**(11–12), 1740–1747, DOI: 10.1111/jocn.13193.

197 W. Cao, Q. Lu, J. Li, C. Zhou, J. Zhu, Y. Wan and Y. Liu, Transcatheter arterial infusion with heated saline changes the vascular permeability of rabbit hepatic tumors, *Acad. Radiol.*, 2011, **18**(12), 1569–1576, DOI: 10.1016/j.acra.2011.08.010.

198 S. Kim, Y. Kim, Y. Kim and Y. Cheon, Heating Pretreatment of the Recipient Site Enhances Survival of Transplanted Fat in a Mouse Model, *Plast. Reconstr. Surg.*, 2023, **152**, 787–795, DOI: 10.1097/PRS.0000000000010328.

199 M. Miller, R. Chandra, M. Cuccarese, C. Pfirschke, C. Engblom, S. Stapleton, *et al.*, Radiation therapy primes tumors for nanotherapeutic delivery *via* macrophage-mediated vascular bursts, *Sci. Transl. Med.*, 2017, **9**, eaal0225, DOI: 10.1126/scitranslmed.aal0225.

200 H. Wang, R. Ran, Y. Liu, Y. Hui, B. Zeng, D. Chen, D. Weitz and C. Zhao, Tumor-Vasculature-on-a-Chip for Investigating Nanoparticle Extravasation and Tumor Accumulation, *ACS Nano*, 2018, **12**(11), 11600–11609, DOI: 10.1021/acsnano.8b06846.

201 R. Ngoune, A. Peters, D. Elverfeldt, K. Winkler and G. Pütz, Accumulating nanoparticles by EPR: A route of no return, *J. Controlled Release*, 2016, **238**, 58–70, DOI: 10.1016/j.jconrel.2016.07.028.

202 J. Perry, K. Reuter, J. Luft, C. Pecot, W. Zamboni and J. Desimone, Mediating Passive Tumor Accumulation through Particle Size, Tumor Type, and Location, *Nano Lett.*, 2017, **17**(5), 2879–2886, DOI: 10.1021/acs.nanolett.7b00021.

203 P. Zhao, M. Zheng, C. Yue, Z. Luo, P. Gong, G. Gao, Z. Sheng, C. Zheng and L. Cai, Improving drug accumulation and photothermal efficacy in tumor depending on size of ICG loaded lipid-polymer nanoparticles, *Biomaterials*, 2014, **35**(23), 6037–6046, DOI: 10.1016/j.biomaterials.2014.04.019.

204 M. Sznol, S. Lin, D. Bermudes, L. Zheng and I. King, Use of preferentially replicating bacteria for the treatment of cancer, *J. Clin. Invest.*, 2000, **105**(8), 1027–1030, DOI: 10.1172/JCI9818.

205 S. Luo, X. Luo, X. Wang, L. Li, H. Liu, B. Mo, H. Gan, W. Sun, L. Wang, H. Liang and S. Yu, Tailoring Multifunctional Small Molecular Photosensitizers to *In Vivo* Self-Assemble with Albumin to Boost Tumor-Preferential Accumulation, NIR Imaging, and Photodynamic/Photothermal/Immunotherapy, *Small*, 2022, e2201298, DOI: 10.1002/smll.202201298.

206 R. Rachakatla, S. Balivada, G. Seo, C. Myers, H. Wang, T. Samarakoon, R. Dani, M. Pyle, F. Kroh, B. Walker, X. Leaym, O. Koper, V. Chikán, S. Bossmann, M. Tamura and D. Troyer, Attenuation of mouse melanoma by A/C magnetic field after delivery of bi-magnetic nanoparticles by neural progenitor cells, *ACS Nano*, 2010, **4**(12), 7093–7104, DOI: 10.1021/nn100870z.

207 Z. Fridlender, J. Sun, S. Kim, V. Kapoor, G. Cheng, L. Ling, G. Worthen and S. Albelda, Polarization of tumor-associated neutrophil phenotype by TGF-beta: "N1" *versus* "N2" TAN, *Cancer Cell*, 2009, **16**(3), 183–194, DOI: 10.1016/j.ccr.2009.06.017.

208 Z. Ma, K. Han, X. Dai and H. Han, Precisely Striking Tumors without Adjacent Normal Tissue Damage *via* Mitochondria-Templated Accumulation, *ACS Nano*, 2018, **12**(6), 6252–6262, DOI: 10.1021/acsnano.8b03212.

209 M. Dreher, W. Liu, C. Michelich, M. Dewhirst and A. Chilkoti, Thermal cycling enhances the accumulation of a temperature-sensitive biopolymer in solid tumors, *Cancer Res.*, 2007, **67**(9), 4418–4424, DOI: 10.1158/0008-5472.CAN-06-4444.

210 E. Cazares-Cortes, S. Cabana, C. Boitard, É. Nehlig, N. Griffete, J. Fresnais, C. Wilhelm, A. Abou-Hassan and C. Ménager, Recent insights in magnetic hyperthermia: From the "hot-spot" effect for local delivery to combined magneto-photo-thermia using magneto-plasmonic hybrids, *Adv. Drug Delivery Rev.*, 2019, **138**, 233–246, DOI: 10.1016/j.addr.2018.10.016.

211 D. Zhang, J. Yang, S. Ye, Y. Wang, C. Liu, Q. Zhang and R. Liu, Combination of Photothermal Therapy with Anti-Inflammation Therapy Attenuates the Inflammation Tumor Microenvironment and Weakens Immunosuppression for Enhancement Antitumor Treatment, *Small*, 2022, e2107071, DOI: 10.1002/smll.202107071.

212 S. Uthaman, S. Pillarisetti, H. Hwang, A. Mathew, K. Huh, J. Rhee and I. Park, Tumor Microenvironment-Regulating Immunosenescence-Independent Nanostimulant Synergizing with Near-Infrared Light Irradiation for Antitumor Immunity, *ACS Appl. Mater. Interfaces*, 2021, **13**(22), 25895–25902, DOI: 10.1021/acsami.0c20063.

213 L. Huang, Y. Li, Y. Du, Y. Zhang, X. Wang, Y. Ding, X. Yang, F. Meng, J. Tu, L. Luo and C. Sun, Mild photothermal therapy potentiates anti-PD-L1 treatment for immunologically cold tumors *via* an all-in-one and all-in-control strategy, *Nat. Commun.*, 2019, **10**, 1–13, DOI: 10.1038/s41467-019-12771-9.

214 C. Wang, Y. H. Xu, H. Z. Xu, K. Li, Q. Zhang, L. Shi, L. Zhao and X. Chen, PD-L1 blockade TAM-dependently potentiates mild photothermal therapy against triple-negative breast cancer, *J. Nanobiotechnol.*, 2023, **21**(1), 476, DOI: 10.1186/s12951-023-02240-3.

215 S. Fu, Q. Ma, J. Li, Y. Wang, C. Yang, P. Gu, W. Zhang, Y. Liu and N. Zhang, Blockage of HSP90 and IDO1 pathway by α-MSH modified nanoelicitor to dual-facilitate mild photothermal therapy, *Pharm. Sci. Adv.*, 2023, **1**(2), 100009, DOI: 10.1016/j.pscia.2023.100009.

216 H. Liu, J. Xu, M. Ye, *et al.*, Self-shrinking supramolecular nanoparticles syndicate energy suppression and NIR-II mild photothermal amplification of mitochondrial oxidative stress for breast cancer therapy, *Nano Res.*, 2024, **17**, 4314–4328, DOI: 10.1007/s12274-023-6296-4.

217 P. Wang, B. Chen, Y. Zhan, L. Wang, J. Luo, J. Xu, L. Zhan, Z. Li, Y. Liu and J. Wei, Enhancing the efficiency of mild temperature photothermal therapy for cancer assisting with various strategies, *Pharmaceutics*, 2022, **14**(11), 2279, DOI: 10.3390/pharmaceutics14112279.

218 R. Meyer, R. Braun, G. Rosner and M. Dewhirst, Local 42°C Hyperthermia Improves Vascular Conductance of the R3230Ac Rat Mammary Adenocarcinoma during Sodium Nitroprusside Infusion, *Radiat. Res.*, 2000, **154**, 196–201, DOI: 10.1667/0033-7587(2000)154[01962:lchivc]2.0.CO;2.

219 C. Babbs, D. DeWitt, W. Voorhees, J. McCaw and R. Chan, Theoretical feasibility of vasodilator-enhanced local tumor heating, *Eur. J. Cancer Clin. Oncol.*, 1982, **18**(11), 1137–1146, DOI: 10.1016/0277-5379(82)90095-5.

220 M. Horsman, K. Christensen and J. Overgaard, Hydralazine-induced enhancement of hyperthermic damage in a C3H mammary carcinoma in vivo, *Int. J. Hyperthermia*, 1989, **5**(2), 123–136, DOI: 10.3109/02656738909140442.

221 G. Nussbaum, C. Babbs and M. Mintun, Results of a preliminary study of the potential of vasodilators for improving thermotherapy of deep-seated tumours, *Int. J. Hyperthermia*, 1986, **2**(2), 61–64, DOI: 10.3109/02656738609019994.

222 T. Suganuma, K. Irie, E. Fujii, T. Yoshioka and T. Muraki, Effect of heat stress on lipopolysaccharide-induced vascular permeability change in mice, *J. Pharmacol. Exp. Ther.*, 2002, **303**, 656–663, DOI: 10.1124/jpet.102.035758.

223 S. Tabatabaei, H. Girouard, A. Carret and S. Martel, Remote control of the permeability of the blood–brain barrier by magnetic heating of nanoparticles: a proof of concept for brain drug delivery, *J. Controlled Release*, 2015, **206**, 49–57, DOI: 10.1016/j.jconrel.2015.02.027.

224 C. Song, Effect of hyperthermia on vascular functions of normal tissues and experimental tumors; brief communication, *J. Natl. Cancer Inst.*, 1978, **60**(3), 711–713, DOI: 10.1093/JNCI/60.3.711.

225 S. Lorenzo and C. Minson, Heat acclimation improves cutaneous vascular function and sweating in trained cyclists, *J. Appl. Physiol.*, 2010, **109**(6), 1736–1743, DOI: 10.1152/japplphysiol.00725.2010.

226 A. Ven, P. Kim, O. Haley, J. Fakhoury, G. Adriani, J. Schmulen, P. Moloney, F. Hussain, M. Ferrari, X. Liu, S. Yun and P. Decuzzi, Rapid tumoritropic accumulation of systemically injected plateloid particles and their biodistribution, *J. Controlled Release*, 2012, **158**(1), 148–155, DOI: 10.1016/j.jconrel.2011.10.021.

227 S. Golombek, J. May, B. Theek, L. Appold, N. Drude, F. Kiessling and T. Lammers, Tumor targeting *via* EPR: strategies to enhance patient responses, *Adv. Drug Delivery Rev.*, 2018, **130**, 17–38, DOI: 10.1016/j.addr.2018.07.007.

228 T. Tanaka, S. Shiramoto, M. Miyashita, Y. Fujishima and Y. Kaneo, Tumor targeting based on the effect of enhanced permeability and retention (EPR) and the mechanism of receptor-mediated endocytosis (RME), *Int. J. Pharm.*, 2004, **277**(1–2), 39–61, DOI: 10.1016/J.IJPHARM.2003.09.050.

229 C. England, H. Im, L. Feng, F. Chen, S. Graves, R. Hernandez, H. Orbay, C. Xu, S. Cho, R. Nickles, Z. Liu, D. Lee and W. Cai, Re-assessing the enhanced permeability and retention effect in peripheral arterial disease using radiolabeled long circulating nanoparticles, *Biomaterials*, 2016, **100**, 101–109, DOI: 10.1016/j.biomaterials.2016.05.018.

230 F. Yoshino, T. Amano, Y. Zou, J. Xu, F. Kimura, Y. Furusho, T. Chano, T. Murakami, L. Zhao and N. Komatsu, Preferential tumor accumulation of polyglycerol functionalized nanodiamond conjugated with cyanine dye leading to near-infrared fluorescence *in vivo* tumor imaging, *Small*, 2019, **15**(14), e1901930, DOI: 10.1002/smll.201901930.

231 W. Liu, M. Dreher, D. Furgeson, K. Peixoto, H. Yuan, M. Zalutsky and A. Chilkoti, Tumor accumulation, degradation, and pharmacokinetics of elastin-like polypeptides in nude mice, *J. Controlled Release*, 2006, **116**(2), 170–178, DOI: 10.1016/J.JCONREL.2006.06.026.

232 S. Tanimura, R. Kadomoto, T. Tanaka, Y. Zhang, I. Kouno and M. Kohno, Suppression of tumor cell invasiveness by hydrolyzable tannins (plant polyphenols) *via* the inhibition of matrix metalloproteinase-2/-9 activity, *Biochem. Biophys. Res. Commun.*, 2005, **330**(4), 1306–1313, DOI: 10.1016/J.BBRC.2005.03.116.

233 P. Xu and F. Liang, Nanomaterial-based tumor photothermal immunotherapy, *Int. J. Nanomed.*, 2020, **15**, 9159–9180, DOI: 10.2147/IJN.S249252.

234 G. S. R. Raju, E. Pavitra, G. L. Varaprasad, S. S. Bandaru, G. P. Nagaraju, B. Farran, Y. S. Huh and Y. K. Han, Nanoparticles mediated tumor microenvironment modulation: current advances and applications, *J. Nanobiotechnol.*, 2022, **20**(1), 274, DOI: 10.1186/s12951-022-01476-9.

235 Q. Lu, D. Kou, S. Lou, *et al.*, Nanoparticles in tumor microenvironment remodeling and cancer immunotherapy, *J. Hematol. Oncol.*, 2024, **17**, 16, DOI: 10.1186/s13045-024-01535-8.

236 J. Wu, The enhanced permeability and retention (EPR) effect: the significance of the concept and methods to enhance its application, *J. Pers. Med.*, 2021, **11**(8), 771, DOI: 10.3390/jpm11080771.

237 M. Overchuk, R. A. Weersink, B. C. Wilson and G. Zheng, Photodynamic and photothermal therapies: synergy opportunities for nanomedicine, *ACS Nano*, 2023, **17**(9), 7979–8003, DOI: 10.1021/acsnano.3c00891.

238 W. Islam, T. Niidome and T. Sawa, Enhanced targeting of solid tumors, *J. Pers. Med.*, 2022, **12**(12), 1964, DOI: 10.3390/jpm12121964.

239 D. Huang, L. Sun, L. Huang and Y. Chen, Nanodrug delivery systems modulate tumor vessels to increase the enhanced permeability and retention effect, *J. Pers. Med.*, 2021, **11**(2), 124, DOI: 10.3390/jpm11020124.

240 Y. Wen, X. Chen, X. Zhu, Y. Gong, G. Yuan, X. Qin and J. Liu, Photothermal-chemotherapy integrated nanoparticles with tumor microenvironment response enhanced the induction of immunogenic cell death for colorectal cancer efficient treatment, *ACS Appl. Mater. Interfaces*, 2019, 43393–43408, DOI: 10.1021/acsami.9b17137.

241 N. Aghda, S. Abdulsahib, C. Severson, E. Lara, S. Hurtado, T. Yildiz, J. Castillo, J. Tunnell and T. Betancourt, Induction of immunogenic cell death of cancer cells through nanoparticle-mediated dual chemotherapy and photothermal therapy, *Int. J. Pharm.*, 2020, 119787, DOI: 10.1016/j.ijpharm.2020.119787.

242 S. Todryk, A. Melcher, N. Hardwick, E. Linardakis, A. Bateman, M. Colombo, A. Stoppacciaro and R. Vile, Heat shock protein 70 induced during tumor cell killing induces Th1 cytokines and targets immature dendritic cell precursors to enhance antigen uptake, *J. Immunol.*, 1999, **163**(3), 1398–1408, DOI: 10.4049/jimmunol.163.3.1398.

243 J. Zhu, Y. Lou, P. Liu and L. Xu, Tumor-related HSP70 released after cryo-thermal therapy targeted innate immune initiation in the antitumor immune response, *Int. J. Hyperthermia*, 2020, **37**, 843–853, DOI: 10.1080/02656736.2020.1788173.

244 D. Hinshaw and L. Shevde, The tumor microenvironment innately modulates cancer progression, *Cancer Res.*, 2019, 4557–4566, DOI: 10.1158/0008-5472.CAN-18-3962.

245 H. Udono, D. Levey and P. Srivastava, Cellular requirements for tumor-specific immunity elicited by heat shock proteins: tumor rejection antigen gp96 primes CD8+ T cells in vivo, *Proc. Natl. Acad. Sci. U.S.A.*, 1994, **91**, 3077–3081, DOI: 10.1073/pnas.91.8.3077.

246 M. Melancon, A. Elliott, A. Shetty, Q. Huang, R. Stafford and C. Li, Near-infrared light modulated photothermal effect increases vascular perfusion and enhances polymeric drug delivery, *J. Controlled Release*, 2011, **156**(2), 265–272, DOI: 10.1016/j.jconrel.2011.06.030.

247 A. Sen, M. Capitano, J. Spernyak, J. Schueckler, S. Thomas, A. Singh, S. Evans, B. Hylander and E. Repasky, Mild elevation of body temperature reduces tumor interstitial fluid pressure and hypoxia and enhances efficacy of radiotherapy in murine tumor models, *Cancer Res.*, 2011, **71**(11), 3872–3880, DOI: 10.1158/0008-5472.CAN-10-4482.

248 I. Biancacci, F. Lorenzi, B. Theek, X. Bai, J. May, L. Consolino, *et al.*, Monitoring EPR effect dynamics during nanotaxane treatment with theranostic polymeric micelles, *Adv. Sci.*, 2022, **9**, e2103745, DOI: 10.1002/advs.202103745.

249 V. Torchilin, Tumor delivery of macromolecular drugs based on the EPR effect, *Adv. Drug Delivery Rev.*, 2011, **63**(3), 131–135, DOI: 10.1016/j.addr.2010.03.011.

250 A. Karageorgis, S. Dufort, L. Sancey, M. Henry, S. Hirsjärvi, C. Passirani, *et al.*, An MRI-based classification scheme to predict passive access of 5 to 50-nm large nanoparticles to tumors, *Sci. Rep.*, 2016, **6**, 21417, DOI: 10.1038/srep21417.

251 E. Jäger, A. Jäger, T. Etrych, F. Giacomelli, P. Chytil, A. Jigounov, *et al.*, Self-assembly of biodegradable copolyester and reactive HPMA-based polymers into nanoparticles as an alternative stealth drug delivery system, *Soft Matter*, 2012, **8**, 9563–9575, DOI: 10.1039/C2SM26150B.

252 Y. Tian, Z. Gao, N. Wang, M. Hu, Y. Ju, Q. Li, *et al.*, Engineering poly(ethylene glycol) nanoparticles for accelerated blood clearance inhibition and targeted drug delivery, *J. Am. Chem. Soc.*, 2022, 18419–18428, DOI: 10.1021/jacs.2c06877.

253 B. Tesarova, S. Dostalova, V. Šmídová, Z. Goliasova, Z. Skubalova, H. Michalkova, *et al.*, Surface-PASylation of ferritin to form stealth nanovehicles enhances *in vivo* therapeutic performance of encapsulated ellipticine, *Appl. Mater. Today*, 2020, **18**, 100501, DOI: 10.1016/j.apmt.2019.100501.

254 E. Bellido, T. Hidalgo, M. Lozano, M. Guillevic, R. Simón-Vázquez, M. Santander-Ortega, *et al.*, Heparin-engineered mesoporous iron metal-organic framework nanoparticles: toward stealth drug nanocarriers, *Adv. Healthcare Mater.*, 2015, **4**, 1246–1257, DOI: 10.1002/adhm.201400755.

255 G. Song, C. Ji, C. Liang, X. Song, X. Yi, Z. Dong, *et al.*, TaOx decorated perfluorocarbon nanodroplets as oxygen reservoirs to overcome tumor hypoxia and enhance cancer radiotherapy, *Biomaterials*, 2017, **112**, 257–263, DOI: 10.1016/j.biomaterials.2016.11.034.

256 Z. Miao, P. Liu, Y. Wang, K. Li, D. Huang, H. Yang, Q. Zhao, Z. Zha, L. Zhen and C. Xu, PEGylated tantalum nanoparticles: a metallic photoacoustic contrast agent for multiwavelength imaging of tumors, *Small*, 2019, e1903596, DOI: 10.1002/smll.201903596.

257 X. Cheng, Y. Wei, X. Jiang, C. Wang, M. Liu, J. Yan, L. Zhang and Y. Zhou, Insight into the prospects for tumor therapy based on photodynamic immunotherapy, *Pharmaceuticals*, 2022, **15**(11), 1359, DOI: 10.3390/ph15111359.

258 M. Yousefi, M. Hantehzadeh and A. Sari, Synthesis of tantalum nanoparticles by laser ablation in liquid method and investigating the effect of electric field on the structural properties, *Int. J. Mod. Phys. B*, 2023, 2450340, DOI: 10.1142/s0217979224503405.

259 H. Liao, C. Nehl and J. Hafner, Biomedical applications of plasmon resonant metal nanoparticles, *Nanomedicine*, 2006, **1**(2), 201–208, DOI: 10.2217/17435889.1.2.201.

260 S. Boonstra, S. Roffel, E. Dompeling, M. Helderman-van der Laan, M. Sosef, W. van der Meijden, *et al.*, Safety of autologous adipose-derived stem cell therapy in patients with chronic non-healing wounds: results of a prospective

study, *Wound Repair Regen.*, 2022, **30**(4), 554–563, DOI: 10.1111/wrr.13061.

261 I. Mannelli and M. Marco, Recent advances in analytical and bioanalysis applications of noble metal nanorods, *Anal. Bioanal. Chem.*, 2010, **398**, 2451–2459, DOI: 10.1007/s00216-010-3937-8.

262 D. Paramasivam, N. Kayambu, A. Rabel, A. Sundramoorthy and A. Sundaramurthy, Anisotropic noble metal nanoparticles: synthesis, surface functionalization and applications in biosensing, bioimaging, drug delivery and theranostics, *Acta Biomater.*, 2017, **49**, 45–65, DOI: 10.1016/j.actbio.2016.11.066.

263 N. Khlebtsov and L. Dykman, Optical properties and biomedical applications of plasmonic nanoparticles, *J. Quant. Spectrosc. Radiat. Transf.*, 2010, **111**, 1–35, DOI: 10.1016/j.jqsrt.2009.07.012.

264 C. S. Tiwari, A. Pratap and P. K. Jha, Influence of size, shape and dimension on glass transition and Kauzmann temperature of silver (Ag) and tantalum (Ta) nanoparticles, *J. Nanoparticle Res.*, 2020, **22**(8), 218, DOI: 10.1007/s11051-020-04955-y.

265 A. Espinosa, J. Reguera, A. Curcio, A. Muñoz-Noval, C. Kuttner, A. Walle, L. Liz-Marzán and C. Wilhelm, Janus magnetic-plasmonic nanoparticles for magnetically guided and thermally activated cancer therapy, *Small*, 2020, **16**, e1904960, DOI: 10.1002/smll.201904960.

266 Y. X. Leng, J. Y. Chen, P. Yang, H. Sun, J. Wang and N. Huang, The biocompatibility of the tantalum and tantalum oxide films synthesized by pulse metal vacuum arc source deposition, *Nucl. Instrum. Methods Phys. Res., Sect. B*, 2006, **242**(1–2), 30–32, DOI: 10.1016/j.nimb.2005.08.002.

267 C. Ji, M. Zhao, C. Wang, R. Liu, S. Zhu, X. Dong, C. Su and Z. Gu, Biocompatible tantalum nanoparticles as radiosensitizers for enhancing therapy efficacy in primary tumor and metastatic sentinel lymph nodes, *ACS Nano*, 2022, **16**(6), 9428–9441, DOI: 10.1021/acsnano.2c02314.

268 C. Yang, J. Li, C. Zhu, Q. Zhang, J. Yu, J. Wang, Q. Wang, J. Tang, H. Zhou and H. Shen, Advanced antibacterial activity of biocompatible tantalum nanofilm *via* enhanced local innate immunity, *Acta Biomater.*, 2019, **99**, 450–460, DOI: 10.1016/j.actbio.2019.03.027.

269 C. Kang, Y. Wang, L. Li, *et al.*, Assessment of *in vivo* article-induced MC3T3-E1 proliferation and underlying mechanisms, *J. Mater. Sci. Mater. Med.*, 2021, **32**, 133, DOI: 10.1007/s10856-021-06606-7.

270 H. Yi, G. Yan, J. He, J. Zhuang, C. Jin and D. Y. Zhang, Tantalum nitride-based theranostic agent for photoacoustic imaging-guided photothermal therapy in the second NIR window, *Nanomaterials*, 2023, **13**(11), 1708, DOI: 10.3390/nano13111708.

271 D. Ding, Q. Zeng, F. He and Z. Chen, The effect of thermal oxidation on the photothermal conversion property of tantalum coatings, *Materials*, 2021, **14**(14), 4031, DOI: 10.3390/ma14144031.

272 R. Kant, Surface plasmon resonance-based fiber–optic nanosensor for the pesticide fenitrothion utilizing Ta2O5 nanostructures sequestered onto a reduced graphene oxide matrix, *Microchim. Acta*, 2019, **186**, 575, DOI: 10.1007/s00604-019-4002-8.

273 M. Tran, E. Turner, S. Segro, L. Fang, E. Seyyal and A. Malik, Tantala-based sol-gel coating for capillary microextraction on-line coupled to high-performance liquid chromatography, *J. Chromatogr. A*, 2017, **1522**, 38–47, DOI: 10.1016/j.chroma.2017.09.048.

274 Y. Sun, T. Liu, H. Hu, Z. Xiong, K. Zhang, X. He, W. Liu, P. Lei and Y. Hu, Differential effect of tantalum nanoparticles *versus* tantalum micron particles on immune regulation, *Mater. Today Bio*, 2022, **16**, 100340, DOI: 10.1016/j.mtbio.2022.100340.

275 M. Calzada and A. Gonzalez, Tantalum penta-glycolate sol as a precursor of strontium bismuth tantalate ferroelectric thin films, *J. Am. Ceram. Soc.*, 2005, **88**, 2702–2708, DOI: 10.1111/j.1551-2916.2005.00505.x.

276 S. Chakravarty, J. M. L. Hix, K. A. Wiewiora, M. C. Volk, E. Kenyon, D. D. Shuboni-Mulligan, B. Blanco-Fernandez, M. Kiupel, J. Thomas, L. F. Sempere and E. M. Shapiro, Tantalum oxide nanoparticles as versatile contrast agents for X-ray computed tomography, *Nanoscale*, 2020, **12**(14), 7720–7734, DOI: 10.1039/d0nr01234c.

277 S. Ambreen, N. D. Pandey, P. Mayer and A. Pandey, Characterization and photocatalytic study of tantalum oxide nanoparticles prepared by the hydrolysis of tantalum oxo-ethoxide, *Beilstein J. Nanotechnol.*, 2014, **5**(1), 1082–1090, DOI: 10.3762/bjnano.5.121.

278 E. E. Khawaja and S. G. Tomlin, The optical properties of thin films of tantalum pentoxide and zirconium dioxide, *Thin Solid Films*, 1975, **30**(2), 361–369, DOI: 10.1016/0040-6090(75)90100-5.

279 A. Chan, J. Tetzlaff, D. Altman, A. Laupacis, P. Gøtzsche, K. Krleza-Jeric, A. Hrõbjartsson, H. Mann, K. Dickersin, J. Berlin, C. Doré, W. Parulekar, W. Summerskill, T. Groves, K. Schulz, H. Sox, F. Rockhold, D. Rennie and D. Moher, SPIRIT 2013 statement: defining standard protocol items for clinical trials, *Ann. Intern. Med.*, 2013, **158**(3), 200–207, DOI: 10.7326/0003-4819-158-3-201302050-00583.

280 T. Kendall, M. Robinson, D. Brierley, S. Lim, D. O'Connor, A. Shaaban, I. Lewis, A. Chan and D. Harrison, Guidelines for cellular and molecular pathology content in clinical trial protocols: the SPIRIT-Path extension, *Lancet Oncol*, 2021, **22**(10), e435–e445, DOI: 10.1016/S1470-2045(21)00344-2.

281 S. Lim, K. Gurusamy, D. O'Connor, A. Shaaban, D. Brierley, I. Lewis, *et al.*, Recommendations for cellular and molecular pathology input into clinical trials: a systematic review and meta-aggregation, *J. Pathol.: Clin. Res.*, 2021, **7**, 191–202, DOI: 10.1002/cjp2.199.

282 G. Bao, S. Mitragotri and S. Tong, Multifunctional nanoparticles for drug delivery and molecular imaging, *Annu. Rev. Biomed. Eng.*, 2013, **15**, 253–282, DOI: 10.1146/annurev-bioeng-071812-152409.

283 N. Bertrand, P. Grenier, M. Mahmoudi, E. Lima, E. Appel, F. Dormont, *et al.*, Mechanistic understanding of *in vivo*

protein corona formation on polymeric nanoparticles and impact on pharmacokinetics, *Nat. Commun.*, 2017, **8**, 777, DOI: 10.1038/s41467-017-00600-w.

284 L. Grislain, P. Couvreur, V. Lenaerts, M. Roland, D. Deprezdecampeneere and P. Speiser, Pharmacokinetics and distribution of a biodegradable drug-carrier, *Int. J. Pharm.*, 1983, **15**, 335–345, DOI: 10.1016/0378-5173(83)90166-7.

285 Z. Cao, L. Gan, W. Jiang, J. Wang, H. Zhang, Y. Zhang, *et al.*, Protein binding affinity of polymeric nanoparticles as a direct indicator of their pharmacokinetics, *ACS Nano*, 2020, 3563–3575, DOI: 10.1021/acsnano.9b10015.

286 T. Dubaj, K. Kozics, M. Šrámková, A. Manová, N. Bastús, O. Moriones, *et al.*, Pharmacokinetics of PEGylated gold nanoparticles: in vitro—in vivo correlation, *Nanomaterials*, 2022, **12**, 511, DOI: 10.3390/nano12030511.

287 Y. Chen, G. Song, Z. Dong, X. Yi, Y. Chao, C. Liang, *et al.*, Drug-loaded mesoporous tantalum oxide nanoparticles for enhanced synergetic chemoradiotherapy with reduced systemic toxicity, *Small*, 2017, **13**(8), 1602869, DOI: 10.1002/smll.201602869.

288 S. Su and P. Kang, Systemic review of biodegradable nanomaterials in nanomedicine, *Nanomaterials*, 2020, **10**, 656, DOI: 10.3390/nano10040656.

289 Y. Liu, K. Ai and L. Lu, Nanoparticulate X-ray computed tomography contrast agents: from design validation to *in vivo* applications, *Acc. Chem. Res.*, 2012, **45**(10), 1817–1827, DOI: 10.1021/ar300150c.

290 C. He, D. Liu and W. Lin, Self-assembled core-shell nanoparticles for combined chemotherapy and photodynamic therapy of resistant head and neck cancers, *ACS Nano*, 2015, **9**(1), 991–1003, DOI: 10.1021/nn506963h.

291 J. Nam, S. Son, K. Park, W. Zou, L. Shea and J. Moon, Cancer nanomedicine for combination cancer immunotherapy, *Nat. Rev. Mater.*, 2019, **4**, 398–414, DOI: 10.1038/s41578-019-0108-1.

292 F. Gong, J. Chen, X. Han, J. Zhao, M. Wang, L. Feng, *et al.*, Core-shell TaOx@MnO2 nanoparticles as a nano-radiosensitizer for effective cancer radiotherapy, *J. Mater. Chem. B*, 2018, **6**(15), 2250–2257, DOI: 10.1039/C8TB00070K.

293 F. Mogheri, E. Jokar, R. Afshin, A. Akbari, M. Dadashpour, A. Firouzi-amandi, *et al.*, Co-delivery of metformin and silibinin in dual drug loaded nanoparticles synergistically improves chemotherapy in human non-small cell lung cancer A549 cells, *Nat. Rev. Mater.*, 2021, **66**, 102752, DOI: 10.1016/j.jddst.2021.102752.

294 Y. Liu, L. Qiao, S. Zhang, G. Wan, B. Chen, P. Zhou, *et al.*, Dual pH-responsive multifunctional nanoparticles for targeted treatment of breast cancer by combining immunotherapy and chemotherapy, *Acta Biomater.*, 2018, **66**, 310–324, DOI: 10.1016/j.actbio.2017.11.010.

295 M. Mirrahimi, J. Beik, M. Mirrahimi, Z. Alamzadeh, S. Teymouri, V. Mahabadi, *et al.*, Triple combination of heat, drug and radiation using alginate hydrogel co-loaded with gold nanoparticles and cisplatin for locally synergistic cancer therapy, *Int. J. Biol. Macromol.*, 2020, 617–626, DOI: 10.1016/j.ijbiomac.2020.04.272.

296 B. Xiao, X. Si, M. Han, E. Viennois, M. Zhang and D. Merlin, Co-delivery of camptothecin and curcumin by cationic polymeric nanoparticles for synergistic colon cancer combination chemotherapy, *J. Mater. Chem. B*, 2015, **3**(39), 7724–7733, DOI: 10.1039/C5TB01245G.

297 J. He, Y. Zhou, Y. Liu, R. Guo, J. Jiang and M. Bruchez, Fluorogen-activating-protein-loaded tantalum oxide nanoshells for *in vivo* on-demand fluorescence/photoacoustic imaging, *ACS Appl. Bio Mater.*, 2022, 1057–1063, DOI: 10.1021/acsabm.1c01113.

298 K. Wang, X. He, X. Yang and H. Shi, Functionalized silica nanoparticles: a platform for fluorescence imaging at the cell and small animal levels, *Acc. Chem. Res.*, 2013, **46**(7), 1367–1376, DOI: 10.1021/ar3001525.

299 J. Crowder, N. Bates, J. Roberts, A. Torres and P. Bonitatibus, Determination of tantalum from tantalum oxide nanoparticle X-ray/CT contrast agents in rat tissues and bodily fluids by ICP-OES, *J. Anal. At. Spectrom.*, 2016, **31**, 1311–1317, DOI: 10.1039/C5JA00446B.

300 U. Dhawan, S. Wang, Y. Chu, G. Huang, Y. Lin, Y. Hung, *et al.*, Nanochips of tantalum oxide nanodots as artificial microenvironments for monitoring ovarian cancer progressiveness, *Sci. Rep.*, 2016, **6**, 31998, DOI: 10.1038/srep31998.

301 X. He, K. Wang and Z. Cheng, In vivo near-infrared fluorescence imaging of cancer with nanoparticle-based probes, *Wiley Interdiscip. Rev.: Nanomed. Nanobiotechnol.*, 2010, **2**(4), 349–366, DOI: 10.1002/wnan.85.

302 E. L. Irede, O. R. Aworinde, O. K. Lekan, *et al.*, Medical imaging: a critical review on X-ray imaging for the detection of infection, *Biomed. Mater. Devices*, 2024, 307–317, DOI: 10.1007/s44174-024-00212-1.

303 E. L. Irede, R. F. Awoyemi, B. Owolabi, O. R. Aworinde, R. O. Kajola, A. Hazeez, *et al.*, Cutting-edge developments in zinc oxide nanoparticles: synthesis and applications for enhanced antimicrobial and UV protection in healthcare solutions, *RSC Adv.*, 2024, **14**, 20992–21034, DOI: 10.1039/D4RA02452D.

304 T. P. Okonkwo, O. D. Amienghemhen, A. N. Nkwor and I. H. Ifijen, Exploring the versatility of copper-based nanoparticles as contrast agents in various imaging modalities, *Nano-Struct. Nano-Objects*, 2024, **40**, 101370, DOI: 10.1016/j.nanoso.2024.101370.

305 I. C. Omoruyi, J. I. Omoruyi, O. N. Aghedo, U. D. Archibong and I. H. Ifijen, Application of Magnetic Iron Oxide Nanostructures in Drug Delivery: A Compact Review, in *TMS 2023 152nd Annual Meeting & Exhibition Supplemental Proceedings*, Springer, Cham, 2023, DOI: 10.1007/978-3-031-22524-6_22.